UNIVERSITÉ DE MONTRÉAL

DESIGN PROCEDURES AND FINITE ELEMENT ANALYSIS OF POT BEARINGS

KIMIYA ZAKIKHANI
DÉPARTEMENT DES GÉNIES CIVIL, GÉOLOGIQUE, ET DES MINES
ÉCOLE POLYTECHNIQUE DE MONTRÉAL

MÉMOIRE PRÉSENTÉ EN VUE DE L'OBTENTION
DU DIPLÔME DE MAÎTRISE ÈS SCIENCES APPLIQUÉES
(GÉNIE CIVIL)
AVRIL 2014

UNIVERSITÉ DE MONTRÉAL

ÉCOLE POLYTECHNIQUE DE MONTRÉAL

Ce mémoire intitulé :

DESIGN PROCEDURES AND FINITE ELEMENT ANALYSIS OF POT BEARINGS

présenté par : ZAKIKHANI Kimiya
en vue de l'obtention du diplôme de : Maîtrise ès sciences appliquées
a été dûment accepté par le jury d'examen constitué de :

Mme KOBOEVIC Sanda, Ph.D., présidente
M. BOUAANANI Najib, Ph.D., membre et directeur de recherche
M. LAMARCHE Charles-Philippe, Ph.D., membre

To my mother, Sadat Feiznia
and my father Mohammad Sadegh Zakikhani

ACKNOWLEDGEMENTS

During my graduate studies at Polytechnique Montreal, I was fortunate to benefit from care, help and support of many people, among them, my family, friends and the academic community of Polytechnique Montreal. Without all this kindness, I could not be able to complete my program.

First, I would like to thank my research director, Prof. Najib Bouaanani who supervised all the stages of my program. His advice, attention, patience and support made completion of my studies possible and I will benefit from the knowledge he has offered me in the next professional phases of my life.

Part of this research was financed by the Natural Sciences and Engineering Research Council of Canada (NSERC), namely through the MITACS-Accelerate internship program with industrial partner GoodCo-Ztech. I would like to thank Ms. Parinaz Pakniat, design engineer at GoodCo-Ztech for her guidance and help during my internship program.

I would also like to express my appreciation to all the members of Research Group for Structural Engineering (GRS) of Polytechnique Montreal and my friend Masood Meidani who has genuinely helped me since the beginning of my graduate studies.

Finally, I could not thank enough my family in particular my mother and father whose support in every aspect of my life made my dreams come true and I feel so fortunate to have them by my side. I also want to thank my sister for her sincere encouragements and companionship as my best friend.

RÉSUMÉ

Au Canada, les infrastructures des ponts vieillissent rapidement. En 2007, un grand nombre de ponts ont dépassé 57% de leur durée de vie, estimée à 43,3 années. Ce ratio augmenté 72% au Québec, ce qui indique qu'un bon nombre de ces ponts sont structurellement ou fonctionnellement déficient (Gagnon and Gaudreault 2011). Ce contexte met l'accent sur la nécessité de ce basér sur la performance, la rentabilité et l'optimisation des techniques de construction et l'amélioration des stratégies de rénovation. L'appui du pont est un élément essentiel de l'ensemble de la structure. Étant donné que la durée de vie d'un appui de pont est plus courte que celle du pont lui-même, un nombre considérable de déficiences dans les ponts peut être dû à un dysfonctionnement de l'appui du pont. Le type d'appui du pont qui est largement utilisé est appui de type pot (élastomère confiné), qui a été développé en Europe au début des années 1960. Comme d'autres types d'appuis, l'appui de type pot est utilisé pour supporter une superstructure de pont et accommoder ses mouvements indépendamment des éléments de support, c'est-à-dire piles et culées (Tonias 1994).

Quelques codes de pratique et spécifications qui ont mis l'accent sur la conception des appuis de type pot sont la norme européenne EN 1337-5 (EN 2005), AASHTO LRFD spécifications de conception de pont (AASHTO 2012), le rapport NCHRP 432 (NCHRP 1999) et CAN/CSA-S6-06 (CAN/CSA 2006). Certaines des règles prescrites par ces codes ne sont pas claires et devraient être validées pour assurer que la conception répond à la pratique de l'ingénierie actuelle. D'autre part, l'étude du comportement de l'appui de pont exige des techniques d'analyse de modélisation dictées par la présence de l'élastomère, qui est un matériau incompressible fortement non linéaire, couplé aux mécanismes complexes impliquant des interactions de contact non linéaires entre les différentes parties du BPE. Ces analyses avancées sont généralement fastidieuses et demande beaucoup d'expertise, ce qui explique principalement le manque des publications scientifiques dans ce domaine.

L'objectif principal de cette recherche est d'étudier les performances structurelles d'appuis à pot fixes par modélisation des éléments finis simplifiés. Dans le chapitre 2, les normes et les directives les plus importantes de la conception de BPE ont été introduites et l'origin des équations a été discutée en se référant des études théoriques disponibles. Ce chapitre répond à la nécessité de fournir un document qui étudie les raisons derrières les spécifications des normes. Par la suite, avant de procéder à l'analyse des éléments finis, la précision du logiciel pour les conditions de contact a été évaluée au chapitre 3. Dans ce chapitre, les résultats de la modélisation par éléments finis de deux corps cylindriques en contact ont été comparés aux formulations disponibles de contact analytiques. Le chapitre 4 présente le processus de

conception des appuis de pont de type pot comme une procédure à suivre étape par étape par le concepteur. Après avoir évalué la convergenc du logiciel d'analyse des éléments finis pour le problème de contact, chapitre 5 présente la méthode et les hypothèses utilisées pour générer des modèles éléments finis 3D. Ces modèles comprennent les modèles d'appui à pot ainsi que des modèles disque et anneau développé pour simuler les conditions de contact dans un appui de pot. à la fin de ce chapitre une étude paramétrique de régression a été effectuée sur les résultats de l'angle de contact obtenus par modélisation EF. Cette étape a été prise en compte due à l'impact important de l'angle de contact entre le piston et le pot dans la procédure de conception de l'appui à pot et son efficacité dans les formulations de conception recommandées dans les normes.

ABSTRACT

Bridge infrastructure in Canada is aging rapidly, with a large number of bridges exceeding 57% of their service life estimated at 43.3 years in 2007 (Gagnon and Gaudreault 2011). This ratio increases to 72% in Quebec, indicating that many of these bridges are structurally or functionally deficient. This context emphasizes the need for performance-based, cost-effective and optimized construction techniques and retrofit strategies. A bridge bearing is a crucial part of the whole structure. Since the total lifetime of a bearing is much less than that of the bridge itself, considerable number of deficiencies in bridges can be due to bearing malfunction. A widely used type of bridge bearings are elastomeric pot bearings (EPBs), which are developed in Europe in the early 1960s. As other bearing types, they are used to support a bridge superstructure and accommodate its movements independently from the supporting elements, i.e. piers and abutments (Tonias 1994).

Some of the specifications and codes of practice that address the design of pot bearings include the European Standard EN 1337-5 (EN 2005), AASHTO LRFD bridge design specifications (AASHTO 2012), the NCHRP Report 432 (NCHRP 1999) and Canadian Highway Bridge Design Code CAN/CSA-S6-06 (CAN/CSA 2006). Very often, the underlying assumptions behind the requirements prescribed by these codes for the design pot bearings are unclear. On the other hand, the investigation of the behaviour of EPBs requires advanced modeling analysis techniques dictated by the presence of the elastomeric pad, which is a highly nonlinear incompressible material, coupled to the complex mechanisms involving nonlinear contact interactions between the different parts of EPBs. Such advanced analyses are usually expertise demanding, time-consuming, and usually manufacturer proprietary, which mainly explains the lack of published research in this field.

The main objective of this research is to investigate the structural performance of fixed pot bearings through finite element modeling and simplified analytical formulations. For this purpose, the most important standards and guidelines for design of EPBs have been introduced, and the rationale underlying main design equations was discussed by referring to available theoretical work. Before performing finite element analyses on a series of pot bearings, the accuracy of the contact formulation programmed in the finite element software was assessed by comparing to classical contact problems for which analytical formulations are available, such as two cylindrical bodies in contact. The design process of pot bearings as a step by step procedure to be followed by the practicing engineer was highlighted. The

assumptions and method pursued to generate 3D finite element models were presented. A simplified finite element model including a piston and a truncated pot was also proposed and validated. A regression parametric study was performed on the results of contact angle between the pot and piston obtained from finite element modeling. The results of these simplified formulations of contact angle are original and important for the improvement of design procedures of pot bearings.

TABLE OF CONTENTS

LIST OF TABLES

LIST OF FIGURES

LIST OF APPENDICES

LISTE OF ABBREVIATIONS AND SYMBOLS

Abbreviations

EPB	Elastomeric pot bearing
FE	Finite Element
FEM	Finite Element Modeling

Symbols

a	Effective throat thickness of weld
a_{d}	Safety factor
A_{p}	Pot bearing base area
A_{R}	Pot wall area
a'	semi-major axis of contcat
b	Piston and pot contact width
b'	semi-minor axis of contcat
b_{Ring}	thickness of the ring and disk
c	Correction factor for slide path
c_1	Clearance between diameter of pot and piston
d_{Pad}	Diameter of the elastomeric pad
d_{Pot}	Internal diameter of the pot
dR	Difference in radius of bodies in Persson method
D_{Pot}	External diameter of the pot
E_{d}	Design modulus of elasticity
E	Modulus of elasticity of each body
F	Concentrated horizontal load applied to a node at upper body
$f_{\mathrm{e,\,k}}$	Characteristic contact strength of the elastomer
$F_{\mathrm{vw,\,d}}$	Design shear strength of butt weld
$F_{\mathrm{w,\,Rd}}$	Butt weld design resistance per unit length
F_{y}	Yield strength
F_{u}	Ultimate strength
h_{P}	Vertical clearance between top of piston and top of pot wall
t_{Pad}	Total height of the elastomeric pad
h_{Wall}	Height of pot wall
H	Horizontal loads applied to disk and ring model
H_{u}	Lateral load from ultimate load combinations
l_{a}	The lever arm of horizontal loads

N_{Rd}	Design resistance of the elastomeric pad
N_{Rk}	Characteristic value of resistance of the elastomeric pad
N_{Sd}	Design axial force of the elastomeric pad
n_{v}	Number or vehicles moving along the bridge
p	Pressure between two bodies per square length
P_0	Maximum pressure between piston and the pot per unit length
$P(x)$	Horizontal pressure between piston and pot per unit length
Q	Distributed load in ring and disk models
r and r_1 and r_2	Radii of cylinders
R	Radius of curved piston wall
r_{Disk}	Radius of the disk
r_{Ring}	Inner radius of the ring
R_{Ring}	External radius of the ring
R_0	Radial distance from center of pot to object in question
r_{Pad}	Radius of the elastomeric pad
$S_{\mathrm{A,\,d}}$	Accumulated slide path of the bearing
S_{T}	Accumulated slide path derived from testing
t_{Pot}	Height of the base of the pot
t_{Wall}	Thickness of the pot wall
$V_{\mathrm{e,\,Sd}}$	Design transverse forces due to elastomer pressure
$V_{\mathrm{Fx,\,Sd}}$	Horizontal forces along x axis
$V_{\mathrm{Fxy,\,Sd}}$	Total lateral forces
$V_{\mathrm{Fy,\,Sd}}$	Horizontal forces along y axis
V_{Rd}	Design resistance transverse forces
V_{Sd}	Design transverse forces
V_{u}	Vertical load from ultimate load combinations
V'_{Rd}	Shear resistance within pot walls per unit length
V'_{Sd}	Design shear forces within pot walls per unit length
w	Width of piston face
w_{Ring}	width of the ring
X, Y, Z	Axes of the global system of coordinates
α	Value of contact angle
α_1	Angle of contact obtained from first regression analysis
α_f	Angle of contact obtained from final regression analysis
α_{Perm}	Rotation angle from permanent loads according to EN 1337
α'_{min}	Negative rotation angles caused by variable loads according to EN 1337

$\alpha'_{\max}$	Positive rotation angles caused by variable loads according to EN 1337
$\alpha_{\max}$	Design value of maximum rotation angle according to EN 1337
β_{w}	Correlation factor
Δ	Parameter related to body properties
$\Delta\alpha_2$	Range of rotation angles due to extreme positions of variable loads
Δt_{Pad}	Deflection of elastomer due to rotation
δ_{u}	Vertical deflection due to factored load
γ_{M}	Partial safety factor
γ_{M2}	Connector resistance partial safety factor
γ'	Ratio of vertical to horizontal loads in ultimate limit state
ν	Poisson's ratio
ϕ	Central angle measured positive counterclockwise from the $x-$axis
r'	Equal to $tan(\alpha/4)$ in Persson method
σ_{s}	Stress due to hydrostatic pressure
σ_{u}	Ultimate tensile strength
σ_{xx}	Principal stress in x direction
σ_{yy}	Principal stress in y direction
σ_{zz}	Principal stress in z direction
γ	Factor of contact pressure

CHAPTER 1

INTRODUCTION

1.1 Problem statement

Bridges are one of the first structures built in human history. According to statistics, considerable number of bridges are deficient in Canada. Some part of this deficiency may be due to the use of bridge bearings. Elastomeric pot bearings, which were developed in Europe in the early 1960s, are the most common type of bridge bearings used to support a bridge superstructure and accommodate its movements independently from supporting elements, i.e. piers and abutments. These bearings are part of High Load Multi-Rotational bearings with the ability to transmit large force demands from superstructure to substructure and to accommodate rotation about any horizontal axis as a function of the applied loads. EPBs have usually been designed according to a mix of empirical and theoretical procedures.

Different standards, specifications and codes of practice have focused on the design of pot bearings such as the European Standard EN 1337-5 (EN 2005), AASHTO LRFD bridge design specifications (AASHTO 2012), NCHRP Report 432 (NCHRP 1999) and Canadian Highway Bridge Design Code (CAN/CSA 2006). Some of the rules prescribed by these codes and guidelines were validated by experimental tests, and others are only based on theoretical considerations, engineering judgment or in-house practice of various bearing manufacturers. Very often, the rationale behind some of these design rules is unclear and a detailed study to clarify the underlying assumptions in these documents is essential for the practicing engineer.

The investigation of the behaviour of EPBs requires advanced modeling analysis techniques dictated by the presence of the elastomeric pad, which is a highly nonlinear incompressible material, coupled to the complex mechanisms involving nonlinear contact interactions between different parts of EPBs. Such advanced analyses are usually expertise demanding and time-consuming, which mainly explains the lack of published research in this field. Also by performing an advanced finite element modeling of numerous pot bearings, the assumptions stated in the specifications mentioned can be studied further and a numerical method to estimate design parameters may be developed.

1.2 Objectives

The main objective of this research is to investigate structural performance of fixed pot bearings (EPBs) through finite element modeling and analytical formulations of pot bearings. This objective is achieved through finite element analysis of pot bearings while adopting some simplifying assumptions under different values of applied loadings. The second objective of this research project is to prepare a detailed literature review related to the development and use of EPBs. This step is taken due to lack of a coherent document that focuses on the most reliable methods specified in different design specifications and discusses the rationale behind them. The results of this research can be used to modify pot bearing design using the equation developed in this thesis to estimate contact angle between bearing parts.

1.3 Methodology

One of the main objectives of this research project is to provide a coherent literature review on different aspects of pot bearings. Numerous sources were consulted such as library databases, journal articles, conference papers, standards and guidelines, and available technical reports. The internship at the industrial partners provided valuable information on various design and manufacturing procedures. The first objective of the research program was fulfilled by covering the following information regarding pot bearings :

- Introduction to main parts of an a fixed pot bearing and their fundamental mechanical functions ;
- Mechanical and geometrical properties of pot bearings ;
- Review of standards, specifications and design guidelines of pot bearings.

The literature review shows that some of the existing rules concerning design of EPBs were validated by experimental testing while others were based on some theoretical contact considerations which need to be studied further. These theoretical contact formulations are then applied to some case studies and the results are compared to those obtained from finite element modeling. This step is taken to verify the accuracy of the results obtained from the software. By referring to the literature review, the steps that should be followed to design pot bearings according to various specifications are highlighted.

In the second part of the research project, 3D finite element models of actual pot bearings are built and the assumptions used to generate the finite element models are discussed. Since preparing and running finite element model of a pot bearing is a very time consuming due to nonlinear behaviour of the elastomeric pad and complexities of 3D contact modeling between piston and the pot, as the next step a simplified finite element model is developed which includes disk and ring. The accuracy of the disk and ring model is examined by comparing the

contact angle obtained from both finite element models. Then numerous finite element models were generated for various loading and geometrical properties for disk and ring model. The type of mesh chosen was optimized so that it provided accurate results and at the same time reduced computational burden. To achieve the most acceptable results, some of the prepared models had to be modified and run again. Then, due to the importance of distribution of contact forces between piston and pot, the angle of contact through which these forces were distributed was obtained manually for each model.

After obtaining the angle of contact values from numerical modeling of disk and ring models, a parametric regression analysis was performed on the results. In this analysis the effective parameters in contact values between disk and the ring were selected from numerical modeling and Persson method (as an accurate method for 2D contact problem of a disk and an infinite ring) and the regression analysis was performed in two steps. In the first step angle of contact of α_1 was obtained from regression analysis of models with one constant parameter. In the second step, the final angle of contact of α_f was obtained from performing regression analysis on all the numerical results. After presenting an angle of contact in terms of the available variables, the equations in specifications which consider angle of contact as $180\,^\circ$ can be modified to the value obtained from parametric regression analysis.

1.4 Contents of the thesis

This thesis is organized as follows

- Chapter 1 presents the problem statements, objectives of the research and the methodology followed ;
- Chapter 2 presents a literature review on EPBs and the important guidelines and codes to design pot bearings ;
- Chapter 3 focuses on verifying finite element modeling with analytical contact formulations ;
- Chapter 4 presents design steps according to the specifications as a continuous procedure ;
- Chapter 5 focuses on generation of finite element models and parametric regression analysis on contact angles ;
- Chapter 6 provides a conclusion of the research project and discusses the results.

CHAPTER 2

LITERATURE REVIEW

2.1 Introduction

Bridge infrastructure is aging rapidly, with a large number of bridges exceeding their service life, and many of which being structurally or functionally deficient (Alampalli et al. 2002 ; Gagnon and Gaudreault 2011 ; Nystrom et al. 2003). A bridge bearing is a crucial component having a lifetime generally much less than that of the bridge itself. Therefore, a considerable number of deficiencies in bridges is due to bearing malfunction. A widely used type of bridge bearings are pot bearings with confined elastomeric pads, which were developed initially in Europe in the early 1960s (Atkinson 1991). These bearings are used to support bridge superstructure and accommodate its movements independently from the supporting elements, i.e. piers and abutments.

Pot bearings are part of High Load Multi-Rotational bearings since they can (i) transmit large force demands from the superstructure to the substructure, and (ii) accommodate rotation about any horizontal axis as a function of the applied loads. This type of bearings can also accommodate translational movements when coupled with a PTFE (Polytetrafluoroethylene) layer and stainless steel slider. Pot bearings have usually been designed according to a mix of empirical and theoretical procedures.

Failures of first generation pot bearings raised the need for more firm design specifications and guidelines. The first technical documents were produced without extensive practical research and little data describing the complexities of the behavior of pot bearing components such as the elastomeric pad was available. Critical issues related to the efficiency of sealing and lubrication were not addressed appropriately. Past experience has shown that clear and detailed specifications are necessary for the production of high quality bearing devices while ensuring minimum uniform standards common to design engineers, manufacturers and bridge inspectors. Such standardization of production techniques was expected to lead to consistent quality and reduced costs (Atkinson 1991). As such, different standards, specifications and codes of practice have focused on the design of pot bearings such as the European Standard EN 1337-5 (EN 2005), American Association of State Highway and Transportation-AASHTO (AASHTO 2012) and the NCHRP Report 432 (NCHRP 1999). Some of the rules prescribed by these codes and guidelines were validated by experimental tests, and others are only based on theoretical considerations, engineering judgment or in-house practice of

various bearing manufacturers. Very often, the rationale behind some of these design rules is unclear and should be understood to assure that the design still meets current engineering needs. The investigation of the structural behavior of pot bearings requires advanced modeling analysis techniques dictated by the presence of the elastomeric pad, which is a highly nonlinear incompressible material, coupled to the complex mechanisms involving nonlinear contact interactions between the different parts of pot bearings. Such advanced analyses are usually expertise-demanding, time-consuming and usually manufacturer's proprietary, which can explain the lack of published research in this field.

The main objective of this chapter is to provide a detailed literature review on the mechanical behaviour of fixed pot bearings and their design guidelines.

2.2 History of contact problem

One of the most important disciplines of engineering science is contact mechanics and physics of friction. They have numerous applications in civil engineering such as bearings and hinges. The problem of contact mechanics depends on various conditions such as existence of lubrication and material specifications (Popov, 2010).

Contact stresses are caused by pressure of one solid on another over limited areas of contact. In some cases contact stresses have significant values and are of high importance since the stresses on or beneath the surface of the contact is the major cause of failure of one or both of the bodies (Boresi et al. 1978). In contact problems (such as the case of bridge pot bearings) the contact between the elements does not remain in fixed conditions since stresses are often cyclic in nature and are repeated several times which may lead to fatigue failure starting from local fractures. Thus these stresses may limit the load carrying capacity of the members (Boresi et al. 1978).

Over the years, several researchers have tried to solve the problem of contact between two bodies. Classical contact mechanics is one of the most reliable results of studying contact problems between two materials which is associated to Heinrich Hertz. He has solved the problem of finding principal contact stresses between two elastic bodies with smooth and continuous surfaces in 1882 with a satisfactory solution by assuming the contact area is small compared to the dimensions of the bodies (non conforming), the frictional forces in the contact area can be ignored and that the contact area is infinitely long in one direction (elastic half-space) (Popov, 2010 ; Johnson 1985).

After presentation of Hertz contact theory, several researchers focused on solving contact problems for which the assumptions made in Hertz method are not satisfied. For example as conforming surfaces, case of two dimensional contact of a cylindrical pin in a hole with

slightly larger radius was studied by Allan Persson who managed to provide a complex solution for contact angle in 1964 (Persson 1964 ; Ciavarella 2001 ; Johnson 1985). Goodman and Keer studied contact problem of a frictionless sphere in a conforming cavity with a slightly larger radius in 1965, (Roark et. al 1989 ; Johnson 1985). Also instead of assuming contact area to be infinitely long along one direction Flynn and Roll studied contact problem for a very short cylinder and a plate having a width less than five or six times that of the contact area (Roark et. al 1989 ; Flynn and Roll 1967). Regarding to effects of friction in at the interface of two non-conforming bodies it is proved that this factor plays a part only if the material of the elastic bodies are different (Johnson 1985). If the materials of the two solids are dissimilar, the tangential displacements will be different too. This leads to slip between the bodies (Johnson 1985).

The contact conditions in a pot bearing can be represented as contact between a disk and a ring with finite width. In the context of this research the attention was directed to Hertz and Persson method to solve contact problem between two cylindrical bodies. This is due to the fact that the assumptions made in these theories correspond well to the requirements of a pot bearing comparing to those defined in other procedures.

2.3 Basic definitions of pot bearings

Pot bearings are generally used when there is a demand of longer spans and higher loads while the number of girders is to be minimized (AASHTO/NSBA 2004 ; NCHRP 1999). This type of bearing can accommodate movements which may be either translational, rotational or both. A basic pot bearing can permit rotation but no translation. However, translational movements can be accommodated easily too by introducing PTFE stainless steel sliders. The direction of the translational movement can be controlled by using guide bars (NCHRP 1999 ; Valvezan and Farhangi 1996). Fig. 2.1 illustrates a typical pot bearing consisting of an elastomeric pad confined within a cylindrical shallow container called pot while pressured by a flat plate called piston.

A pot bearing transmits horizontal and vertical loads from the superstructure to the bridge supports, i.e. piers and/or abutments. For this purpose, the elastomer pad acts like a fluid in a hydraulic cylinder transmitting the load from superstructure through the piston plate to the pot base and walls. This load is finally transferred from the pot to the pier or abutment (Roeder and Stanton 1998 ; Valvezan and Farhangi 1996). The base of the pot may rest on a masonry plate and a bedding layer, or is occasionally directly placed on the pier or abutment (Roeder and Stanton 1998). The fixed pot bearing illustrated in Fig. 2.1 can permit rotational movements. However in order to accommodate horizontal mo-

vements, a PTFE slider can be fixed to the top of the piston plate which allows the bearing to slide against a sole plate while the direction of sliding can be controlled using guiding bars (Valvezan and Farhangi 1996).

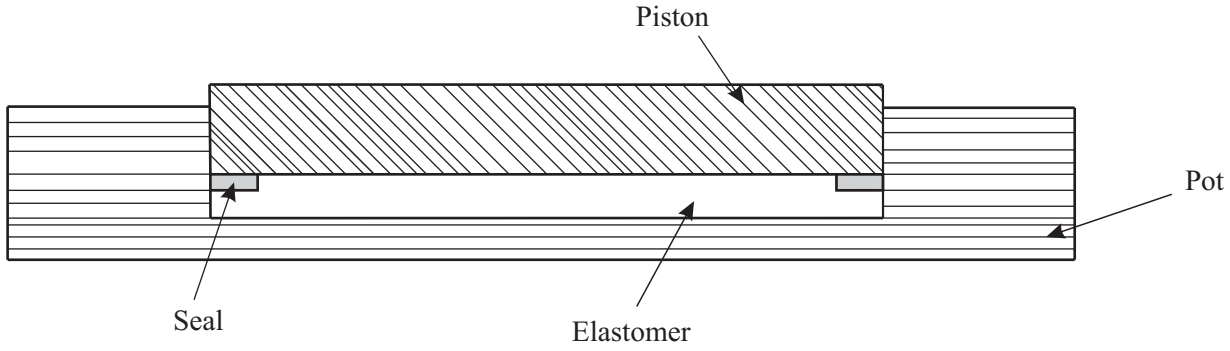

FIGURE 2.1 Principal elements of a fixed EPB

2.4 Material specifications of pot bearings

The material used for different parts of a pot bearing depends on the specification used for designing the pot to satisfy specific requirements. Some of these requirements include resistance, durability, weldability and operating temperatures for piston and pot, stiffness and and resistance to wear and abrasion for elastomeric pad and frictional resistance, effect on escape of elastomer and resistance to wear for sealing rings (EN 2005 ; NCHRP 1999).

Regarding to material of the pot, it is usually made of either structural carbon, stainless steel or aluminum (Steel Bridge Bearing and Design Guide 2011) among which stainless steel is the most popular considering corrosion resistance, durability and weldability requirements (Roeder and Stanton 1998).

Until now various types of elastomers have been used in bridge applications, such as neoprene, butyl rubber and urethane. However, the most common elastomers are by far natural rubber which is commonly used in UK and Switzerland and neoprene which is more popular in France and Germany (Muscarella 1995 ; Roeder and Stanton 1998). In comparison with natural rubber, neoprene has better resistance to deterioration in the presence of oil, ozone and other agents (Agrawal et al. 2005 ; Roeder and Stanton 1998). However when subjected to vertical forces, it exhibits outward bulging which restricts the height of a neoprene pad to be used effectively for transferring vertical loads (Agrawal et al. 2005). On the other hand, natural rubber generally costs less and appears to be less susceptible to low temperature stiffening than neoprene (Muscarella 1995 ; Roeder and Stanton 1998).

The internal seals can be made of different materials such as brass, polyoxymethylene-delrin (POM), carbon filled PTFE and stainless steel. In the first pot bearings use of PTFE seals was very common since they are cheaper than brass and create less frictional resistance to the rotation of the piston. However, it became clear that elastomer leaked through them relatively easily (Roeder and Stanton 1998). Brass sealing rings are one of the most common internal seals used today. They may either be flat or have a circular cross section. Brass rings with a solid circular cross section provide a tight seal but may experience wear during cyclic rotation. However, their long-term performance can be improved by reducing friction and wear of the rings. On the other hand flat brass rings are more susceptible to leakage and ring fracture, but they behave less severe wear. To improve ring performance, use of heavier flat brass rings has been suggested (NCHRP 1999).

POM sealing ring include individual beads which snap together and form a closed chain which is vulcanized. Comparing to brass rings they are deeper and friction between seal and the pot wall appears to be less which reduces resistance to rotation (Roeder and Stanton 1998).

2.5 Design criteria for pot bearings

In this section, important design criteria of pot bearings according to the most reliable specifications including European Standard EN 1337-5 (EN 2005), American Association of State Highway and Transportation - AASHTO (AASHTO 2012) and Canadian Highway Bridge Design Code (CAN/CSA 2006) are presented. The general design method of fixed pot bearings according to these codes remains the same which includes determining design parameters of pad, pot and piston. However the rationales behind these specifications to design each element are different. In the next sections the assumptions and methods of designing principal elements of a pot bearing according to each of these specifications will be discussed.

2.5.1 Rotation limitations

Rotations of a bridge deck with respect to its supports under the effect of dead or live loads causes the rotation of the piston plate, thus generating a non-uniform pressure on the elastomeric pad which deforms accordingly. We denote by $\alpha_{\max}$ the design angle corresponding to the maximum rotation under the combined effects of dead and live loads. In addition to the effects of applied loads, AASHTO (2012) requires that the limiting value of $\alpha_{\max}$ should account for : (i) maximum rotation caused by fabrication and instrumentation tolerances, taken as 0.005 rad or less if justified by an approved quality control plan, and (ii) allowance for uncertainties, taken as 0.005 rad or less if justified by an approved quality control plan.

Regarding to rotation limitation, EN 1337-5 requires that maximum rotation should take into account rotations due to permanent loads as well as the variable loads. The following angles can be defined to assess such rotations which may originate from permanent or variable loads :

- the rotation angle α_{Perm} caused by permanent loads,
- the minimum rotation angle $\alpha'_{\min}$ caused by variable loads,
- the maximum rotation angle $\alpha'_{\max}$ caused by variable loads,
- rotation angle due to extreme positions of variable loads $\Delta\alpha_2$ which can be obtained from sum of $\alpha'_{\min}$ and $\alpha'_{\max}$.

  According to the experimental results, this rotation due to traffic and temperature effects is in order of 0.005 rad (Gase 2011) which is also the limiting bound for rotation angle due to extreme position of variable loads according to EN 1337-5.

  According to EN 1337-5 another criteria that should be considered regarding to the variable rotations is the accumulated slide path of $S_{\text{A, d}}$ generated from variable rotations in a pot bearing which effects durability of the internal seals.

  As illustrated in Fig. 2.2, the accumulated slide path in a pot bearing due to variable rotation when one vehicle is moving can be obtained as $\Delta\alpha_2 \dfrac{d_{\text{Pad}}}{2}$. By Assuming that n_{v} number of lorries pass the bridge during the intended life of the bearing, accumulated slide path generated from variable rotation can be obtained from

$$S_{\text{A, d}} = n_{\text{v}}\, \Delta\alpha_2\, \frac{d_{\text{Pad}}}{2} \tag{2.1}$$

  The accumulated slide path of the bearing obtained from Eq. (2.1) should not exceed the one obtained from experimental testing (S_{T}), as specified in annex E-EN 1337-5 multiplied by the correcting factor of c. This factor is applied due to the fact that in a bridge bearing accumulated slide path is performed in much more severe conditions than that of experimental testing (due to high velocity of cyclic rotations and constant

value of rotations in testing conditions) (Marioni 2006)

$$S_{\mathrm{A,d}} \leqslant cS_{\mathrm{T}} \tag{2.2}$$

where

– $S_{\mathrm{A,d}}$ is the accumulated slide path of the bearing (mm),
– d_{Pad} is the diameter of elastomer (mm),
– n_{v} is the number of vehicles moving along the bridge during intended life of bearing,
– c is the correction factor to take account of difference between the constant amplitude of slide path prescribed in the tests (annex E of EN 1337-5) and the variable amplitude movements which actually occur in traffic conditions,
– S_{T} is the accumulated slide path derived from testing in accordance with annex E of EN 1337-5 (mm),

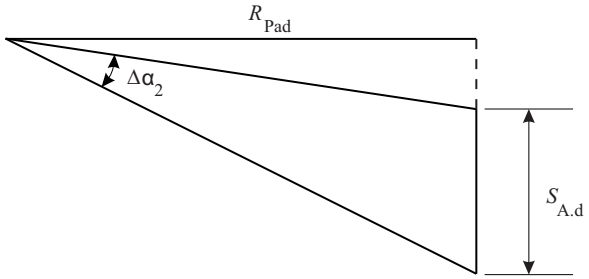

FIGURE 2.2 Representation of sliding path due to $\Delta\alpha_2$

– α_{max} is the maximum rotation (rad) caused by both permanent and variable loads which should not exceed 0.03 rad according to EN 1337-5.

$$\alpha_{\mathrm{max}} = \alpha_{\mathrm{Perm}} + \alpha'_{\mathrm{max}} \tag{2.3}$$

Fig. 2.3 presents rotations caused permanent and variable loads.

2.5.2 Horizontal load distribution

In the specifications, it is assumed that the elastomeric pad has hydrostatic characteristics under pressure. Also, the pressure between piston and pot walls resulting from external horizontal actions is assumed to be parabolically distributed over half of the perimeter of the pot. For this reason, the maximum value of this pressure is taken as 1.5 times its mean value as will be shown next.

For clarity, the case of a pot bearing subjected to a horizontal load along the x direction is considered as illustrated in Fig. 2.4. Assuming that the distribution of horizontal forces P

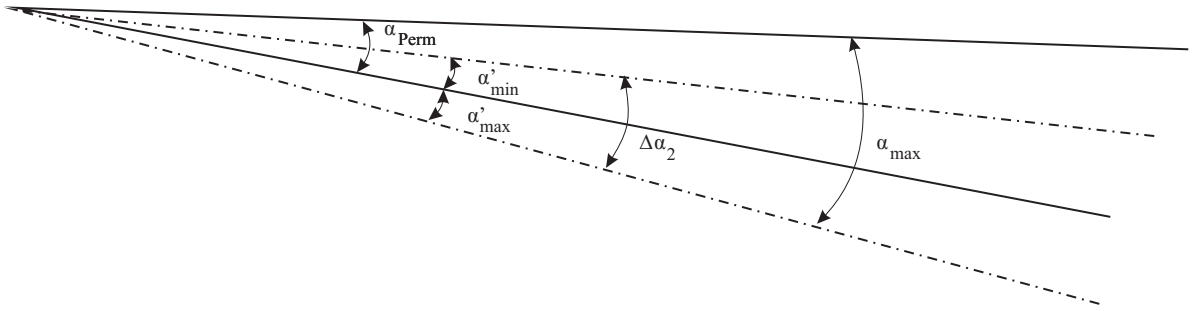

FIGURE 2.3 Representation of rotation angles

transferred from the piston to the pot per unit thickness follows a parabolic shape as shown in Fig. 2.4, the resulting total horizontal force can then be expressed as

$$V_{\mathrm{Fx,\,Sd}} = \int_{-r_{\mathrm{Pad}}}^{r_{\mathrm{Pad}}} P(x)\,\mathrm{d}x \tag{2.4}$$

or

$$V_{\mathrm{Fx,\,Sd}} = 2\int_{0}^{\frac{\pi}{2}} P(\phi)\,\mathrm{d}\phi \tag{2.5}$$

where r_{Pad} is the interior radius of the pot, x is the coordinate along the diameter axis of the pot parallel to the direction of applied horizontal load and ϕ is a central angle measured positive counterclockwise from the $x-$axis. Considering the boundary conditions

$$P(x) = 0 \text{ at } x = -r_{\mathrm{Pad}}\,; \qquad P(x) = 0 \text{ at } x = r_{\mathrm{Pad}}\,; \qquad P(x) = P_0 \text{ at } x = 0 \tag{2.6}$$

we can write

$$P(x) = -\frac{P_0}{r_{\mathrm{Pad}}^2}\,x^2 - P_0 \tag{2.7}$$

We also have

$$x = r_{\mathrm{Pad}}\,\sin(\phi)\,; \qquad \mathrm{d}x = r_{\mathrm{Pad}}\,\cos(\phi)\,\mathrm{d}\phi \tag{2.8}$$

Eq. (5.4) becomes then

$$V_{\mathrm{Fx,\,Sd}} = 2\int_{0}^{\frac{\pi}{2}} \left[-P_0\left(\frac{r_{\mathrm{Pad}}^2\sin^2(\phi)}{r_{\mathrm{Pad}}^2} - 1\right)\right] r_{\mathrm{Pad}}\cos(\phi)\,\mathrm{d}\phi \tag{2.9}$$

$$= \frac{4}{3}\,P_0 r_{\mathrm{Pad}} \tag{2.10}$$

yielding

$$P_0 = 1.5\,\frac{V_{\mathrm{Fx,\,Sd}}}{d_{\mathrm{Pad}}} \tag{2.11}$$

where $\dfrac{V_{\mathrm{Fx,\,Sd}}}{d_{\mathrm{Pad}}}$ represents the mean value of horizontal forces per unit thickness along the diameter. In the general case, the total lateral forces $V_{\mathrm{Fxy,\,Sd}}$ due to applied horizontal loads along any direction can be obtained as

$$V_{\mathrm{Fxy,\,Sd}} = \sqrt{V^2_{\mathrm{Fx,\,Sd}} + V^2_{\mathrm{Fy,\,Sd}}} \tag{2.12}$$

where $V_{\mathrm{Fx,\,Sd}}$ and $V_{\mathrm{Fy,\,Sd}}$ are the resulting forces along x and y directions, respectively. This

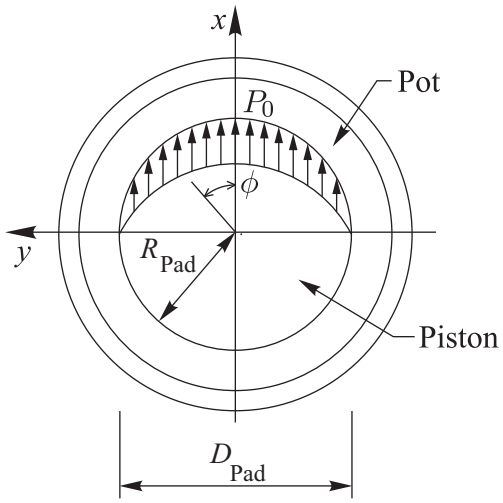

FIGURE 2.4 Representation of horizontal forces

is also denoted that in previous versions of EN 1337, distribution of applied horizontal loads was assumed to have cosine shape. Thus factor of 1.5 in Eq. (2.11) changes to 1.3 for cosine distribution of contact forces.

2.5.3 Elastomeric pad

After determining the maximum rotations in a pot bearing, thickness and diameter of the elastomeric pad can be determined from the allowable pressure induced on the pad from applied vertical loads as well as pad deflection limit as discussed further.

Allowable pressure on pad

According to the early work in Germany and physical test results, European designs were usually based on allowable pressure of 25 MPa exerted on the elastomeric pad and a pad diameter to thickness ratio of about 16. The stress limit of 25 MPa mentioned in the early European designs appears to be appropriate since this value was a common concrete bearing stress at the early years of development of pot bearings (Roeder and Stanton 1998). This upper limit is also retained for the current version of AASHTO due to satisfactory bearing performance except a few seal failures. However, this stress limit is specified as 40 MPa in CHBDC.

Comparing to these specifications EN 1337-5, relates the allowable stress on the pad to its contact strength properties ($f_{\mathrm{e,k}}$). This means that the design axial force of the elastomeric pad (N_{Sd}) has to be less than or equal to axial resistance of the pad (N_{Rd}), i.e.

$$N_{\mathrm{Sd}} \leqslant N_{\mathrm{Rd}} \tag{2.13}$$

The value of N_{Rd} can be obtained as

$$N_{\mathrm{Rd}} = \frac{N_{\mathrm{Rk}}}{\gamma_{\mathrm{M}}} \tag{2.14}$$

and

$$N_{\mathrm{Rk}} = \frac{\pi}{4} d_{\mathrm{Pad}}^2 f_{\mathrm{e,k}} \tag{2.15}$$

where

- N_{Rk} is the characteristic value of resistance of the elastomeric pad
- $f_{\mathrm{e,k}}$ is the characteristic contact strength of the elastomer which is a statistically-based material property (ASTM 2012). According to EN 1337-5 for pot bearings this value is equal to 60 MPa and is limited by the effectiveness of seal to prevent extrusion of elastomer between piston and pot wall.
- γ_{M} is a partial safety factor. In EN 1337, the recommended value of this factor is equal to 1.30. For this parameter characteristic values of uncertain loads and resistances are specified and partial safety factors are applied to ensure safety of the structure. Partial safety factors are usually based on experience or calibrated to existing codes or to measures of the reliability obtained from probabilistic techniques (Sorensen 2011).

Thickness of the pad

The minimum thickness requirement of elastomeric pad is of high importance due to its influence on rotation capacity of the bearing. Generally rotation capacity of the bearing can be increased by using a thicker pad. According to the specifications dimensions of elastomeric pad should be such that under the characteristic combination of the applied actions the total rotation of $\alpha_{\max}$ does not cause a deflection of Δt at the perimeter more than 15 percent of the pad thickness ($\Delta t \leqslant t \times 0.15$). This strain limit is based more on past practice than the research results (NCHRP 1999) which prevents seal from escaping and the bearing from locking up. To comply with this requirement, the specifications state that the minimum thickness of an elastomeric pad shall be obtained from

$$t_{\mathrm{Pad}_{min}} = 3.33\,\alpha_{\max}\,d_{\mathrm{Pad}} \tag{2.16}$$

where $t_{\mathrm{Pad}_{min}}$ is the minimum thickness of the elastomer (mm).

Eq. (2.16) finds its justification in what follows,

The value of deflection due to elastomer rotation of $\alpha_{\max}$ can be determined as

$$\Delta t_{\mathrm{Pad}} = \frac{d_{\mathrm{Pad}}}{2}\,\tan(\alpha_{\max}) \tag{2.17}$$

Another criterion specified in European Standard EN 1337-5 is

$$\Delta t_{\mathrm{Pad}} \leqslant 0.15\,t_{\mathrm{Pad}} \tag{2.18}$$

Eqs. (2.17) to (2.18) result in

$$t_{\mathrm{Pad}} \geqslant \frac{10}{3}\,\alpha_{\max}\,d_{\mathrm{Pad}} \approx 3.33\,\alpha_{\max}\,d_{\mathrm{Pad}} = t_{\mathrm{Pad}_{min}} \tag{2.19}$$

In addition according to EN 1337-5 the pad thickness should not be less than $d_{\mathrm{Pad}}/16$.

2.5.4 Piston

Corresponding to piston design, the main difference between EN 1337-5 and AASHTO is in the type of piston wall. According to EN 1337-5 the designer can choose from two types of contact surface for the piston, (i) flat contact surface or (ii) curved contact surface. Also in AASHTO it is stated that contact rim may be cylindrical or spherical. However there is no indication regarding to the diversity in design procedure for the two types.

Flat contact surface

According to EN 1337-5 designing piston wall as flat is allowed when the width of the piston w is less than 15 mm. Also design value of transverse force and should be less than the resistance force. To satisfy this requirement, maximum pressure from the applied horizontal loads (which has a parabolic distribution as discussed in section 2.5.2) should be less than the yielding stress of the material used or in other words

$$\frac{P_0}{w} \leqslant \frac{F_\mathrm{y}}{\gamma_\mathrm{M}} \tag{2.20}$$

where w is the width of piston face as illustrated in Fig. 5.1. Using Eq. (2.11) yields

$$\frac{1.5\, V_{\mathrm{Fxy,\,Sd}}}{d_\mathrm{Pot}\, w} \leqslant \frac{F_\mathrm{y}}{\gamma_\mathrm{M}} \tag{2.21}$$

This equation can also be written as

$$w \geqslant \frac{1.5 V_{\mathrm{Fxy,\,Sd}} \gamma_\mathrm{M}}{d_\mathrm{Pot} F_\mathrm{y}} \tag{2.22}$$

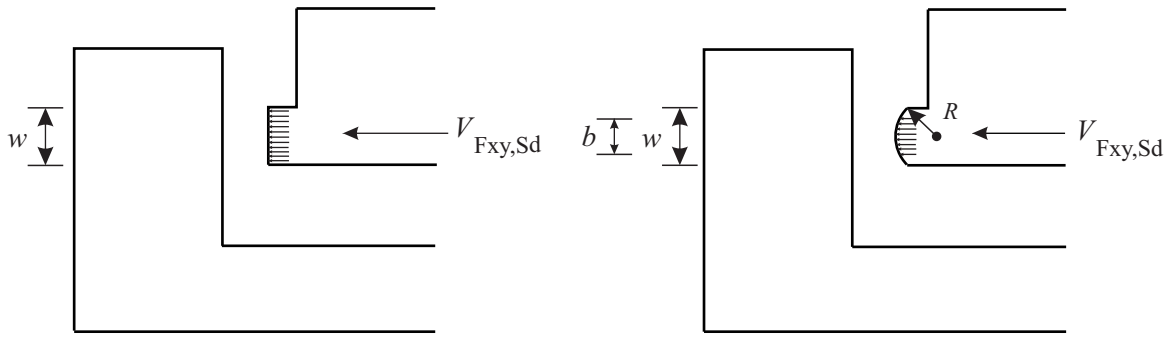

FIGURE 2.5 Flat and curved contact surface

The requirement for width of piston face according to AASHTO is similar to Eq. (2.22)

$$w \geq \frac{1.5 V_{\mathrm{Fxy,\,Sd}}}{d_\mathrm{Pot} F_\mathrm{y}} \tag{2.23}$$

also in CHBDC, contact area is assumed as 0.33 $w d_\mathrm{Pad}$ instead of $w d_\mathrm{Pad}$. According to CHBDC and AASHTO the following limit bounds for this parameter should be respected regarding to width of piston face,

$$w \geqslant 3\,\mathrm{mm} \tag{2.24}$$

$$w \geqslant 0.03\ d_{\mathrm{Pot}} \tag{2.25}$$

In CHBDC limit bound of 3 mm is replaced with 6 mm.

Curved contact surface

According to EN 1337, the radius of the curved contact surface should satisfy the following criterion

$$R \geqslant \max(0.5\, d_{\mathrm{Pot}}, 100) \tag{2.26}$$

Similar to the case of flat contact surface, design transverse forces shall be less than resistance of the curved contact surface to transverse forces, i.e.

$$V_{\mathrm{Sd}} \leqslant V_{\mathrm{Rd}} \tag{2.27}$$

where

$$V_{\mathrm{Rd}} = \frac{15 F_{\mathrm{u}}^2\, R\, d_{\mathrm{Pot}}}{E_{\mathrm{d}}\, \gamma_{\mathrm{M}}^2} \tag{2.28}$$

in which, as illustrated in Fig. 5.1

- R is the radius of contact surface
- F_{u} is the ultimate strength of the material
- E_{d} is design modulus of elasticity
- d_{Pot} is the internal diameter of the pot.

Eq. (2.28) is based on Hertz theory of contact between a flat and a cylindrical surface. The ability of curved surfaces and plates to withstand deformation under applied loads is dependent upon the hardness of materials from which they are made. As it is clear there is not a constant relationship between hardness and yield stress of the material contrary to ultimate strength. Therefore, Eq. (2.28) is based on ultimate strength of the material assuming Hertz contact conditions apply (Johnson 1985)

- The strains are small and within the elastic limit
- Each body can be considered an elastic half-space, i.e., the area of contact is much smaller than the characteristic radius of the body
- The surfaces are continuous and non-conforming, and
- The surfaces are frictionless.

According to Hertz theory, if two cylinders with radii r_1 and r_2, made of the same material with Youn modulus E_{d}, and Poisson's ratio $\nu = 0.3$, are in contact as illustrated in Fig. 3.2,

then the resulting pressure can be obtained as (Srinath 2009)

$$p = 0.418\sqrt{\frac{F\,(r_1 + r_2)\,E_\mathrm{d}}{r_1\,r_2}} \tag{2.29}$$

where F is the force applied per unit length of the cylinder. In a pot bearing with curved piston wall contact takes place between a cylinder with radius of r and a plane surface. Therefor Eq. (2.29) changes to (Srinath 2009)

$$p = 0.418\sqrt{\frac{F E_\mathrm{d}}{r}} \tag{2.30}$$

In the previous edition of EN 1337, contact stress was limited to 1.75 times the ultimate tensile strength σ_u to limit the deformation of the pot and the piston to an acceptable level (Lee 1994). However as a conservative assumption contact stresses are limited to $2F_\mathrm{u}$ in the latest version of EN 1337-5. considering that $F = P_0$,

$$0.418\,\sqrt{P_0\,E\,\frac{1}{r}} = 2\,\sigma_\mathrm{u} \tag{2.31}$$

where

$$\sigma_\mathrm{u} = \frac{F_\mathrm{u}}{\gamma_M} \tag{2.32}$$

Eq. (2.28) can be obtained.

Also according to EN 1337, piston and pot contact width for a bearing with curved piston wall Fig. 5.1 can be obtained from

$$b = 3.04\sqrt{\frac{1.5V_{\mathrm{Fxy,\,Sd}}\,r}{E_\mathrm{d}\,d_\mathrm{Pot}}} \tag{2.33}$$

By referring to the case of two cylinders in contact and assuming that contact takes place approximately along a straight line element before loads are applied, the semi-major axis of area will be infinitely large, therefore the semi-minor axis of area will be considered as the radius of contact. In this case, contact width can be calculated from Hertz theory for 2D contact between two cylinders (Boresi et al. 1978)

$$\frac{b}{2} = \sqrt{\frac{2P_0\,\Delta}{\pi}} \tag{2.34}$$

If both of the cylinders are made from the same material with modulus of elasticity of E_{d} and Poisson's ratio ν, parameter Δ can be expressed as

$$\Delta = 4\,r\,\frac{1-\nu^2}{E_{\mathrm{d}}} \tag{2.35}$$

Replacing Eq. (2.35) into Eq. (2.34) yields to Eq. (2.33).

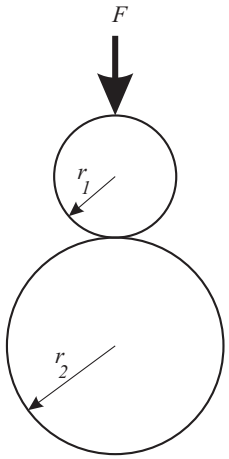

FIGURE 2.6 Two cylindrical bodies in contact

2.5.5 Pot

One of the main differences in design procedure of pot bearings according to AASHTO specifications and European Standard EN 1337-5 is in design of the pot. In AASHTO specifications and CHBDC, design of pot is based on assuming that walls and base of the pot provide sufficient resistance against the bending moments applied and that all the elements of the pot act as a single structural unit. However in EN 1337-5 design procedure of the pot is performed by taking account of the tensile and shear forces due to applied horizontal loads and pressures from the pad rather than bending moments and assuming that base and pot walls act as separate components. On the other hand method of pot design in CHBDC is quite similar to AASHTO specifications.

Pot walls

According to AASHTO specifications if pot bearing is subjected to lateral loads the thickness of the pot wall should satisfy the following condition (AASHTO 2012)

$$t_{\text{Wall}} \geqslant \sqrt{\frac{25 H_{\text{u}}\, \alpha_{\max}}{F_{\text{y}}}} \tag{2.36}$$

This requirement is based on the assumption that applied horizontal loads are carried by bending mechanism while the bursting effects of pot wall from hydrostatic stresses are carried by hoop tension in the wall (NCHRP 1999). Then according to Fig. 2.7 the lever arm of horizontal loads can be obtained from

$$l_{\text{a}} = t_{\text{Pad}} + \alpha_{\max} \frac{d_{\text{Pad}}}{2} + \frac{w}{2} \tag{2.37}$$

and as discussed before,

$$t_{\text{Pad}_{min}} = 3.33\, \alpha_{\max}\, d_{\text{Pad}} \tag{2.38}$$

Considering that the maximum stress in the bearing is 3.5 kips, the vertical load can be obtained from (NCHRP 1999)

$$V_{\text{u}} = 3.5 \frac{\pi d_{\text{Pad}}^2}{4} \tag{2.39}$$

Also by assuming that applied horizontal load is a percentage of the vertical loads

$$H_{\text{u}} = \gamma' V_{\text{u}} \tag{2.40}$$

From equations 2.39 and 2.40 and assuming parabolic distribution of horizontal forces

$$w = \frac{1.5H_{\mathrm{u}}}{d_{\mathrm{Pad}}F_{\mathrm{y}}} = \frac{1.5\gamma' V_{\mathrm{u}}}{d_{\mathrm{Pad}}F_{\mathrm{y}}} = \frac{5.25\gamma' d_{\mathrm{Pad}}}{F_{\mathrm{y}}} \tag{2.41}$$

Then from equations 2.38 and 2.41, Eq. 2.37 changes to

$$l_{\mathrm{a}} = 3.33\,\alpha_{\mathrm{max}}\,d_{\mathrm{Pad}} + \alpha_{max}\frac{D_{Pad}}{2} + 2.625\frac{\gamma' d_{\mathrm{Pad}}}{F_{\mathrm{y}}} = (3.83\,\alpha_{\mathrm{max}} + \frac{2.625\gamma'}{F_{\mathrm{y}}})d_{\mathrm{Pad}} \tag{2.42}$$

By limiting the moments due to applied horizontal loads per unit length to 0.6 times the plastic bending moment strength of pot wall with unit length in circumferential direction we have,

$$\frac{H_{\mathrm{u}}}{d_{\mathrm{Pad}}}l_{\mathrm{a}} \leq 0.6F_{\mathrm{y}}\frac{t_{\mathrm{Wall}}^2}{4} \tag{2.43}$$

Then finally

$$t_{\mathrm{Wall}} \geq \sqrt{\frac{25H_{\mathrm{u}}\,\alpha_{\mathrm{max}}d}{F_{\mathrm{y}}}} \tag{2.44}$$

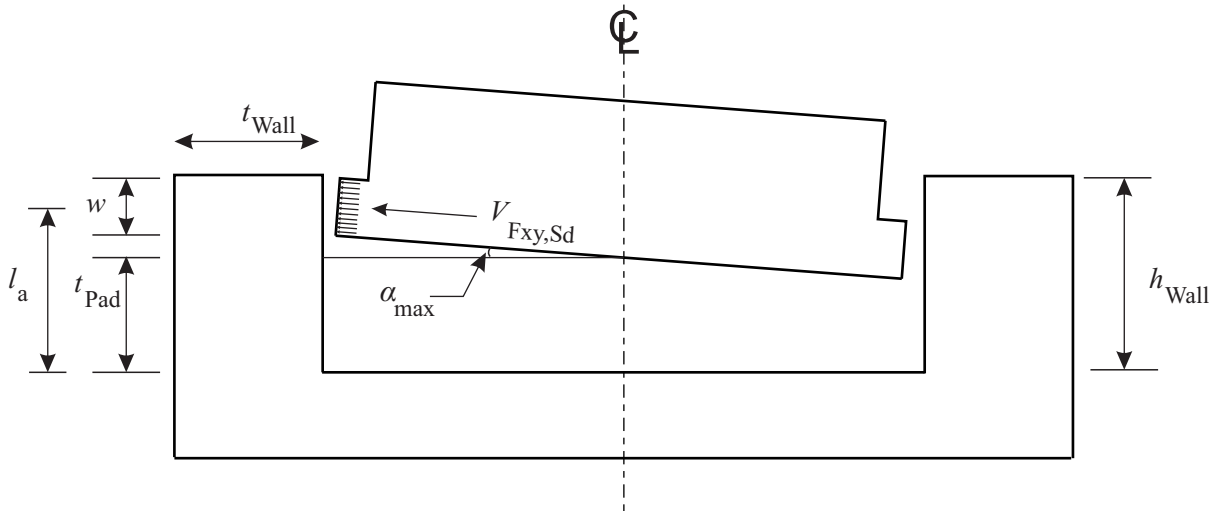

FIGURE 2.7 Lever arm of applied horizontal forces according to AASHTO

Considering Fig. 2.7, after obtaining width of piston face (w), pot cavity depth (h_{Wall}) should respect the following requirement according to AASHTO,

$$h_{\mathrm{Wall}} \geqslant (0.5\,\alpha_{\mathrm{max}}\,d_{\mathrm{Pot}}) + t_{\mathrm{Pad}} + w \tag{2.45}$$

Comparing to AASHTO specification, as mentioned before design method of pot walls according to EN 1337-5 is based on providing sufficient resistance against applied tensile and shear forces to the pot wall rather than bending moment resistance. In EN 1337, the simplified formulae for design of pot bearings consider that the pot walls and the pot base act as separate components at the ultimate limit state (Eggert and Kauschke 2002). The transverse force within pot walls subjected to tensile force have to satisfy

$$V_{\mathrm{Sd}} \leqslant V_{\mathrm{Rd}} \tag{2.46}$$

where V_{Sd} includes the force $V_{\mathrm{e,\,Sd}}$ corresponding to hydrostatic pressure from the elastomeric pad and the lateral load $V_{\mathrm{Fxy,\,Sd}}$ corresponding to applied horizontal forces

$$V_{\mathrm{Sd}} = V_{\mathrm{e,\,Sd}} + V_{\mathrm{Fxy,\,Sd}} \tag{2.47}$$

The force $V_{\mathrm{e,\,Sd}}$ can be obtained as follows. The stress applied to the pot walls due to hydrostatic pressure is given by

$$\sigma_{\mathrm{s}} = \frac{N_{\mathrm{Sd}}}{\pi \, \dfrac{d_{\mathrm{Pot}}^2}{4}} \tag{2.48}$$

According to the Hook stress equation, the transverse force $V_{\mathrm{e,\,Sd}}$ can be obtained as

$$V_{\mathrm{e,\,Sd}} = \frac{N_{\mathrm{Sd}} \, d_{\mathrm{Pot}} \, t_{\mathrm{Pad}}}{\pi \, \dfrac{d_{\mathrm{Pot}}^2}{4}} = \frac{4 N_{\mathrm{Sd}} \, t_{\mathrm{Pad}}}{\pi d_{\mathrm{Pot}}} \tag{2.49}$$

The design resistance transverse force of V_{Rd} corresponds to the design stresses within the pot, which shall not exceed the design value of the yield strength F_{y} at any section of the pot wall. The force V_{Rd} can then be obtained as

$$V_{\mathrm{Rd}} = \frac{F_{\mathrm{y}} \, A_{\mathrm{R}}}{\gamma_{\mathrm{M}}} \tag{2.50}$$

where A_{R} is twice the area of the cross-section of the pot wall given by

$$A_{\mathrm{R}} = (D_{\mathrm{Pot}} - d_{\mathrm{Pot}}) h_{\mathrm{Wall}} \tag{2.51}$$

According to EN 1337-5, determination of shear forces applied to pot walls from pad pressures and applied horizontal loads reformulate applied load per unit height of pot walls.

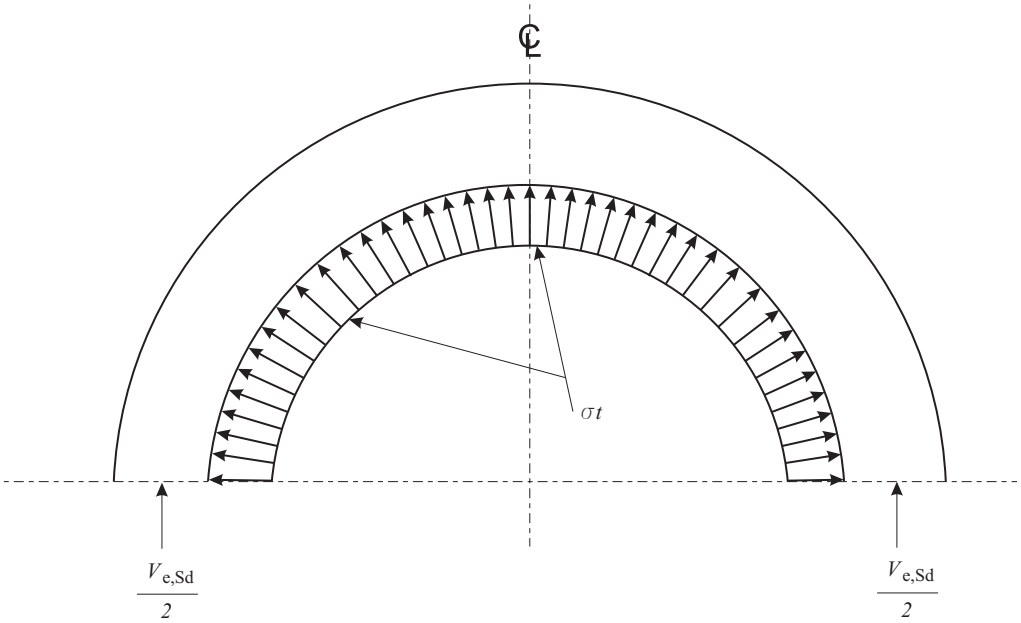

FIGURE 2.8 Representation of elastomer pressure on pot wall

Therefore, the design shear forces within pot walls have to satisfy the following relationship

$$V'_{\mathrm{Sd}} \leqslant V'_{\mathrm{Rd}} \tag{2.52}$$

where

$$V'_{\mathrm{Sd}} = \frac{V_{\mathrm{e,\,Sd}} + 1.5V_{\mathrm{Fxy,\,Sd}}}{d_{\mathrm{Pot}}} \tag{2.53}$$

According to distortion energy theory (Bhandari 2010), the yield strength in shear is $\frac{1}{\sqrt{3}}$ times the yield strength in tension. Then, the shear resistance V'_{Rd} of a pot wall per unit height can be obtained as

$$V'_{\mathrm{Rd}} = \frac{F_{\mathrm{y}}\,\dfrac{A_{\mathrm{R}}}{2}}{\gamma_{\mathrm{M}} h_{\mathrm{Wall}}\sqrt{3}} \tag{2.54}$$

where A_{R} was given by Eq. (2.51). Replacing into Eq. (2.54) yields

$$V'_{\mathrm{Rd}} = \frac{F_{\mathrm{y}}(D_{\mathrm{Pot}} - d_{\mathrm{Pad}})}{2\,\gamma_{\mathrm{M}}\sqrt{3}} \tag{2.55}$$

Thus According to EN 1337, by providing sufficient pot wall resistance against applied shear and tensile forces the limit bounds for h_{Wall} and D_{Pot} will be obtained.

Pot base

To determine thickness of pot base, AASHTO and CHBDC specify limiting bounds for the minimum required thickness. These lower bounds are intended to provide the rigidity needed to compensate effects of uneven bearing. This is due to the fact that in case of significant deformation of base plate there will be inadequate volume of elastomer to fill pot cavity resulting to hard contact between bearings parts (AASHTO 2012).

– bearings directly against concrete or grout

$$t_{\mathrm{Pot}} \geqslant 0.06\ d_{\mathrm{Pot}} \tag{2.56}$$

$$t_{\mathrm{Pot}} \geqslant 20\,\mathrm{mm} \tag{2.57}$$

– bearings directly on steel girders or load distribution plates

$$t_{\mathrm{Pot}} \geqslant 0.04\ d_{\mathrm{Pot}} \tag{2.58}$$

However SCEF recommends conservative factor of 0.045 instead of 0.04.

$$t_{\mathrm{Pot}} \geqslant 12.5\,\mathrm{mm} \tag{2.59}$$

In CHBDC the limiting bound of 15 mm is stated in lieu of 12.5 mm limit.

Another criteria specified in AASHTO for base plate thickness is that similar to the pot wall as discussed in section 2.5.5, pot base should be able to resist bending moments generated

$$t_{\mathrm{Pot}} \geqslant \sqrt{\frac{25 H_{\mathrm{u}}\ \alpha_{\max}}{F_{\mathrm{y}}}} \tag{2.60}$$

Determining pot base thickness according to EN 1337-5 is performed by taking account of the tensile forces applied to the base. EN 1337-5 states that base plate of the pot should have sufficient resistance against applied tensile forces similar to the pot walls. Thus the tensile force within the pot base has to be less or equal to the the design resistance

$$V_{\mathrm{Sd}} \leqslant V_{\mathrm{Rd}} \tag{2.61}$$

where as previously

$$V_{\mathrm{Sd}} = V_{\mathrm{e,\,Sd}} + V_{\mathrm{Fxy,\,Sd}} \tag{2.62}$$

In the case of the pot base, the tensile resistance force can be determined as

$$V_{\mathrm{Rd}} = \frac{F_{\mathrm{y}} A_{\mathrm{p}}}{\gamma_{\mathrm{M}}} \tag{2.63}$$

in which the cross-section area A_{p} of the bearing base can be obtained from

$$A_{\mathrm{p}} = D_{\mathrm{Pot}}\, t_{\mathrm{Pot}} \tag{2.64}$$

where t_{Pot} is the thickness of the pot base. However according to EN 1337-5 t_{Pot} should not be less than 12 mm. Finally from the limiting bounds presented in AASHTO, EN 1337-5 or CHBDC and the requirements for tensile or bending moment resistance the thickness of the base plate can be determined.

2.5.6 Sealing rings

Use of internal seal in fixed pot bearing is intended to prevent scape of the pad through the clearance between the recess walls and piston when compressive loads are applied (EN 2005). As discussed in section 2.5.3 the limit of minimum thickness for the elastomeric pad is based on limiting the compressive strain on the pad from rotation to 15%. However since the effective thickness of the pad under sealing recess is reduced, the resulting compressive strain may increase. Then the sealing recess should be shallow relative to total thickness of the elastomeric which will prevent damage to the elastomer layer bellow the rings (Steel Bridge Bearing and Design Guide 2011).

AASHTO allows using seals made of brass either in form of (i) multiple flat rings usually bent from strip and the ends are not joined (Steel Bridge Bearing and Design Guide 2011) or (ii) circular rod brazed into a closed ring. However flat brass rings are more susceptible to ring fracture and leakage of elastomer while circular brass rings are more susceptible to severe wear. AASHTO prohibits use of PTFE rings due to their poor performance while permits use of plastic rings (Steel Bridge Bearing and Design Guide 2011). The specifications stated in AASHTO and CHBDC for rectangular or circular-cross section rings are intended to prevent loss of elastomer pad through the seal due to variable rotations,

– Rings with rectangular cross section :
  In this type of sealing ring three rectangular rings are cut at one point around its circumference with 45 ° to the vertical plane. The position of the rings should be such that the cuts are spaced equally around the circumference of the pot. Also the dimensions of the rings should be such that the width of each ring is not less than either $0.02\, d_{\mathrm{Pot}}$ or 6 mm and not more than 19 mm. Besides the depth of each ring should not be less

than 0.2 times its width.

– Rings with circular cross section :

  In this type of sealing rings, one circular cross sectional ring is used with outside diameter of d_{Pot}. Also cross sectional diameter of the circular sealing ring should not be less than either 0.0175 d_{Pot} or 4 mm

In European Standard EN 1337-5 other than brass sealing rings, use of carbon filled PTFE, stainless steel and POM seals is permitted as well. Also in this code the geometrical considerations are base on the material from which the sealing ring is made of rather than its shape (comparing to AASHTO and CHBDC). Geometrical and material specifications for each of these sealing types are mentioned in detail in Annex A of EN 1337-5. In case of using these types of sealing rings the accumulated slide path from testing (S_{T}) as discussed in section 2.5.1 can be assumed as the following without performing any additional tests,

– For stainless steel seals $S_{\mathrm{T}} = 500\,\mathrm{m}$
– For brass seals $S_{\mathrm{T}} = 1000\,\mathrm{m}$
– For POM and carbon filled PTFE seals $S_{\mathrm{T}} = 2000\,\mathrm{m}$

in case of using alternative sealing rings performing long term rotation and load test is essential to examine behaviour of the sealing ring and test durability of the bearing.

2.6 Fabrication criteria of pot bearings

After performing the primary design of the fixed pot bearing, the procedure to construct the pot from base plate and pot wall should be determined. In this sections the types of connections allowed to be used in the codes will be specified. Also the additional geometrical requirements that should be satisfied for proper behaviour of the bearing are mentioned.

2.6.1 Base plate and pot wall connection

Regarding to the connection procedures between base plate and the ring, EN 1337 focuses more in detail to different types of connections comparing to other specifications. According to AASHTO, the most reliable way of constructing pot is by machining it from a single plate. However, this code allows attaching the pot walls by using full penetration weld for very large bearings to reduce costs and also take account of the high moments where the ring joins the base plate. On the other hand EN 1337 permits use of full penetration butt weld, partial penetration butt weld and fillet weld as means of connection between the base plate and the ring.

Full penetration butt weld

In Fig. 2.9, connection between base plate and the ring using full penetration butt weld according to EN 1337-5 is presented. For this type of connection the properties of the weld is controlled by the elements joined. According to EC3-1-8 full penetration butt weld should have equal or superior properties to those of joined elements so that design resistance is taken as the weaker of the parts connected (Trahair 2008). Then the capacity of butt weld is calculated from capacity of pot base. In other terms, we have

$$V_{\mathrm{Sd}} \leqslant V_{\mathrm{Rd}} \tag{2.65}$$

where

$$V_{\mathrm{Sd}} = V_{\mathrm{e,\,Sd}} + V_{\mathrm{Fxy,\,Sd}} \tag{2.66}$$

and

$$V_{\mathrm{Rd}} \leqslant \frac{F_{\mathrm{y}} A_{\mathrm{p}}}{\gamma_{\mathrm{M}}} \tag{2.67}$$

in which

$$A_{\mathrm{p}} = D_{\mathrm{Pot}}\, t_{\mathrm{Pot}} \tag{2.68}$$

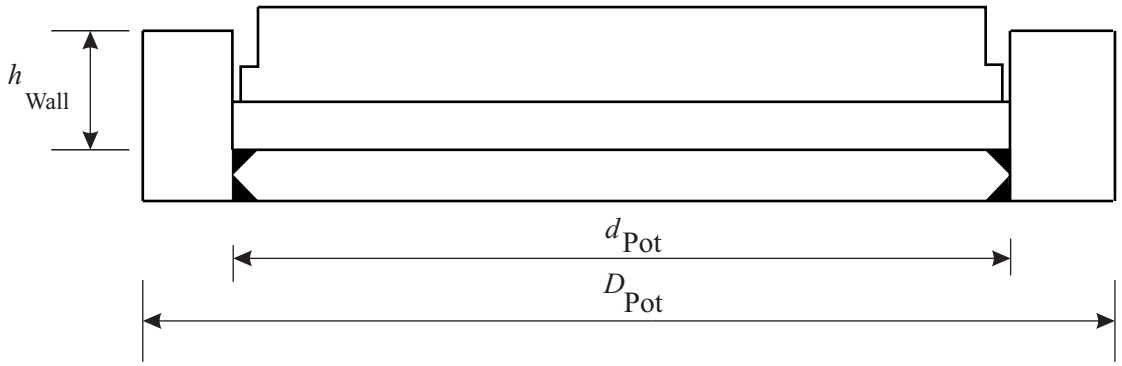

FIGURE 2.9 Full penetration butt weld

Partial penetration butt weld

Comparing to full penetration type, partial penetration butt weld has an effective (throat) thickness which is less than that of the elements joined. In case of connection between base plate and the ring, butt weld has to bear tensile forces applied to the base. Then we have

$$V_{\mathrm{Sd}} \leqslant V_{\mathrm{Rd}} \tag{2.69}$$

where

$$V_{\mathrm{Sd}} = V_{\mathrm{e,\,Sd}} + V_{\mathrm{Fxy,\,Sd}} \tag{2.70}$$

However, the design resistance of partial butt welds is evaluated by

$$V_{\mathrm{Rd}} = \sum F_{\mathrm{w,\,Rd}} d_{\mathrm{Pot}} \tag{2.71}$$

where the design resistance per unit length $F_{\mathrm{w,\,Rd}}$ is given by PrEN 1993-1-8 as

$$F_{\mathrm{w,\,Rd}} = a\, F_{\mathrm{vw,\,d}} \tag{2.72}$$

in which a is the effective throat thickness of weld, and $F_{\mathrm{vw,\,d}}$ is the design shear strength that can be obtained as

$$F_{\mathrm{vw,\,d}} = \frac{\dfrac{F_{\mathrm{u}}}{\sqrt{3}}}{\beta_{\mathrm{w}}\, \gamma_{\mathrm{M2}}} \tag{2.73}$$

where F_{u} is the minimum ultimate strength of the connected parts, β_{w} is a correlation factor, equal to 0.85 for steel grade S275 and 0.9 for steel grade S355 and γ_{M2} is the connector resistance partial safety factor that an be taken equal to 1.25 (Trahair 2008).

Fillet weld

A fillet can be used to connect pot wall to top of the pot base as shown in Fig. 2.10. In this case, the design forces and resistance are determined per unit length. As previously, the following inequality has to be satisfied

$$V'_{\mathrm{Sd}} \leqslant V'_{\mathrm{Rd}} \tag{2.74}$$

in which V'_{Sd} was defined before and V'_{Rd} is given by

$$V'_{\mathrm{Rd}} = \sum F_{\mathrm{w,\,Rd}} \tag{2.75}$$

$F_{\mathrm{w,\,Rd}}$ can be calculated as done for partial penetration butt welds section.

2.6.2 Additional geometrical requirements

The following geometrical conditions need to be satisfied to obtain the required rotational capacity of a pot bearing while preventing escape of the elastomer and locking of bearing components according to EN 1337-5 and AASHTO :

– The edge of the contact interface between the piston and the elastomer must re-

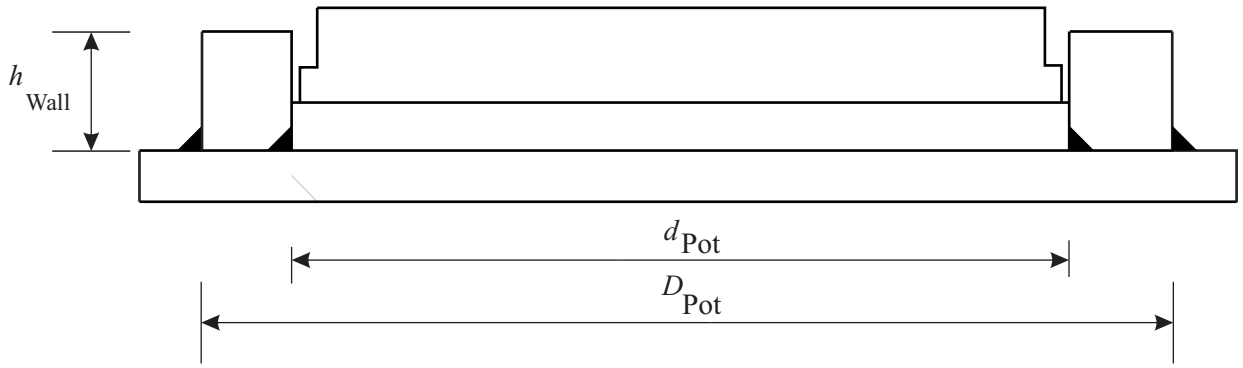

FIGURE 2.10 Fillet Weld

main within the cylindrical recess formed by the pot wall around the whole circumference (EN 2005).

- The top of the pot wall should not be in contact with any other metallic component (EN 2005).
- The seal and piston rim must remain in full contact with the vertical face of the pot wall (AASHTO 2012).
- Contact or binding between metal components should not prevent displacement and rotation (AASHTO 2012).

We show that these criteria imply the following geometric condition according to EN 1337-5 on the height of the pot wall according to figure Fig. 2.11

$$h_{\text{Wall}} \geqslant t_{\text{Pad}} + 0.5 \times (w - b) + \frac{1}{2}\,\alpha_{\max}\, d_{\text{Pad}} + a_{\text{d}} \tag{2.76}$$

where a_{d} is a safety factor which can be evaluated as (EN 2005)

$$a_{\text{d}} = \min\big\{\max(0.01\, d_{\text{Pot}}, 3\,\text{mm}), 10\,\text{mm}\big\} \tag{2.77}$$

If the wall of the piston is flat, i.e. $w = b$, Eq. (2.76) changes to

$$h_{\text{Wall}} \geqslant t_{\text{Pad}} + \frac{1}{2}\,\alpha_{\max}\, d_{\text{Pad}} + a_{\text{d}} \tag{2.78}$$

Regarding to minimum cavity depth for pot bearing with flat contact surface from EN 1337-5 (Eq. (2.78)), AASHTO specifies a more conservative requirement as mentioned in section 2.5.5 by assuming that flat contact area should remain within the pot cavity (Fig. 2.7)

$$h_{\text{Wall}} \geqslant (0.5\,\alpha_{\max}\, d_{\text{Pot}}) + t_{\text{Pad}} + w \tag{2.79}$$

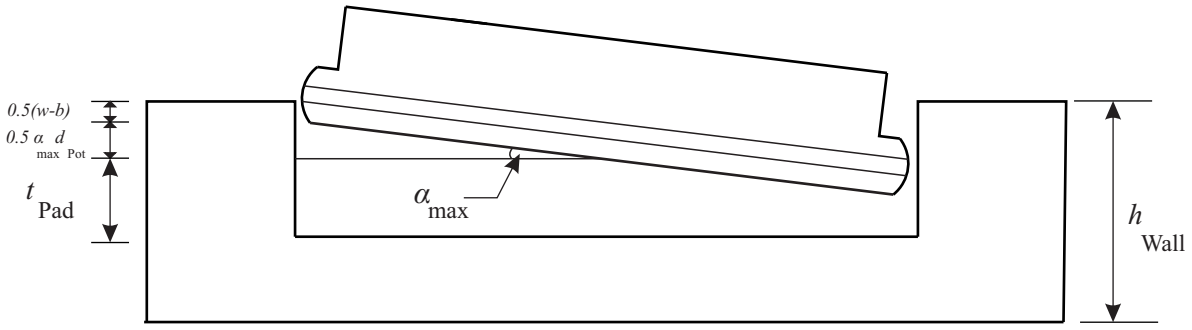

FIGURE 2.11 Geometrical conditions for rotation according to EN 1337

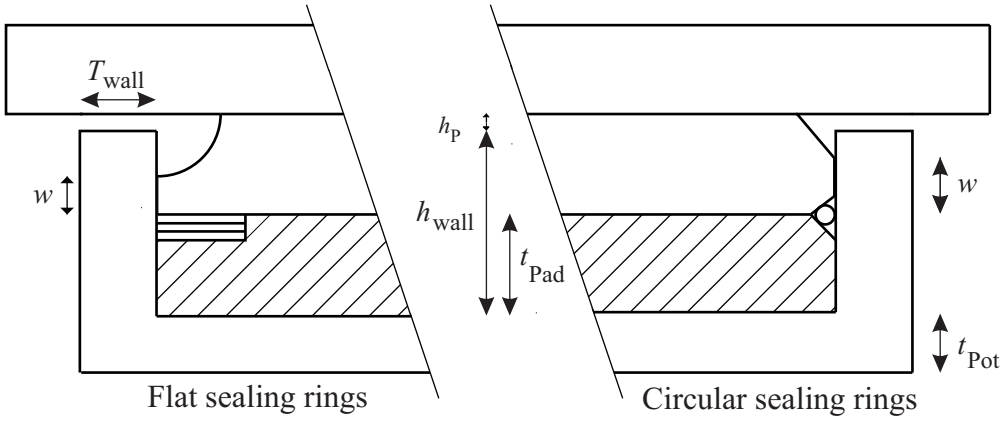

FIGURE 2.12 Critical dimensions for clearances according to AASHTO

Also according to Fig. 2.12 AASHTO specifies that the vertical clearance between top of piston and top of pot wall, h_{P}, as illustrated in Fig. 2.12, should satisfy the following requirement (AASHTO 2012)

$$h_{\mathrm{P}} \geqslant R_0 \alpha_{\max} + 2\delta_{\mathrm{u}} + 3 \tag{2.80}$$

where

- δ_{u} is the compressive deflection due to factored load (mm)
- R_0 is the radial distance from center of pot to object in question (pot wall, anchor bolt, etc) (mm).

Since the actual compressive deflection of δ_{u} is small when compared to the deflection due to rotation (Baker 2006), in SCEF the required minimum clearance is obtained from deflection due to maximum rotation coupled with an extra 3.2 mm.

According to AASHTO the clearance between piston and pot (c_1) is critical to proper functioning of pot bearings. In order to prevent escaping of elastomer AASHTO states that this parameter should be as small as possible in the range of 0.5 to 1 mm. Also in case of designing piston rim as cylindrical the following requirement should be satisfied

$$c_1 \geqslant \alpha_{\max}(w - \frac{d_{\mathrm{Pot}}\, \alpha_{\max}}{2}) \tag{2.81}$$

where

- d_{Pot} is internal diameter of pot (mm)
- w is height of top of rim to underside of piston (mm)
- $\alpha_{\max}$ is design strength limit state rotation (rad)

2.6.3 Lubrication

One of the controversial issues regarding to design of pot bearings is whether it should be lubricated. Some engineers have raised a concern about lubrication making the elastomer slide easily in the pot and consequently reducing the rotational resistance. However some believe that in order to avoid the potential of abrasion and wear of elastomer lubricant should be used. Grease (one common material is Silicon grease) or powdered lubricant are some of the common types of lubricants generally applied before placing the elastomer in the cylinder (Roeder and Stanton 1998). Silicon grease lubrication reduces the rotational resistance during initial cycles of rotation but its beneficial effect is lost in later cycles. The ultimate wear of the elastomeric disk is not reduced significantly by the lubrication, but in contributes in reducing the wear observed in the rings, pot walls and piston (NCHRP 1999).

According to some engineers one of the disadvantages of grease is that when subjected to the same pressure as the elastomeric pad, it makes the pot wall slippery while squeezing

out which leads to leakage of elastomer. Another concern is that some elastomer compounds deteriorate over time when in contact with oil or grease. Also the lubricant tends to migrate and the beneficial effect is lost (Roeder and Stanton 1998).

2.7 Conclusion

This chapter includes a detailed review of design methods of fixed elastomeric pot bearing according to the reliable specifications of AASHTO, EN 1337 and CHBDC was discussed. The requirements stated in each specification were explained and the rationales behind them were presented. It is concluded that the general design method of CHBDC is generally similar to AASHTO. However the main differences between EN 1337-5 and these specifications is in the following requirements,

- Pot design : Design method of pot in AASHTO in mainly based on providing sufficient bending resistance for the applied horizontal loads at interconnection between base and the walls. However in the latest version of EN 1337-5 the design method of pot parts is performed by taking into consideration the shear and tensile forces in the pot rather than the bending moments.
- Piston design : The provisions regarding to piston design in EN 1337-5 seem to be more integrated due to concentration on the requirements for both flat and curved contact face of piston wall. However in AASHTO only the requirements regarding to flat contact area are mentioned.
- Geometrical conditions : In EN 1337-5 the maximum cavity depth of the pot is obtained by assuming that in the most critical condition with maximum rotation of $\alpha_{\max}$ the edge of piston and pad contact face remains within the cylindrical recess. However in AASHTO for the critical condition it is assumed that total width of piston in contact with pot cavity remains within the ring.

CHAPTER 3

ANALYTICAL AND FE MODELING OF CONTACT PROBLEMS

3.1 Introduction

With the advancements in computers and development of new numerical procedures, it seems that method of computing contact parameters and the rational behind it is unclear for many engineers nowadays. Thus it can be concluded that regarding to the importance of contact problem for pot bearings and reliance of the specifications on the analytical methods as it will be discussed further in this chapter, it is important to convey a study on contact parameters (such as angle of contact, principal stresses, contact pressure and contact forces) obtained from both analytical and numerical methods and compare the results.

The objective of this chapter is to apply analytical contact methods of Hertz and Persson and compare the results to the corresponding numerical outputs obtained from modeling two typical cylinders in contact. First a classical case of contact between two cylindrical bodies with the same curvature sign will be considered. The finite element modeling of this type of contact will be developed. The results of the finite element models will be validated against Hertz analytical formulation.

In the next step, the contact angle between a cylinder resting inside another hollow cylindrical body (with different curvature signs) is compared to the analytical methods by referring to both Hertz and Persson analytical methods.

3.2 Analytical methods for contact problems

Hertz has studied contact conditions between two bodies with different geometrical shapes. In a pot bearing, contact between a piston and cylinder can be regarded as contact between two cylindrical bodies. In the following sections Hertizian contact between two cylindrical bodies will be highlighted. Comparing to Hertz, as previously mentioned Persson has limited his theory to contact between two cylindrical bodies which one is resting inside another one. In the following sections a brief introduction to the most important analytical contact methods of Persson and Hertz for two cylindrical bodies is presented.

3.2.1 Hertz theory of contact

The first satisfactory analysis at the contact between two elastic bodies was performed by Hertz by accepting the following assumptions (Johnson 1985) :

- The surfaces are continuous and non-conforming,
- The stresses are small,
- Each solid can be considered as an elastic half-space,
- Area of contact has an elliptical shape,
- and the surfaces are frictionless.

Contact between piston and pot can be regarded as contact between two cylindrical bodies. For two cylinders in contact Hertz assumes that the bodies have parallel axes in which contact area is infinitely long in one direction. In other words, when a distributed load F per unit length is applied to the first body as illustrated in Fig. 3.2, the value of semi-major axis a' will be infinitely long due to the line contact while the semi-minor axis is equal to b'. According to Hertz this type of contact is available for two cylinders with perpendicular line of contact to the paper and also for a small circular cylinder resting on a larger hollow cylinder as illustrated in Fig. 3.3. According to Hertz theory the value of width of contact b' for two cylinders in contact can be obtained from

$$b' = \sqrt{\frac{2F\Delta}{\pi}} \tag{3.1}$$

where

$$\Delta = \frac{1}{\dfrac{1}{2r_1} + \dfrac{1}{2r_2}} \left[\frac{1-\nu_1^2}{E_1} + \frac{1-\nu_2^2}{E_2} \right] \tag{3.2}$$

It should also be noted that for a cylindrical body placed inside another one (case b, Fig. 3.2), r_2 shall be inserted as negative in Eq. (3.2) due to different curvature signs (Boresi et al. 1978). Finally value of contact angle α in the horizontal plane can be obtained from

$$\alpha = 2 \arcsin \left[\frac{b'}{r_1} \right] \tag{3.3}$$

Hertz has also presented analytical equations to obtain values of principal stresses for the cylinders with contact region approximately along a straight line (plane strain). Boresi et. al have simplified Hertizian principal stress equations for linear elastic cylindrical bodies in contact along Z axis (Boresi et al. 1978). This axis originates at the the middle point of contact with maximum contact pressure and passes center of the lower body as illustrated in

Fig. 3.1. The equations for principal stresses obtained by Boresi et. al are,

– Principal stress yy

$$\sigma_{yy} = -2\nu \left[\sqrt{1 + (\frac{z}{b'})^2} - \frac{z}{b'} \right] \frac{b'}{\Delta} \tag{3.4}$$

– Principal stress xx

$$\sigma_{xx} = -\frac{\left[\sqrt{1 + (\frac{z}{b'})^2} - \frac{z}{b'} \right]^2}{\sqrt{1 + (\frac{z}{b'})^2}} \frac{b'}{\Delta} \tag{3.5}$$

– Principal stress zz

$$\sigma_{zz} = -\left[\frac{1}{\sqrt{1 + (\frac{z}{b'})^2}} \right] \frac{b'}{\Delta} \tag{3.6}$$

as previously mentioned, according to Hertz contact theory contact pressure between two parallel cylinders will be represented by a semi elliptical prism over contact length of $2b'$ and the area of contact approaches a rectangle. Fig. 3.1 presents pressure distribution between two cylinders according to this analytical method. This pressure can be obtained from (Lipson et al. 1963)

$$P(y) = P_o \sqrt{1 - \frac{y^2}{b'^2}} \tag{3.7}$$

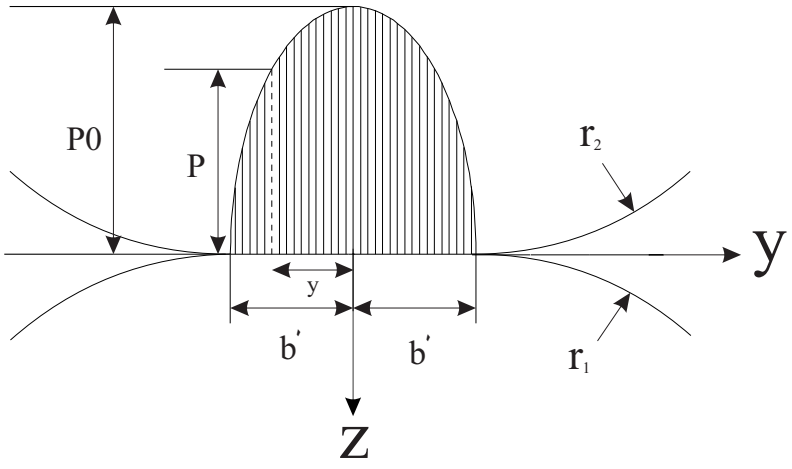

FIGURE 3.1 Hertz pressure distribution

Where the value of P_o is equal to maximum principal stress at the point of contact. Analytical formulations have implied to these values in different types of orientation and

geometrical properties. In the case considered here, since cylinders are made from the same material, value of P_o is obtained from (Lipson et al. 1963)

$$P_0 = 0.418\sqrt{\frac{FE}{a'}\frac{(r_1 + r_2)}{r_1 r_2}} \tag{3.8}$$

In the formulations mentioned above :

- F (N/m) is load per unit length of the contact area
- r_1 and r_2 (m) is smaller and bigger radii of contact of two bodies
- ν is poisson's ratio of each body
- z (m) is the distance below the contact surface
- E (N/m^2) is modulus of elasticity of each of the bodies
- b' is half of contact width of the cylinders
- P_o is the maximum principal stress taking place at the point of contact.

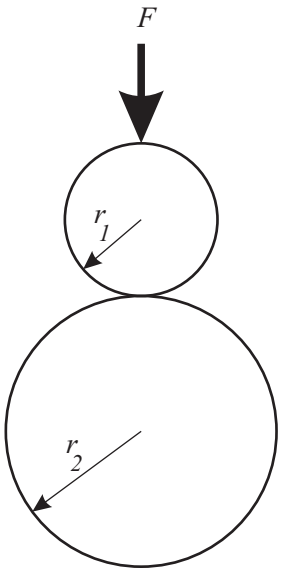

FIGURE 3.2 Two cylindrical bodies in contact with positive curvatures

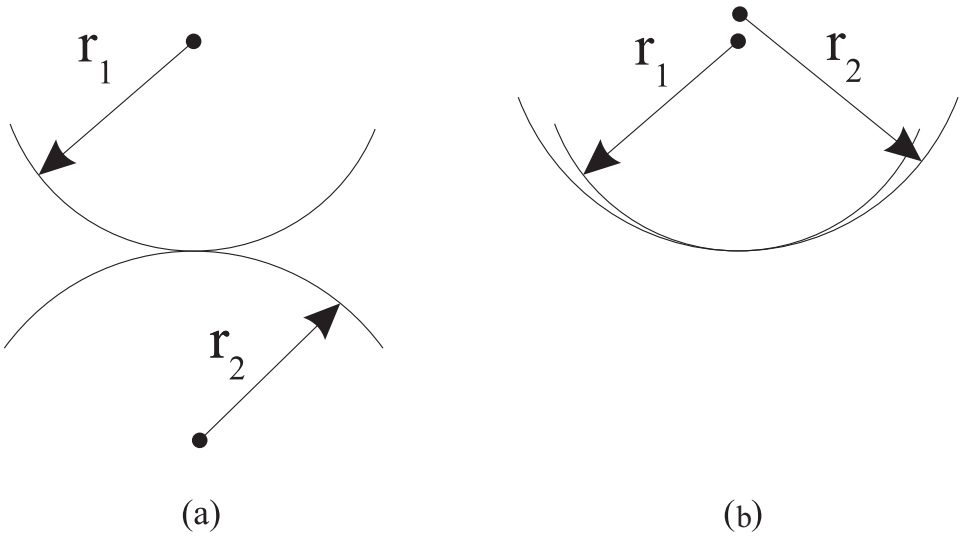

FIGURE 3.3 Hertz contact conditions for two cylindrical bodies

3.2.2 Persson theory of contact

As previously discussed one of the main assumptions of Hertz theory is that contact area is small comparing to the dimensions of the bodies in contact. According to Ciavarella and Persson (Ciavarella 2001 ; Persson 1964) applying the two dimensional case of Hertz theory will not lead to acceptable results for the case of a cylinder in a bore with only a slightly larger radius (Fig. 3.4). This is due to the fact that the contact area between these two bodies is not small compared to the radii of the bodies and the contact angle (conforming contact). An important advance in analyzing an elastic pin in contact with an infinite elastic plate was performed by Persson by providing complex solution for singular integro-differential equation for contact problem between two bodies with the same materials. He has applied stress functions appropriate to a circular disk and a circular hole in an infinite plate to obtain the stress field for both bodies (Johnson 1985). The assumptions considered for this contact problem are,

- The plate is infinite,
- a concentrated force is applied at the center of the plate,
- Both of the bodies are made of isotropic elastic materials,
- The difference of radius of the bodies is very small,
- Contact area is frictionless,
- and plane stress condition is assumed.

In Eq. (3.9), Persson has presented an equation which relates the parameters Δr, E, F and r',

$$\frac{E\Delta r}{Q} = \frac{2}{\pi}\frac{1-r'^2}{r'^2} - \frac{I_6}{\pi^2 r'^2(1+r'^2)} \tag{3.9}$$

where I_6 is an integral which has not been calculated in closed from

$$I_6 = \int_{-r'}^{r'} \frac{\ln \dfrac{\sqrt{r'^2+1}+\sqrt{r'^2-t^2}}{\sqrt{r'^2+1}-\sqrt{r'^2-t^2}}}{1+t^2}\mathrm{d}t \tag{3.10}$$

and E is the modulus of elasticity of the bodies.

Also for maximum stress between the two cylinders Persson has obtained the following equation,

$$\frac{r_2 P_0}{F} = \frac{2r'}{\pi\sqrt{r'^2+1}} + \frac{\ln(\sqrt{r'^2+1}+r')}{\pi r'^2(1+r'^2)} \tag{3.11}$$

where

- F is load per unit length of the contact area

– Δr is the difference of radii of the cylindrical surfaces
– ν is poisson's ratio of each body
– z is the distance below the contact surface
– E is modulus of elasticity of each of the bodies
– b' is half of contact width of the cylinders
– r' is equal to $\tan(\alpha/4)$ (where α is angle of contact)
– Contact forces follow plane stress distribution.

It should also be noted that due to the complexity of calculation of Eq. (3.10), for simplicity Persson has also provided a table which presents value of angle of contact of α and ratio of $r_2 P_0/F$ for each value of $E\Delta r/F$.

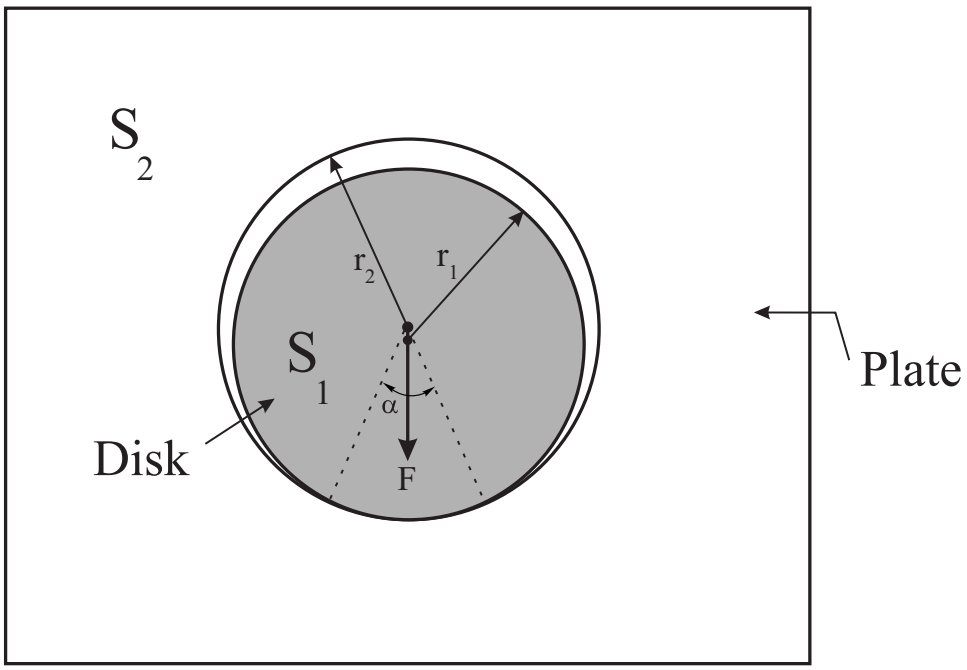

FIGURE 3.4 Persson contact conditions for two cylindrical bodies

3.3 Examples of 2D finite element modeling of contact problems

In this section the properties of the numerical models generated with ADINA software are discussed. In the first step finite element models of two cylindrical bodies with positive curvatures in contact are generated for different meshing types. In the second step numerical models corresponding to two cylindrical bodies with different curvature signs in contact are generated.

3.3.1 Cylinders in contact with positive curvature signs

One cylinder resting on another one (both with positive curvature signs), have been modeled in ADINA finite element software using two dimensional solid elements with a primary contact as illustrated in Fig. 3.5. In order to find the best accordance between analytical and numerical results, finite element models are optimized by using element types with a coarse mesh. The process of generation of model is as follows,

- Material : Both cylinders are made of the same homogeneous, isotropic and elastic steel material with Young's modulus of 200 GPa and Poisson ratio of 0.3.
- Geometry : The radii of upper and lower cylinders have been chosen as 32 mm and 45 mm respectively. These dimensions were extracted from an analytical contact problem of two cylindrical bodies solved by Boresi et al (Boresi et al. 1978).
- Meshing : 2D plain strain cylinders were meshed by nine, eight and four node elements.
- Force : Point force of 40 kN was applied on the upper cylinder.
- Contact : 2D contact group without any friction is chosen as the contact group of the cylinders.

3.3.2 Cylinders in contact with different curvature signs

For two cylinders with different signs in curvature, a small circular cylinder which is resting on a cylindrical ring is modeled in 2D with ADINA (case b Fig. 3.3). In order to have accordance between Persson assumptions and finite element modeling, all the degrees of freedom along perimeter of the outer cylinder were fixed and first point force of 40 kN and then of 154 kN were applied at the center of the inner cylinder. Radius of the inner body is chosen as $r_1 = 104.5$ mm and the internal and external radii of the outer body are chosen as $r_2 = 105$ mm and $r_3 = 242.5$ mm respectively. Also due to the plane stress assumption of calculations in Persson theory, thickness of 6 mm was assigned in 2D finite element model. Geometry of the model is presented in figure Fig. 3.6.

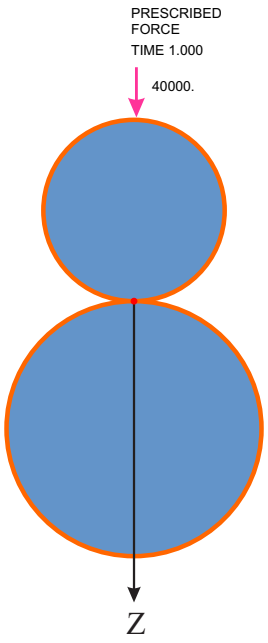

FIGURE 3.5 FE model, two cylinders with positive curvatures

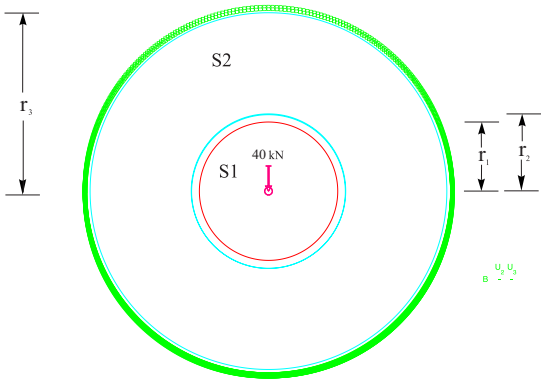

FIGURE 3.6 Cylinders with opposite curvatures

3.4 Comparison of the results of analytical and finite element models

3.4.1 Stress verification for cylinders with positive curvatures,

Values of principal stresses and z coordinates of the nodes which are located along line of contact are extracted (as shown in Fig. 3.5). It must be mentioned that the analytical formulations mentioned for Hertz theory and finite element modeling for this part are both based on plain strain assumption. Therefor, if acceptable results are achieved for yy and zz principal stresses, the accuracy of results can be generalized for xx principal stresses as well. Stress values obtained from both numerical and Hertz analytical methods are compared and finally corresponding tables and figures are provided to present the results. This procedure is pursued for three types of element meshing (9, 8 and 4 node elements).

After comparing the numerical and analytical (Hertz theory) results for two cylinders with positive curvature signs in contact, the following results are obtained ;

- Principal stress zz : By going through the figures and tables illustrated for principal stresses in z direction for the three types of meshing (nine, eight and four node element meshing), it can be concluded that the numerical values have an acceptable accordance with those of analytical formulation.
- Principal stress yy : Similar to the case of principal stress zz, the numerical values of principal stresses yy have an acceptable accordance with the analytical formulation of these stresses.
- Stress xx : Since numerical outputs of both principal stresses zz and yy have led to an acceptable accuracy when compared with analytical formulations, it can be concluded that the values of principal stress xx in finite element modeling are in accordance with analytical outputs due to plain strain assumption.
- Point of contact stresses : By going through the tables and figures illustrated it can be inferred that at the point of contact the results of analytical formulations and ADINA modeling have the highest differences. This is due to concentration of high local stresses at point of contact. However the value of stress ratio at the points very close to contact point (0.3 mm) are found to be very close to one.

Figures 3.7 to 3.12 illustrate the results corresponding to nine node element meshing.

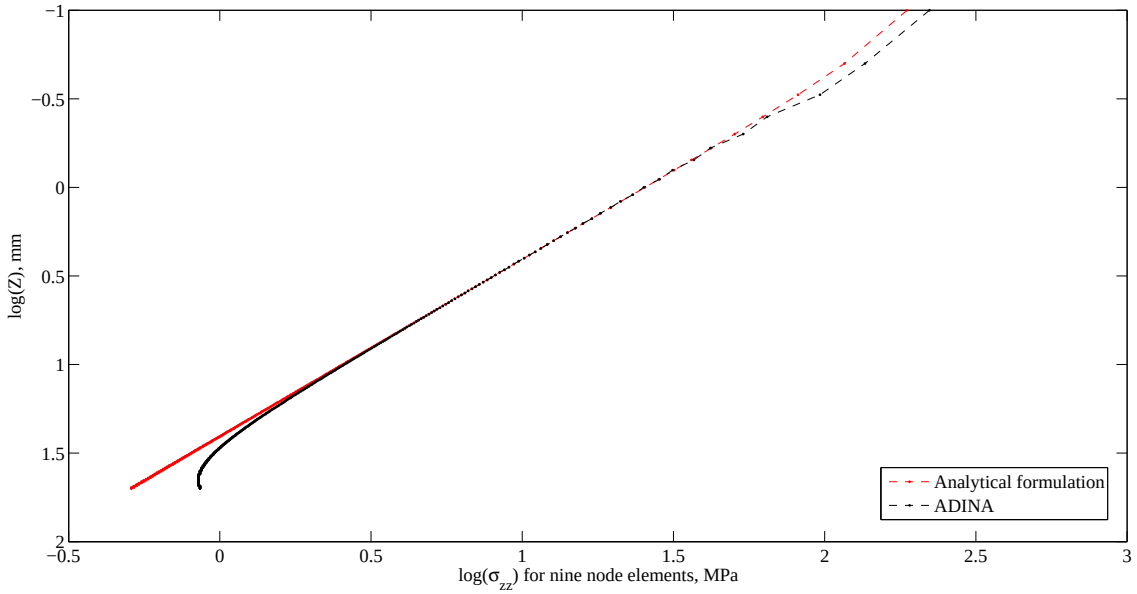

FIGURE 3.7 Stress zz, nine-node FE model, cylinders with positive curvature

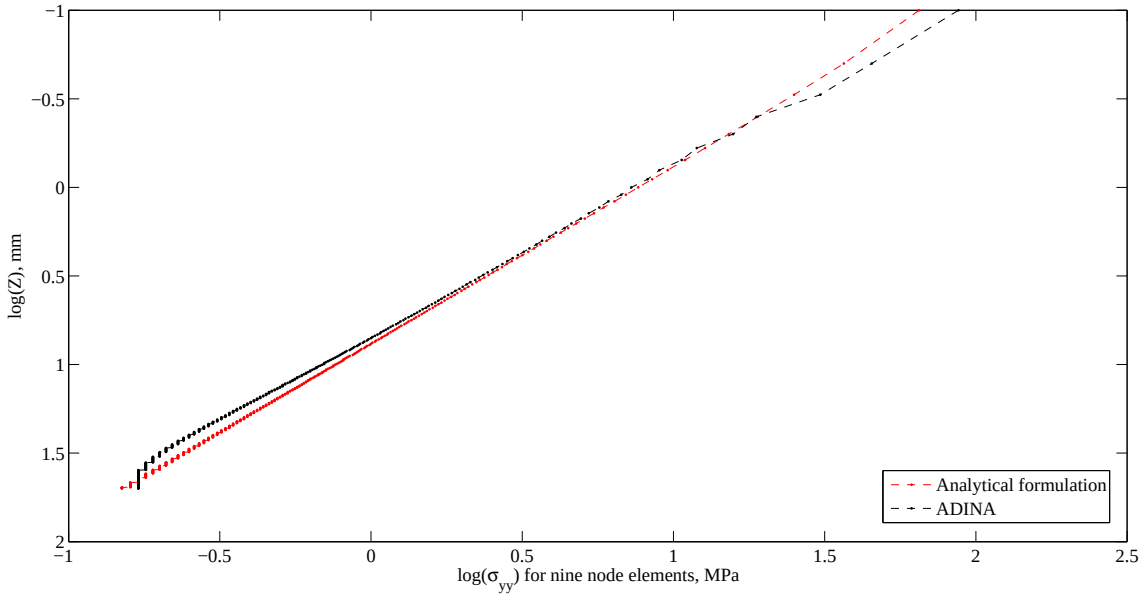

FIGURE 3.8 Stress yy, nine-node FE model, cylinders with positive curvature

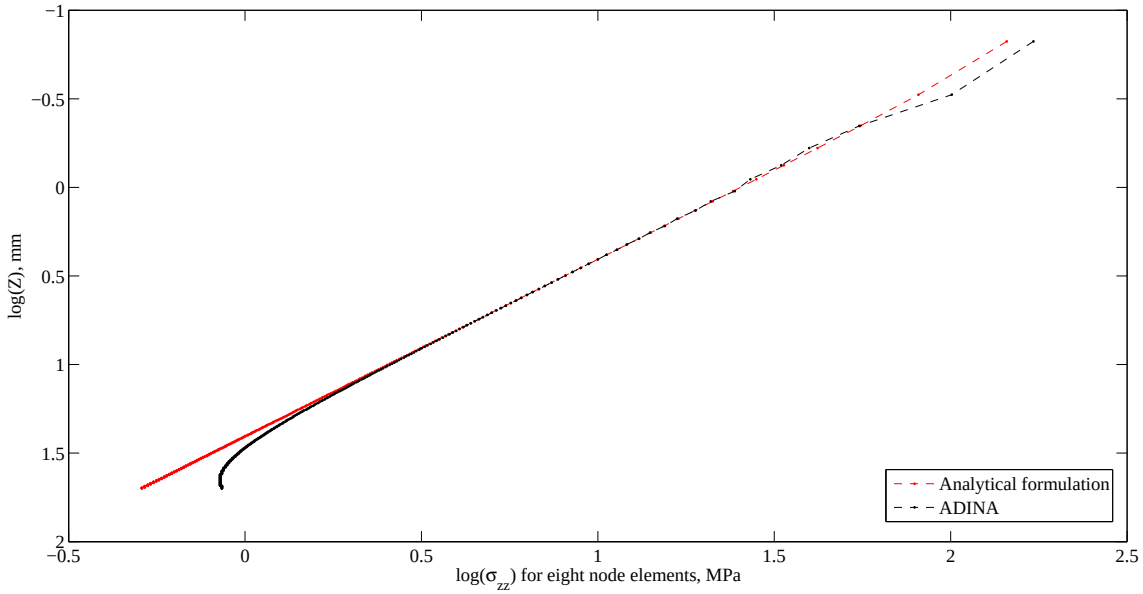

FIGURE 3.9 Stress zz, eight-node FE model, cylinders with positive curvature

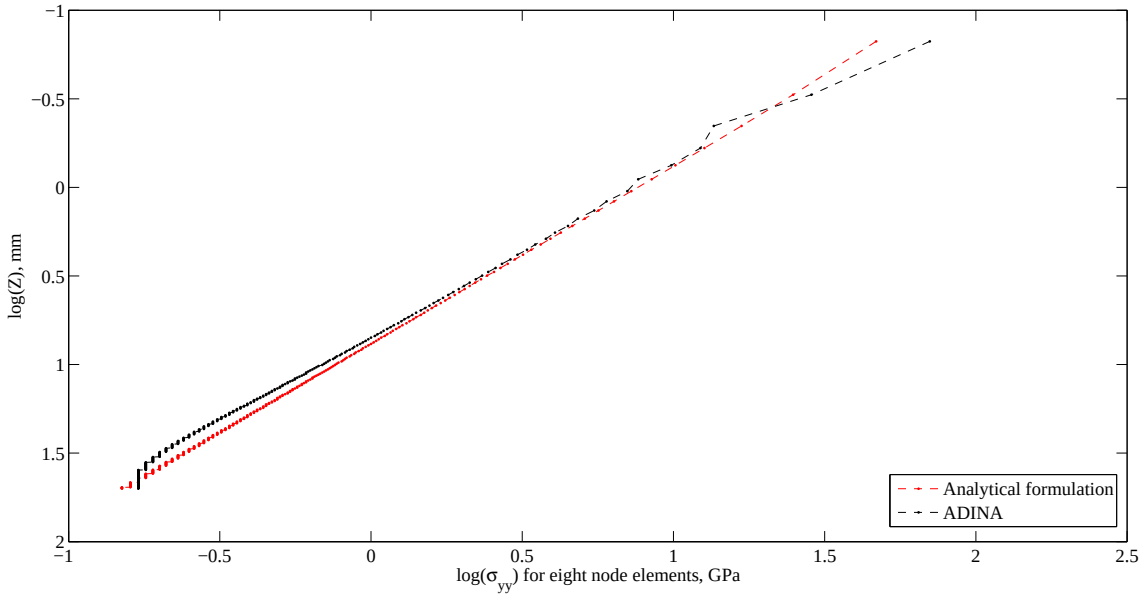

FIGURE 3.10 Stress yy, eight-node FE model, cylinders with positive curvature

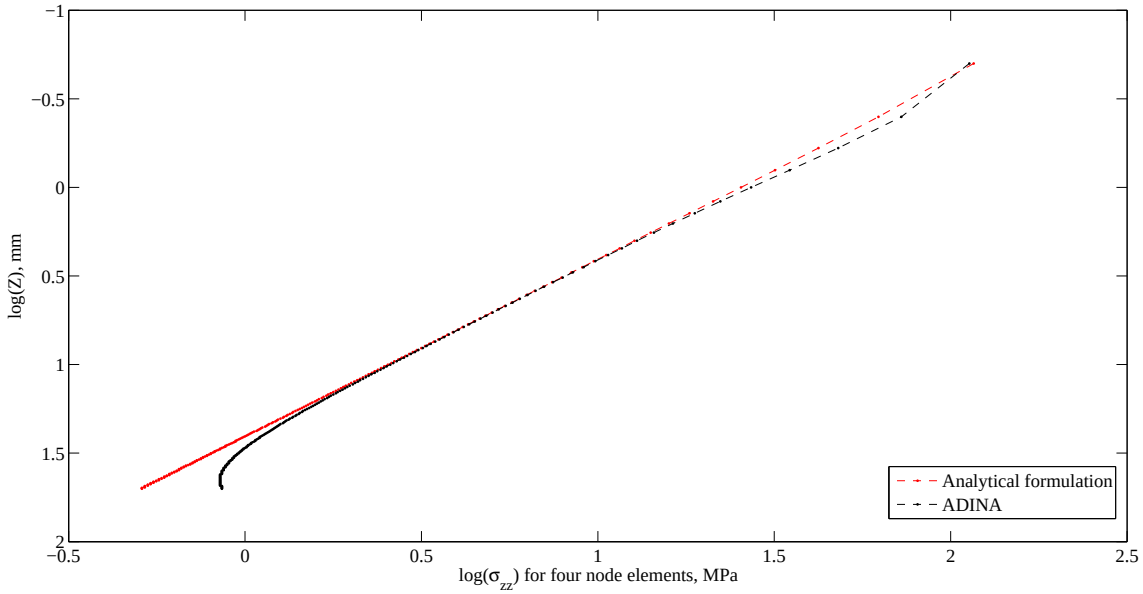

FIGURE 3.11 Stress zz, four-node FE model, cylinders with positive curvature

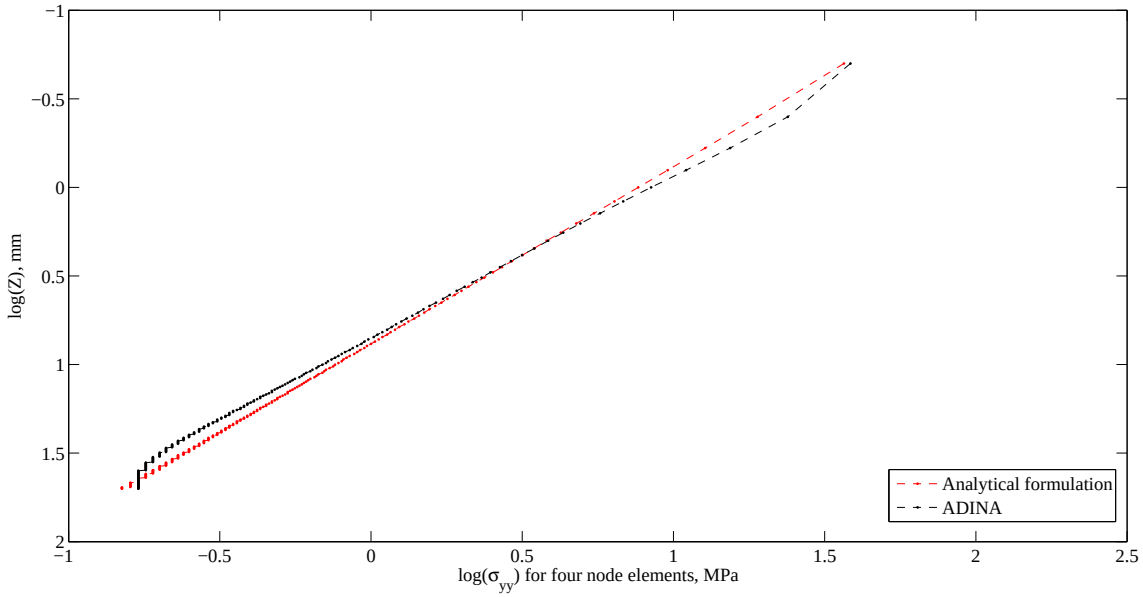

FIGURE 3.12 Stress yy, four-node FE model, cylinders with positive curvature

3.4.2 Contact force verification for cylinders with positive curvatures

In this section contact forces obtained from numerical method are compared to the ones corresponding to Hertz contact theory. As previously discussed in Eq. 3.8, analytical pressure is distributed over contact width (in the range of $-b' \leq y \leq b'$). Thus contact forces obtained from the two methods in three selected nodes (as presented in figures 3.13 and 3.14) are compared.

Analytical contact forces are obtained from Hertz contact pressure induced on each body which is constant for all meshing types. However distribution of analytical contact forces will highly be dependent on the number of nodes in each element. However numerical values of contact forces are directly extracted from finite element modeling. Tables 3.1, 3.2 and 3.3 present values of contact forces at the selected nodes. According to these tables, it can be inferred that for nine, eight and four node element meshing contact forces obtained from of Hertz method are very close to those of FE modeling.

TABLE 3.1 Results for nine-node element model, bodies with similar curvatures

node number	y (mm)	analytical pressure (MPa)	analytical contact force (kN)	ADINA contact force (kN)	ratio
1	-0.199	2.73E+4	-7.26E+3	-7.59E+3	0.96
2	-0.398	2.73E+4	-3.62E+3	-3.74E+3	0.97
3	-0.598	2.72E+4	-7.26E+3	-7.64E+3	0.95

TABLE 3.2 Results for eight-node element model, bodies with similar curvatures

node number	y (mm)	analytical pressure (MPa)	analytical contact force (kN)	ADINA contact force (kN)	ratio
1	-0.199	2.73E+4	-7.26E+3	-7.59E+3	0.96
2	-0.398	2.73E+4	-3.62E+3	-3.74E+3	0.97
3	-0.598	2.72E+4	-7.26E+3	-7.64E+3	0.95

TABLE 3.3 Results for four-node element model, bodies with similar curvatures

node number	y (mm)	analytical pressure (MPa)	analytical contact force (kN)	ADINA contact force (kN)	ratio
1	-0.398	2.73E+4	-1.09E+3	-1.14E+3	0.96
2	-0.797	2.72E+4	-1.09E+3	-1.14E+3	0.96
3	-0.120	2.71E+4	-1.08E+3	-1.13E+3	0.95

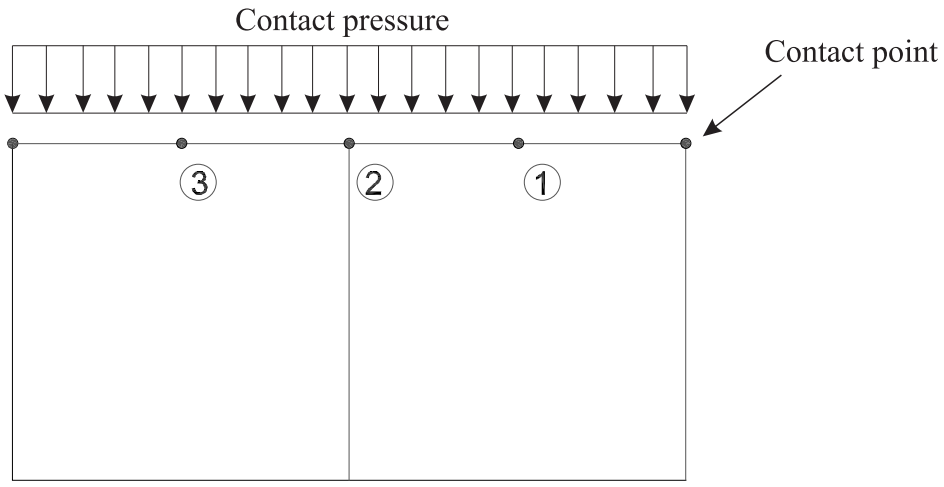

FIGURE 3.13 Nodes chosen for eight and nine node element meshing

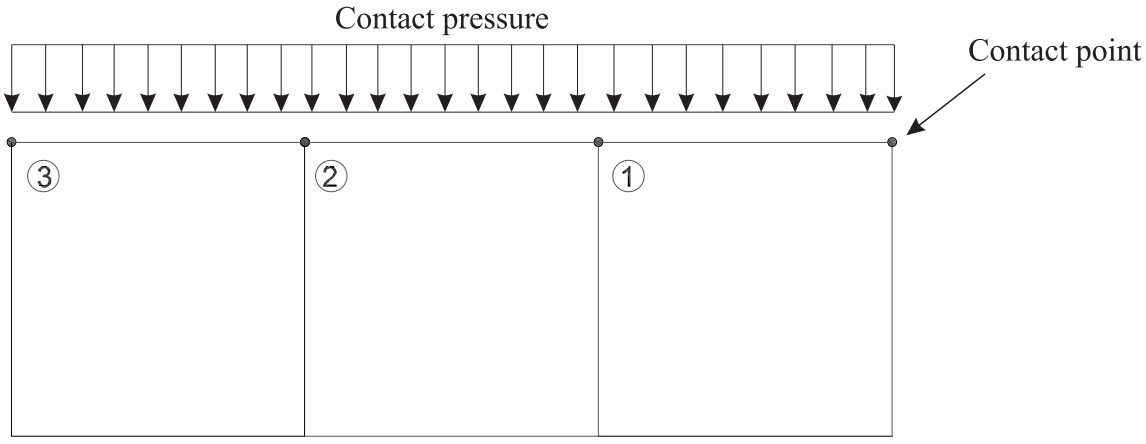

FIGURE 3.14 Nodes chosen for four node element meshing

3.4.3 Angle and stress verification for cylinders with different curvatures

As mentioned before according to the references, limiting case of Hertz contact theory in which contact area becomes infinitely long in one direction will not lead to acceptable results for a cylinder which is in a bore with slightly larger radius (Persson 1964 ; Ciavarella 2001). In such conditions the area of contact is not small anymore. In this section the numerical results obtained by modeling two cylinders in contact with different curvature signs are compared to both Persson and Hertz contact theory and the accuracy of the methods is examined. Fig. 3.15 and 3.16 illustrate distribution of contact forces and angle of contact obtained from numerical modeling for two loading values.

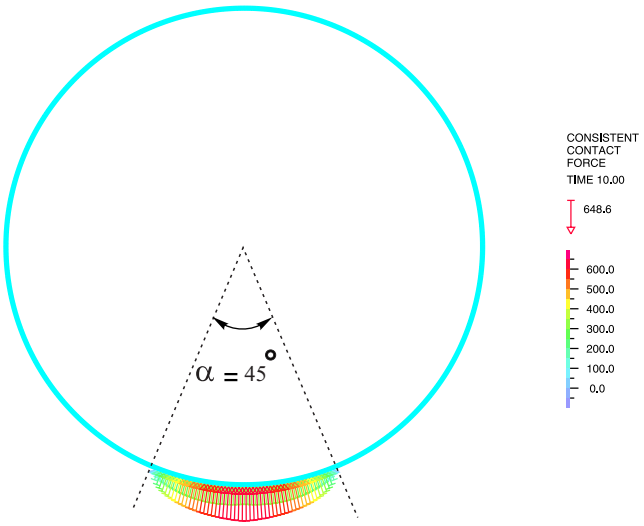

FIGURE 3.15 FEM contact force distribution (H=40 kN)

As mentioned before Persson has purposed an analytical method to obtain contact parameters for the case of contact for a cylinder in a bore of (Eq. (3.9) and Eq. (3.11)). Table 3.4 illustrates the outputs of maximum stresses and angle of contact derived from Hertz and Persson analytical methods as well as finite element modeling of the cylinders for two loading conditions.

From table 3.4 it can be concluded that for contact problem between two cylindrical bodies with opposite curvatures, Persson theory leads to similar results with numerical modeling for both smaller and higher values of loadings. However comparing to Persson, Hertz method leads to less accurate results. By referring to the results it is specifically concluded that when the applied load increases area of contact will become larger for which Hertz outputs will be considerably different from those obtained from Persson method. However comparing to the numerical values Persson leads to accurate results. From the results obtained it is concluded

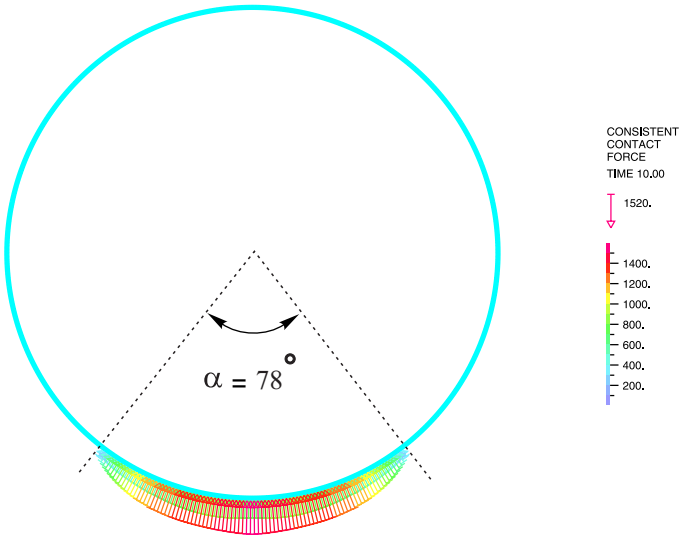

FIGURE 3.16 FEM contact force distribution (H=154 kN)

TABLE 3.4 Numerical and analytical results, bodies with similar curvature sign

	Applied load	Contact angle	Maximum stress
Methods	(kN)	(Deg.)	(MPa)
Numerical method	40	45	108
Persson method	40	45	105
Hertz method	40	47	102
Numerical method	154	78	251
Persson method	154	80	237
Hertz method	154	101	201

that for two cylindrical bodies with contact conditions in which areas of contact is large, contact parameters obtained from Hertz method will not lead to accurate values.

3.5 Conclusions

From the results obtained from finite element modeling and available analytical methods for two cylindrical bodies in contact is is concluded that (i) For two cylinders with positive curvature signs, the numerical method has accordance with that of Hertz theory. Thus this analytical method can be used effectively to estimate contact parameters. (ii) For two cylinders with different curvature signs Hertz method is not always accurate. For cases of with small areas of contact, this method can be accurate. However for larger areas of contact this method is not accurate. However for this case of contact Persson method provides accurate

results for both small and large areas of contact

CHAPTER 4

DISCUSSION ON POT BEARING DESIGN

4.1 Introduction

In chapter 2, the most important specifications which focus on design of pot bearings (European Standard EN 1337-5, AASHTO/NSBA steel bridge bearing design and detailing guidelines and Canadian Highway Bridge Design Code) were introduced and the rules prescribed by these specifications and the rationale behind them were discussed. In this chapter of the thesis, the method of design of pot bearings as a continuous process according to the available codes of practice is highlighted and the important factors as well as the simplifying assumptions made in the design of pot bearings are discussed.

4.2 Design procedure according to European Standard EN 1337-5

4.2.1 Design steps

In Fig. 4.1, the essential steps in design of fixed pot bearings according to European Standard EN 1337-5 are illustrated as a flowchart. As presented in this figure, design procedure begins with specifying elastomer pad dimensions, piston, pot and the sealing rings respectively. In order to begin design process of the bearing it is assumed that the value of some parameters is known to the designer which include, design axial force (N_{Sd}), partial safety factor (γ_{M}), design horizontal force ($V_{\mathrm{Fxy,\,Sd}}$), properties of materials ($f_{\mathrm{e,\,k}}$, F_{y}, E_{d} and F_{y}) and maximum total rotation (α_{max}). In figure 4.2, the important geometrical parameters are presented.

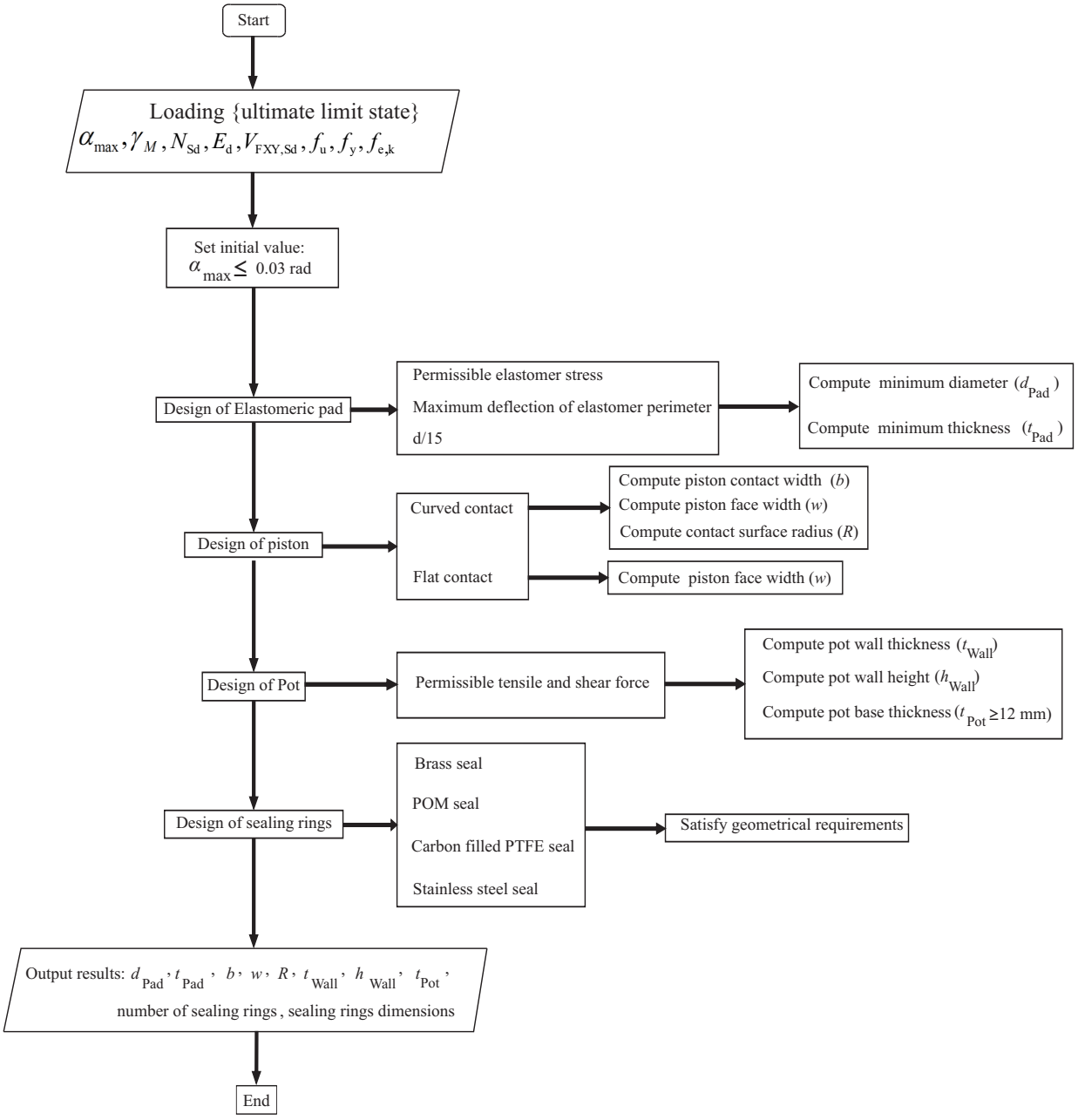

FIGURE 4.1 Pot bearing design flowchart according to EN 1337-5

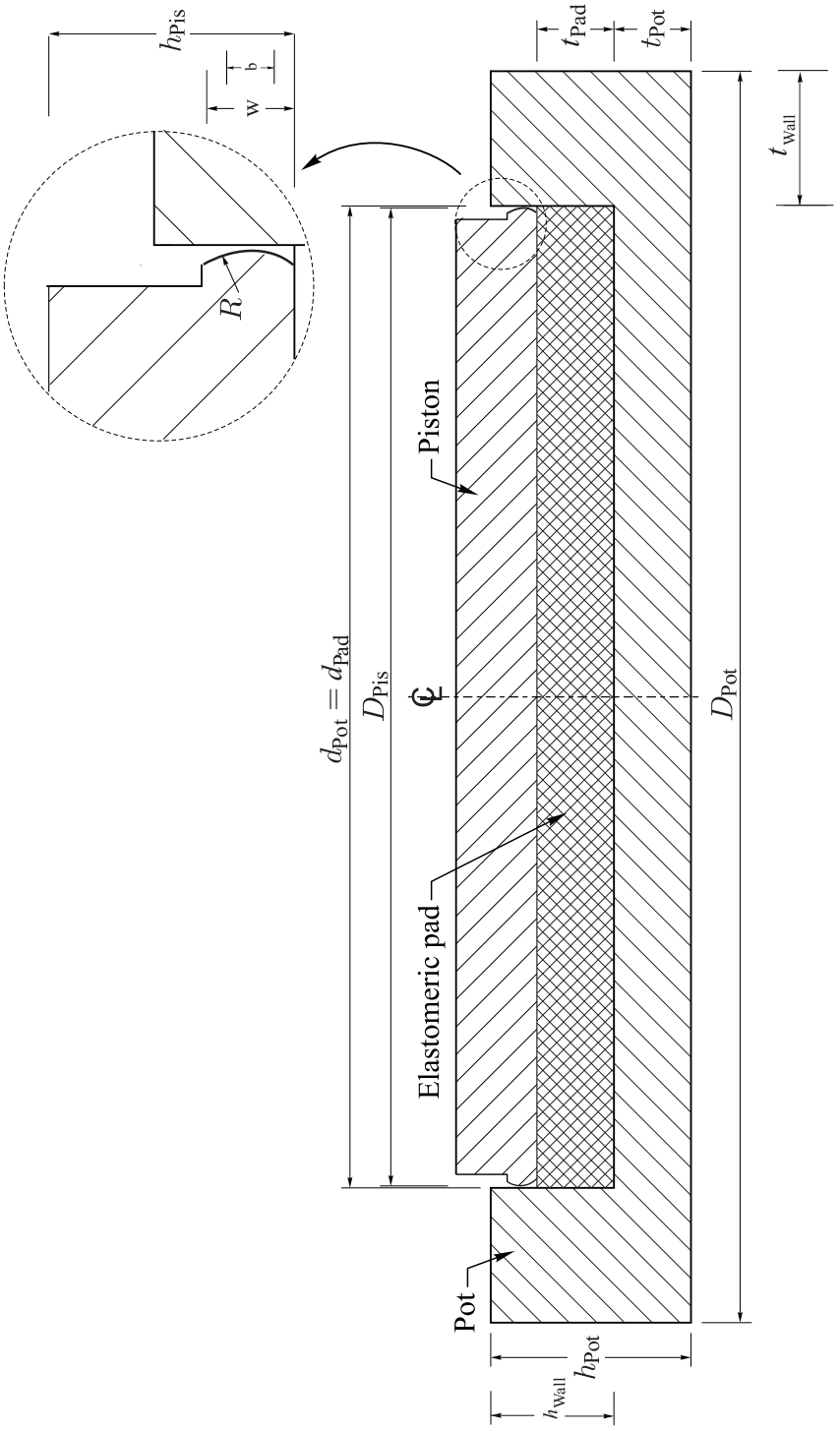

FIGURE 4.2 Geometrical design parameters for an EPB

4.2.2 Design of elastomeric pad

According to European Standard EN 1337-5, in order to specify elastomeric pad dimensions the following verifications shall be made

– Diameter

Elastomeric pad diameter is obtained by assuming design axial forces are less than or equal to the design value of resistance of elastomeric pad

$$N_{\mathrm{Sd}} \leqslant N_{\mathrm{Rd}} \tag{4.1}$$

or

$$N_{\mathrm{Sd}} \leqslant \frac{\pi}{4} d_{\mathrm{Pad}}^2 f_{\mathrm{e,k}} \tag{4.2}$$

– Thickness of the pad

The minimum thickness of the pad is specified by assuming occurrence of the maximum rotation

$$t_{\mathrm{Pad}_{min}} = 3.33\, \alpha_{\mathrm{max}}\, d_{\mathrm{Pad}} \tag{4.3}$$

Another criteria to be considered is,

$$t_{\mathrm{Pad}_{min}} \geq \frac{d_{\mathrm{Pad}}}{15} \tag{4.4}$$

4.2.3 Design of piston

Similar to pot, design of piston is also dependant on the distribution of contact forces in the horizontal plane. According to European Standard EN 1337-5, method of piston design depends on whether the piston wall is flat or curved.

Flat piston

– The width of piston face

This property shall satisfy the following equation

$$\frac{1.5\, V_{\mathrm{Sd}}}{d_{\mathrm{Pot}}\, w} \leqslant \frac{F_{\mathrm{y}}}{\gamma_{\mathrm{M}}} \tag{4.5}$$

Curved piston

– diameter and radii of curvature

These geometrical properties of a curved piston can be obtained by the following crite-

rion,

$$V_{\mathrm{Sd}} \leqslant \frac{15 f_{\mathrm{u}}^2 \, R \, d_{\mathrm{Pot}}}{E_{\mathrm{d}} \, \gamma_{\mathrm{M}}^2} \tag{4.6}$$

– Piston and pot contact width

The piston wall width in which comes into contact with pot can be obtained from

$$b = 3.04 \sqrt{\frac{1.5 V_{\mathrm{Fxy,\,Sd}} \, R}{E_{\mathrm{d}} \, d_{\mathrm{Pot}}}} \tag{4.7}$$

Also width of curved piston is obtained from

$$w = b + \alpha_{\max} d_{\mathrm{Pot}} \tag{4.8}$$

4.2.4 Design of pot

According to the available codes of practice method of design of pot and piston is considerably dependant on the distribution of contact forces in the horizontal plane from piston to the pot. As discussed in chapter 2, in European Standard EN 1337-5 it is assumed that distribution of contact forces in horizontal plane is along half of pot perimeter with a parabolic shape which leads to maximum contact pressure of 1.5 times the mean value. Then it is obvious that this simplifying assumption plays a crucial role in design process of pot bearing. In the next chapter distribution of contact forces in the horizontal plane will be discussed further and in this part of the thesis the design method of piston and pot according to the available specifications will be highlighted.

The geometrical dimensions of the pot to be determined after obtaining properties of the elastomer pad include, external diameter of the pot, height of the pot wall and thickness of pot base plate.

– External diameter of the pot

According to European Standard EN 1337-5 external diameter of the pot can be obtained by providing sufficient resistance to the shear force for the pot walls then

$$V'_{\mathrm{Sd}} \leqslant V'_{\mathrm{Rd}} \tag{4.9}$$

or

$$\frac{4 N_{\mathrm{Sd}} \, t_{\mathrm{Pad}}}{\pi d_{\mathrm{Pot}}^2} + \frac{1.5 V_{\mathrm{Fxy,\,Sd}}}{d_{\mathrm{Pot}}} \leqslant \frac{F_{\mathrm{y}} (D_{\mathrm{Pot}} - d_{\mathrm{Pad}})}{2 \, \gamma_{\mathrm{M}} \sqrt{3}} \tag{4.10}$$

– Height of pot wall

After obtaining external diameter, height of the pot wall can be determined by providing

sufficient resistance against tensile forces from the following equation

$$V_{\mathrm{Sd}} \leqslant V_{\mathrm{Rd}} \tag{4.11}$$

or

$$\frac{4N_{\mathrm{Sd}}\, t_{\mathrm{Pad}}}{\pi d_{\mathrm{Pot}}} + V_{\mathrm{Fxy,\,Sd}} \leqslant \frac{F_{\mathrm{y}}\,(D_{\mathrm{Pot}} - d_{\mathrm{Pot}})h_{\mathrm{Wall}}}{\gamma_{\mathrm{M}}} \tag{4.12}$$

– Thickness of pot base

Pot base thickness can be obtained by providing sufficient resistance against tensile forces applied to the base by

$$V_{\mathrm{Sd}} \leqslant V_{\mathrm{Rd}} \tag{4.13}$$

or

$$\frac{4N_{\mathrm{Sd}}\, t_{\mathrm{Pad}}}{\pi d_{\mathrm{Pot}}} + V_{\mathrm{Fxy,\,Sd}} \leqslant \frac{F_{\mathrm{y}} d_{\mathrm{Pot}}\, t_{\mathrm{Pot}}}{\gamma_{\mathrm{M}}} \tag{4.14}$$

4.2.5 Design of sealing rings

According to European Standard EN 1337-5, sealing rings can be chosen from brass, POM, carbon filled PTFE or stainless steel material. In this standard the dimensions and material properties of the internal seals are based on the experimental tests which led to more satisfactory behaviour of pot bearing. The specifications about diameter, cross section, slits and number of rings and material requirements are stated in Annex A of European Standard EN 1337-5.

4.2.6 Additional conditions

After determining the primary dimensions of elastomeric pad, pot and the piston, according to European Standard EN 1337-5, additional conditions shall be satisfied including

$$h_{\mathrm{Wall}} \geqslant t_{\mathrm{Pad}} + 0.5\,(w - b) + (0.5\,\alpha_{\max}\, d_{\mathrm{Pot}}) + a_{\mathrm{d}} \tag{4.15}$$

and for the parameter h_{p} as illustrated in Fig. 4.3 we have

$$h_{\mathrm{p}} = h_{\mathrm{Wall}} - t_{\mathrm{Pad}} + a_{\mathrm{d}} + (0.5\,\alpha_{\max}\, d_{\mathrm{Pot}}) \tag{4.16}$$

where a_{d} is a safety factor of

$$a_{\mathrm{d}} = \min\left[\max(0.01\, D_{\mathrm{Pot}}, 3\,\mathrm{mm}), 10\,\mathrm{mm}\right] \tag{4.17}$$

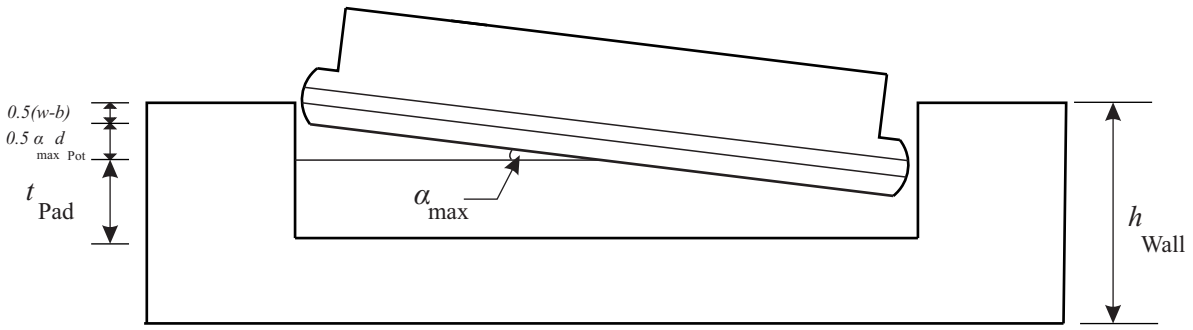

FIGURE 4.3 Geometrical conditions for rotation according to EN 1337-5

4.3 Design procedure according to AASHTO/NSBA

Pot bearing design procedure according to this specification is similar with that of European Standard in determining elastomer dimensions. However comparing to European Standard EN 1337-5, AASHTO Specification assumes transmission of horizontal forces through bending mechanism and bursting moments rather that shear and tensile stresses. This assumption leads to several differences in pot bearing design procedure. The method of pot bearing designed is presented in Fig. 4.4 as a flowchart.

4.3.1 Design of elastomeric pad

– Thickness of the pad
  Similar to European Standard EN 1337-5 the minimum thickness of the pad according to AASHTO is specified by assuming occurrence of the maximum rotation thus the maximum deflection

$$h_{\mathrm{Pad}_{min}} = 3.33\,\alpha_{\max}\,d_{\mathrm{Pad}} \tag{4.18}$$

– Diameter of the pad
  AASHTO specification states maximum compressive stress of 25 MPa which leads to a minimum value of pad and pot diameter.

4.3.2 Design of pot

– Pot wall thickness
  According to AASHTO pot wall thickness can be obtained from

$$t_{\mathrm{Wall}} \geqslant \sqrt{\frac{25 H_{\mathrm{u}}\,\alpha_{\max}}{F_{\mathrm{y}}}} \tag{4.19}$$

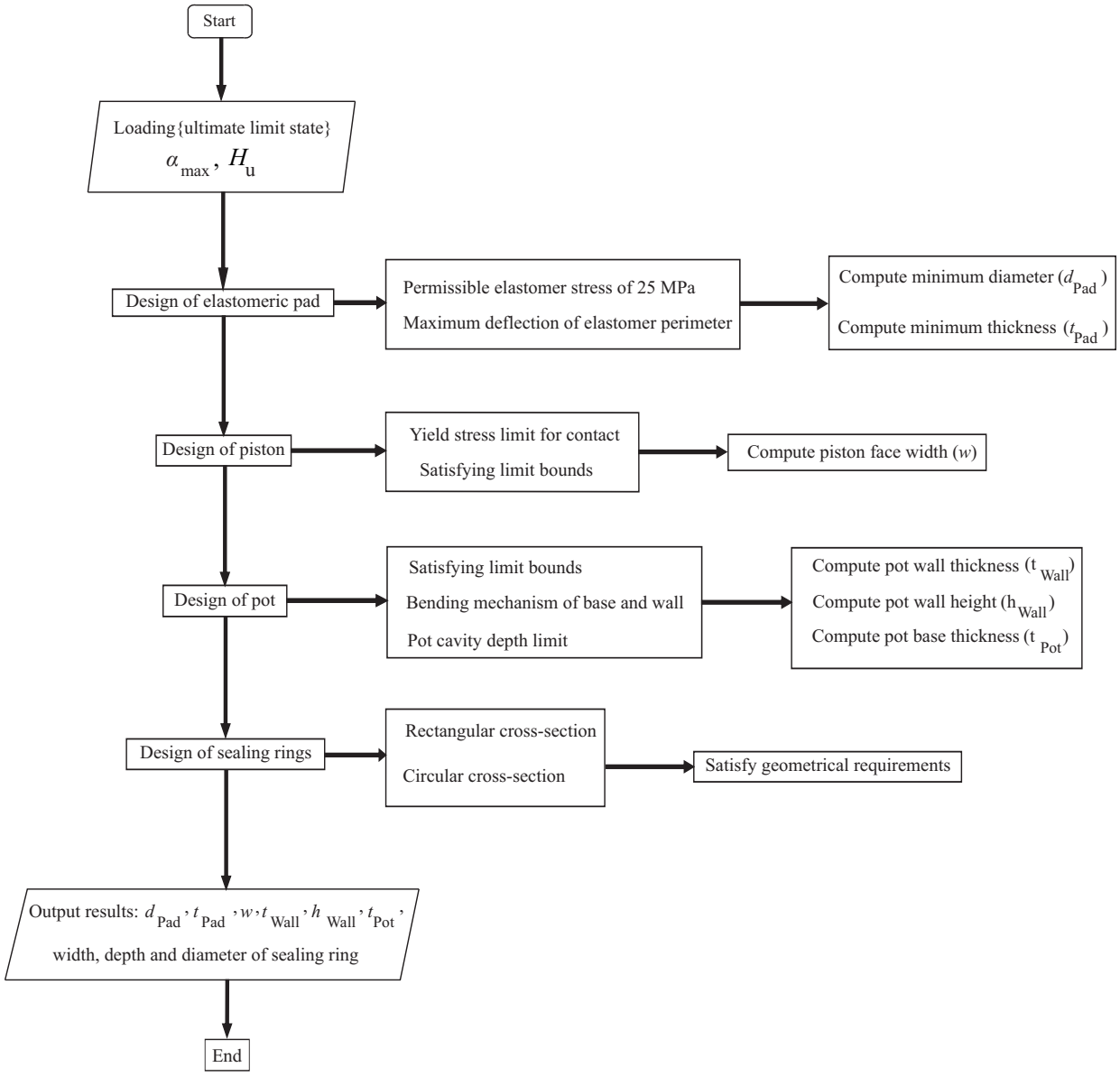

FIGURE 4.4 Pot bearing design flowchart according to AASHTO

– Pot cavity depth
  This parameter according to AASHTO Specifications can be obtained from

$$h_{\text{Wall}} \geqslant (0.5\,\alpha_{\max}\,D_{\text{Pot}}) + t_{\text{Pad}} + w \tag{4.20}$$

– Pot base thickness
  According to AASHTO pot wall thickness can be obtained from

$$t_{\text{Pot}} \geqslant \sqrt{\frac{25 H_{\text{u}}\,\alpha_{\max}}{F_{\text{y}}}} \tag{4.21}$$

  Also depending on where the bearing is placed the following bounds should be satisfied.
  Bearing directly against concrete or grout :

$$t_{\text{Pot}} \geqslant 0.06\,d_{\text{Pot}} \tag{4.22}$$

  and

$$t_{\text{Pot}} \geqslant 20\,\text{mm} \tag{4.23}$$

  bearing directly on steel girders or load distribution plates :

$$t_{\text{Pot}} \geqslant\ 0.04 d_{\text{Pot}} \tag{4.24}$$

  and

$$t_{\text{Pot}} \geqslant 12.5\,\text{mm} \tag{4.25}$$

4.3.3 Design of piston

The specifications related to piston design in AASHTO is only limited to flat piston type by assuming a parabolic distribution of contact forces. According to this specification similar to EN 1337-5 width of piston face can be obtained from

$$w \geq \frac{1.5 H_{\text{u}}}{d_{\text{Pot}} F_{\text{y}}} \tag{4.26}$$

4.3.4 Sealing rings

AASHTO allows use of multiple flat brass rings, circular brass rod formed and brazed into a ring and plastic rings with performing tests which verify proper behaviour of the bearing. However if rings with rectangular or circular cross section are used according to AASHTO specifications, they will not require testing since their behaviour has already been verified.

4.3.5 Additional conditions

– Vertical clearance between top of piston and top of pot wall :
According to AASHTO, this parameter can be determined from

$$h_{\mathrm{P}} \geqslant R_0 \alpha_{\max} + 2\delta_{\mathrm{u}} + 3 \tag{4.27}$$

– Clearance between diameter of piston and pot :
The diameter of piston rim is equal to inside parameter of the pot less the clearance c_1. This value should not be less than 0.5 mm. For cylindrical piston rim,

$$c_1 \geqslant \alpha_{\max}(w - \frac{d_{\mathrm{Pot}}\ \alpha_{\max}}{2}) \tag{4.28}$$

CHAPTER 5

PARAMETRIC ANALYSIS OF POT BEARINGS

5.1 Introduction

As previously discussed, transmission of forces from piston plate to the pot in an elastomeric pot bearings takes place through contact between the two bodies. Thus taking account of contact problem is crucial to design a pot bearing for which hard contact between piston and pot during cyclic rotations does not occur. As discussed in chapters 2 and 4, EN 1337-5 is considered as one of the most comprehensive specifications which introduces the possibility of designing the pot wall as curved or flat. Also the design procedure of bearing parts is based on the assumption that contact forces are transferred through half of bearing perimeter. Also in chapter 3 the accuracy of finite element modeling outputs for Hertz and Persson contact condition was approved by comparing the analytical and numerical procedures for 2D problems. As stated in this chapter for two cylinders with different curvature signs and relatively very close radius, the contact parameters obtained from Hertz theory (angle of contact and maximum stress) are not accurate comparing to Persson method.

In this chapter first available types of contact in a pot bearing will be introduced. Next a finite element model of an elastomeric pot bearing will be developed. The finite element model generated is designated for bearings with small ratios of pad thickness to piston contact width. Also a more simplified finite element model of a disk and a ring in contact will be presented which simulates contact condition between piston and the pot in an elastomeric pot bearing. The model is generated for numerous disk and ring models with similar geometrical and loading conditions in a pot bearing. As the next step, the important parameters which act effective in the contact angle values between the ring and the disk are are combined with those employed in Persson method due to accuracy of this method for 2D problems as discussed in chapter 3. Finally a regression analysis is performed on the contact angle outputs derived from finite element modeling of disk and ring and an equation is developed to obtain contact angle values in disk and ring model.

5.2 Types of contact between piston and pot

In a pot bearing distribution of forces from piston to the pot takes place through two directions. First, the loads are transferred from piston wall to the pot wall in the vertical plane of the bearing. As discussed in chapter 2, in the latest version of EN 1337, this type of

load distribution is studied by classifying piston wall as flat or curved. In this specification parameter b is the length of the piston wall through which contact forces are transferred vertically to pot wall. As previously mentioned, the equations in EN 1337-5 for curved vertical contact are based on assuming contact conditions take place according to Hertz theory. Then in chapter 3 the accuracy of this assumption was verified by comparing the results of two cylindrical bodies in 2D. In Fig. 5.1 the plane in which vertical contact takes place is illustrated. In this chapter it is supposed that piston wall is from flat type.

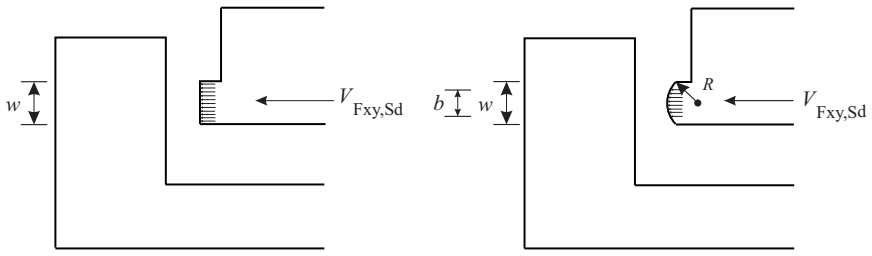

FIGURE 5.1 Distribution of contact forces in vertical plane

The second type of distribution of contact surfaces takes place in the horizontal plane of the bearing. This type of contact force distribution actually takes place through a portion of bearing perimeter. As mentioned in chapter 2, EN 1337-5, AASHTO and CHBDC have prescribed this portion as half of bearing perimeter (or 180 °) as illustrated in Fig. 5.2. In design procedures according to EN-1337 this parameter will take part in determining both piston and pot properties due to taking account shear forces in the pot walls. However in AASHTO and CHBDC, angle of contact plays active only in determining piston dimensions due to taking into account bending mechanism of the pot. As it was stated previously in chapter 2, factor of 1.5 which is available in the equations regarding to design of piston and pot is related to this assumption. Then it can be concluded that value of angle of contact plays an important role in design procedure of the pot bearing.

In the next sections of this chapter more focus will be paid on distribution of contact forces in the horizontal plane of the bearing by performing numerical analysis on pot bearing and disk and ring models.

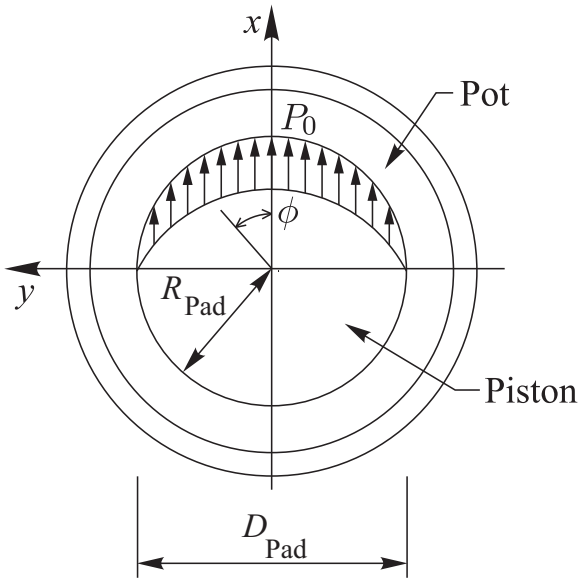

FIGURE 5.2 Distribution of contact forces of EPBs in horizontal plane

5.3 Pot bearing finite element model

As discussed in the previous parts the angle of contact between piston and pot is the parameter that can be used effectively to calculate design tensile and shear forces in a pot bearing. The objective of this section is to develop a 3D finite element model of pot bearing and measure value of contact angle.

Finite element modeling of a pot bearing requires advance modeling analysis techniques due to existence of elastomeric pad as a highly incompressible material and complex mechanisms involving nonlinear contact interactions between different parts of pot bearing in 3D. In this research, numerous types of finite element modeling were generated to simulate behaviour of a pot bearing in 3D by ADINA software. Finally in order to model the bearing the effect of sealing rings was neglecting by assuming that elastomeric pad occupies the whole volume between the piston and the pot. The details of the generated model are highlighted as,

- Geometry

  The geometrical properties and loading values of the bearings were extracted from the properties of fixed pot bearings with flat piston wall designed by D.S.Brwon, a manufacturer of engineered products for the bridges (D.S.Brwon 2013) and also by referring to AASHTO apecifications. The material of piston and the pot is assumed as Grade 350W, with Young's modulus of $E = 200\,\text{GPa}$ and Poisson's ratio of $\nu = 0.287$, ultimate strength of $F_\text{u} = 450\,\text{MPa}$ and yield strength of $F_\text{y} = 350\,\text{MPa}$.
- meshing

  Since contact forces are effective along a portion of bearing perimeter, the pot bearing is subdivided into four quadrants I to IV as illustrated in Fig. 5.3 and the mesh density selected for quadrant I of piston and pot is higher than the other quadrants as presented in figures 5.4 and 5.5. This step is taken to optimize the mesh density to the most critical zones, reduce computational burden, and enhance the quality of the numerical results. The different components are meshed using 3D solid linear isoparametric finite elements and mesh construction is dictated by a compromise between the quality of the numerical models and reasonable computational cost.
- Loading

  As mentioned earlier the effects of the pad in the bearing was taken into account by applying a hydrostatic pressure on base and walls of the pot, therefor a uniform pressure due to the applied vertical loads on the elastomeric pad is assigned to all the faces of the pot in contact with the pad as illustrated in Fig. 5.6 for one quadrant.

  To apply the horizontal forces, since the resulting mesh density is not uniform over

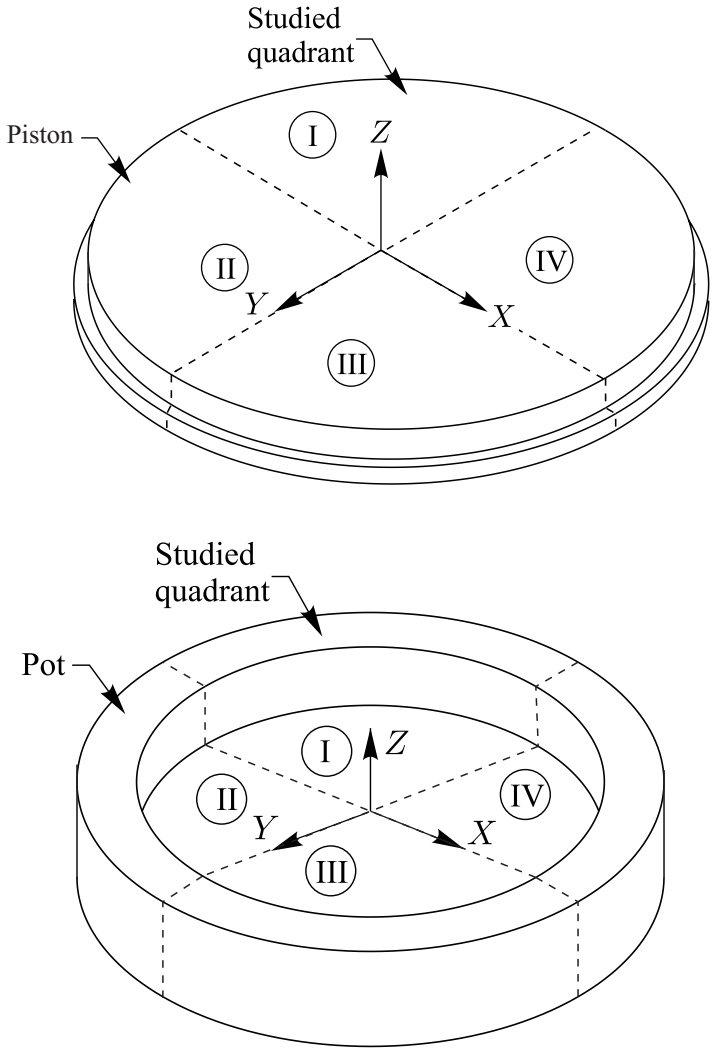

FIGURE 5.3 Geometrical design parameters for pot bearing model

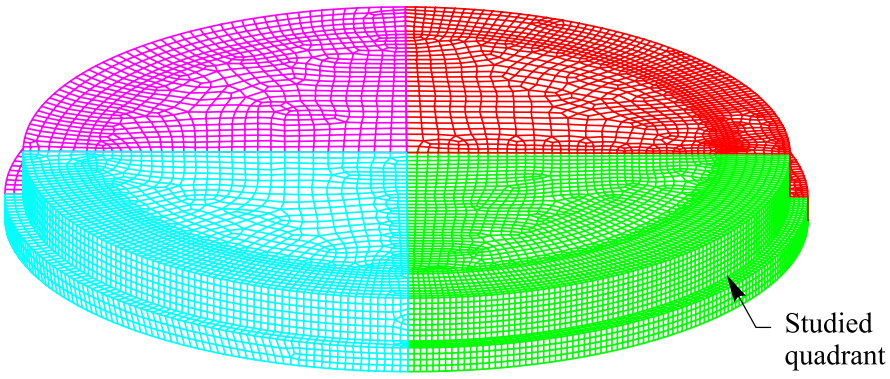

FIGURE 5.4 Generated meshing for piston quadrants

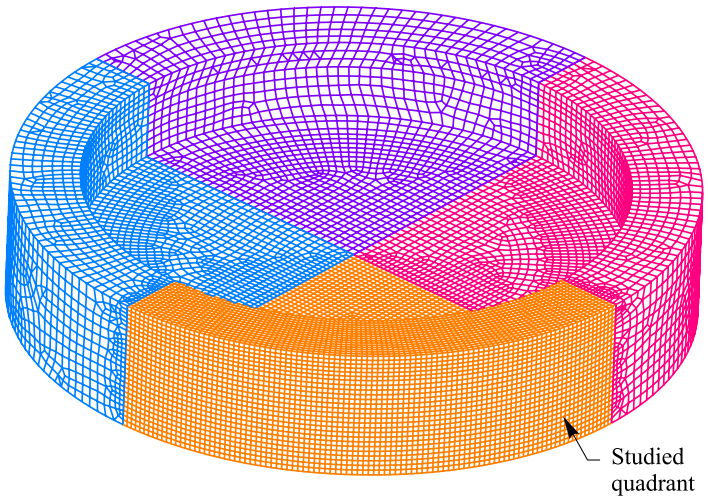

FIGURE 5.5 Generated meshing for pot quadrants

piston upper face, a uniformly meshed thin circular transfert plate is glued to this face to ensure a uniform distribution of the horizontal loads. In Fig. 5.7 the horizontal loads applied to the plate are presented.

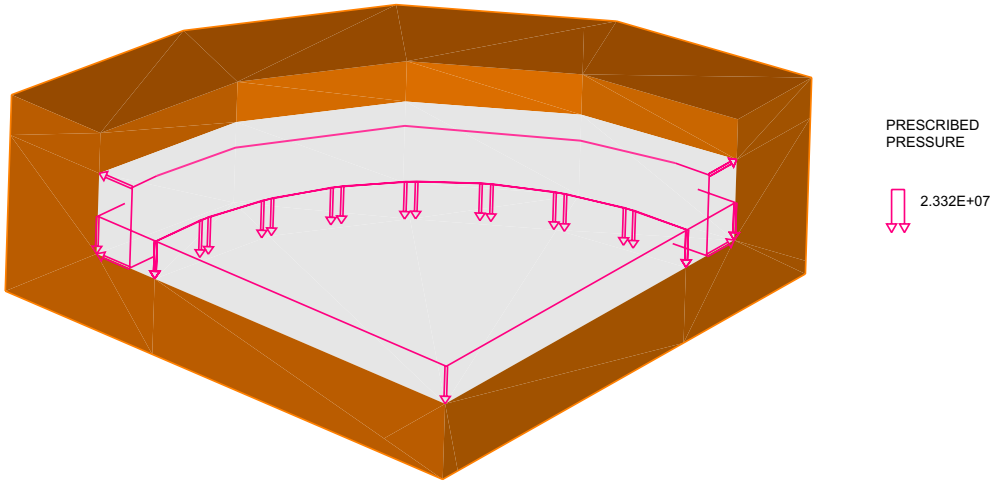

FIGURE 5.6 Applied pressure due to vertical loading

– Boundary conditions

  To simulate the movement of the piston in the bearing, the boundary conditions assigned to the lower face of the piston is such that it can move freely in the horizontal plane of the bearing. Also it is assumed that the bearing is completely fixed in the base of the pot.

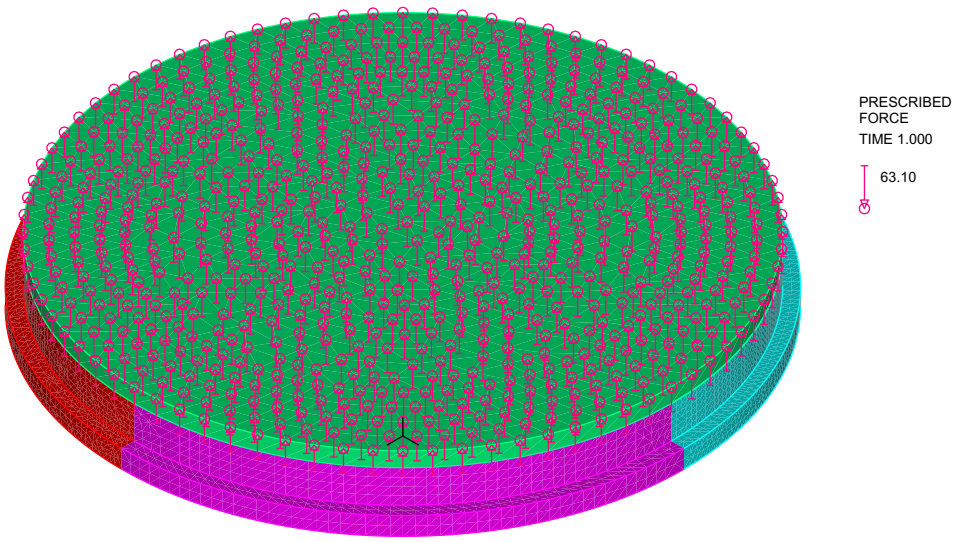

FIGURE 5.7 Loads applied to the transfert plate

5.4 Disk and ring finite element model

The model generated from modeling piston, pot and the base plate discussed in the previous section still imposed computation burden, thus there was an essential need for a more simplified model. To fulfill this objective, numerous trials were performed to generate a more simplified numerical model which simulates contact conditions available in a pot bearing. Finally the simplified model was generated from modeling a disk in a ring with equal thicknesses. Disk and ring were modeled by cutting the piston and the pot at lower and upper sections where they come into contact. For better illustration the sections where the bodies are cut to generate disk and ring models are illustrated in Fig. 5.9. Also the general geometry of disk and ring model is presented in Fig. 5.8.

In order to study variation of contact angle for disk and ring models, numerous samples were created with different geometrical and loading properties of ring and disk models. These properties were extracted from fixed pot bearings designed by D.S.Brwon, a manufacturer of engineered products for the bridges as well as AASHTO design specifications (D.S.Brwon 2013). The material of disk and ring is similar to piston and pot and similar to the case of pot bearing, disk and the ring are meshed for four quadrants for efficient modeling. Also the horizontal loads were applied to a transfert plate which is glued to the disk similar to pot bearing model. Comparing to the bearing, the boundary conditions applied to the ring is such that it is completely fixed along the perimeter instead of the base. However the boundary condition for the disk is similar to the piston in pot bearing model. The vertical loads applied to the bearing were ignored in the simplified models since after

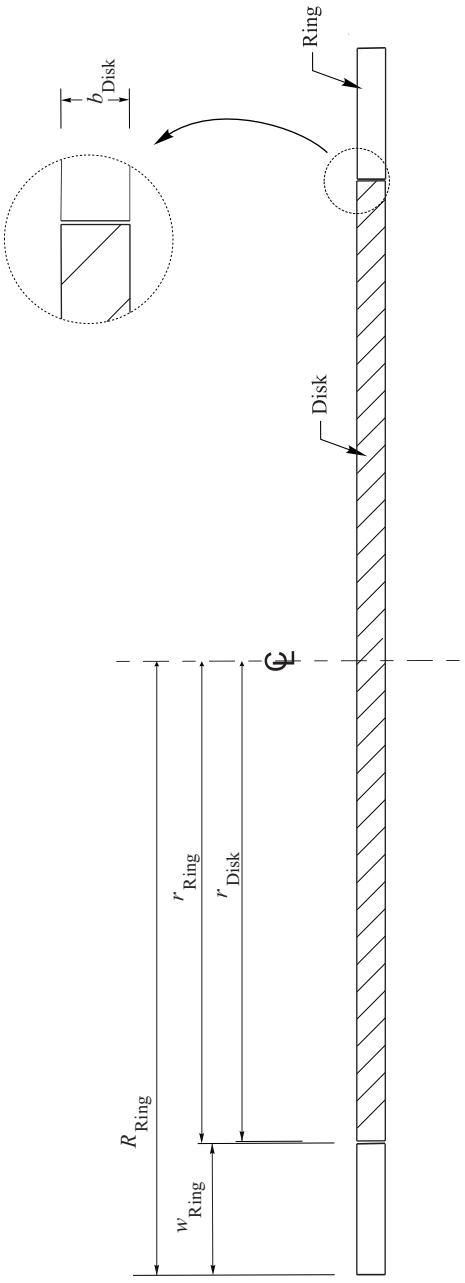

FIGURE 5.8 Geometrical design parameters for disk and ring model

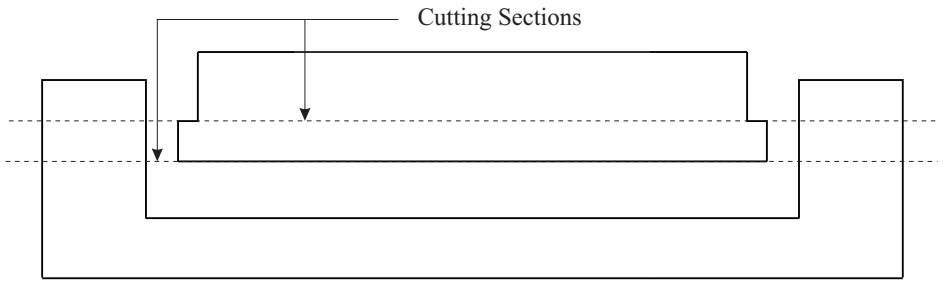

FIGURE 5.9 Sections cut in the bearing to generate ring and disk model

numerous trial and errors it became clear than vertical loads do not play an important role in distribution of contact forces in the horizontal plane.

After generation of the model, contact angles obtained from disk and ring models were compared to the ones corresponding to the pot bearing. Finally disk and ring model was accepted as a simplified model due to very close results with contact angle in pot bearings.

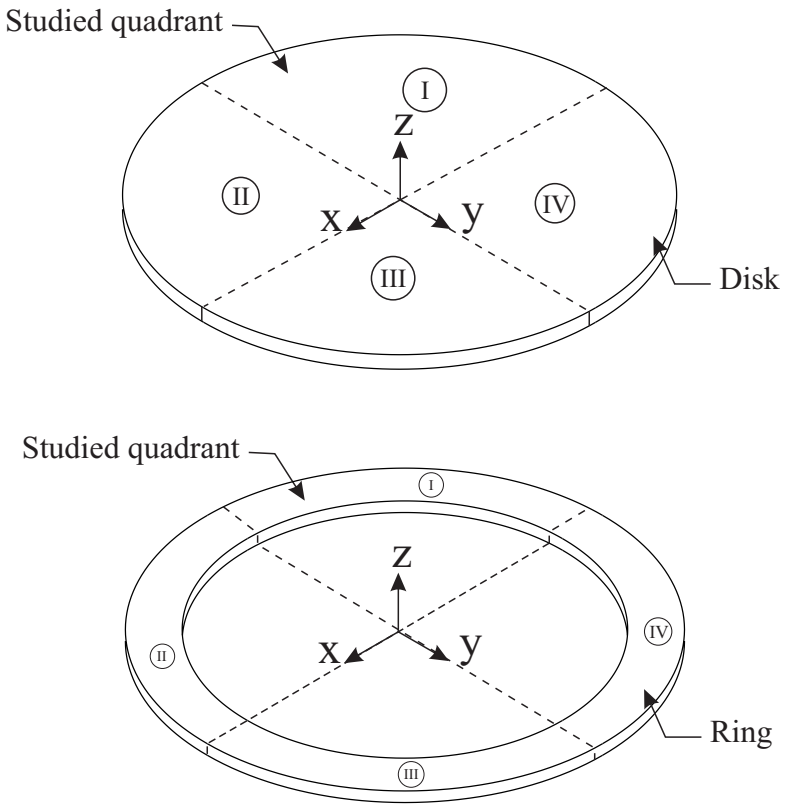

FIGURE 5.10 Subdivision of disk-ring model into four quadrants

5.5 Parametric regression analysis

In chapter 3 the analytical methods to obtain contact angle between two bodies in contact in 2D were discussed and their accuracy were investigated by comparing the numerical results with the analytical outputs. In this chapter it was also proved that for 2D contact between two bodies with small radius difference Hertz method does not provide accurate results while Persson method outputs were still close to the numerical results. In the previous part of current chapter simplified model of disk and ring was presented to simulate contact conditions in a pot bearing.

As it is clear the geometrical conditions available in a pot bearing has more conformity with Persson method comparing to Hertz since piston and pot have very close radii and also because in Persson method cylindrical bodies are assumed as plane stress. On the other hand some assumptions made in Persson method do not exist in contact conditions between disk and ring (or pot bearing). This is due to the fact that Persson method is valid for 2D problems, also the width of the ring is considered as infinite in this method. In the following parts of this chapter it will be illustrated that the angle of contact obtained from Persson method does not lead to accurate results for disk and ring (or pot bearing) by comparing them to those of numerical method.

The objective of this section is to perform a parametric regression analysis by referring to the numerical results obtained from disk and ring models as well as by taking account of parameters effective in Persson method. The parametric regression analysis performed in the context of this research includes the following steps,

- Determining the effective parameters
  The parameters which define geometrical and loading properties of disk and ring models include applied horizontal force (H), radius of the disk (r_{Disk}), inner radius of the ring (r_{Ring}), width of the ring (w_{Ring}) and thickness of the bodies (b_{Ring}).
- Highlighting the parameters effective in Persson method
  Due to the fact that Persson method proved to be accurate for 2D peroblems as discussed in chapter 3 (if the assumptions of the method are satisfied), the parameters effective in this method were used for the parametric analysis. These parameters are in the terms of the ratio $\frac{E\Delta R}{Q}$ where Q is the distributed load ($\frac{H}{b_{\text{Ring}}}$) and ΔR is the difference of disk radius and inner radius of the ring. In the models generated it is assumed that the bodies are made from steel with Young's modulus of $E = 200\,\text{GPa}$ and the difference of disk radius (r_{Disk}) with the inner radius of the ring (r_{Ring}) is 1mm. By using $\frac{E\Delta R}{Q}$, two parameters of the applied force and the thickness of bodies in contact will be taken into account in one parameter.

– Determining the final parameters to be used in regression analysis
  Finally the parameters that will be taken into account for the parametric regression analysis include $\frac{E\Delta R}{Q}$, w_{Ring} and r_{Ring}.

5.5.1 Models generated for regression analysis

After verifying the contact angle obtained from disk and ring numerical model by comparing it to the corresponding pot bearing numerical model, it was decided to perform regression analysis on the numerical contact angles obtained from disk and ring models. Thus numerous models for disk and ring with various loading and geometrical conditions were developed for regression analysis. As mentioned previously, the properties of the ring and disk models were derived from actual pot bearings designed by D.S.Brwon, a manufacturer of engineered products for the bridges (D.S.Brwon 2013) and also by referring to AASHTO specifications (AASHTO 2012). The geometrical properties of these models are presented in annex A. The models generated for disk and ring can be classified into two groups,

– The models with constant inner radius of the ring (r_{Ring})
– The models with various geometrical and loading properties

In other words the parametric study on disk and ring outputs was performed in two steps. This procedure was taken due to the fact that number of variables which play role in the numerical contact angle were more than two. Thus in the first step one model adopted from the ones designed by D.S.Brwon (D.S.Brwon 2013) was chosen (model number 1) from which numerous models were generated by assigning various values for applied horizontal loads ($0.25H$, $0.5H$, $1H$, $2H$ and $3H$) with various values of width of ring ($0.5w_{\text{Ring}}$, $1w_{\text{Ring}}$, $2w_{\text{Ring}}$, $3w_{\text{Ring}}$ and $4w_{\text{Ring}}$). In other words by keeping radius of the ring (r_{Ring}) as constant, number of variables in the parametric study changed from three to two. The properties of these models are included in annex B.

The parametric analysis was performed with fitting feature in MATLAB by assigning the two variables to the program ($E\Delta R/Q$ and w_{Ring}) as x and y and the numerical outputs obtained from model numbers 1 to 25 (Annex B) as z. By performing numerous trial and errors the best fitting function in terms of these two variables to for angle of contact value was obtained as,

$$\alpha_1 = 39.05 \left[\frac{E\Delta R}{Q}\right]^{-0.339} (w_{\text{Ring}})^{0.1704} \tag{5.1}$$

Fig. 5.11 illustrates dispersion of the data of first group of models comparing to α_1 surface obtained from Eq. (5.1). Also in figures 5.12 to 5.16 for different values of horizontal loads changes of α_1 is illustrated for models with a specific w_{Ring} as well as numerical and Persson

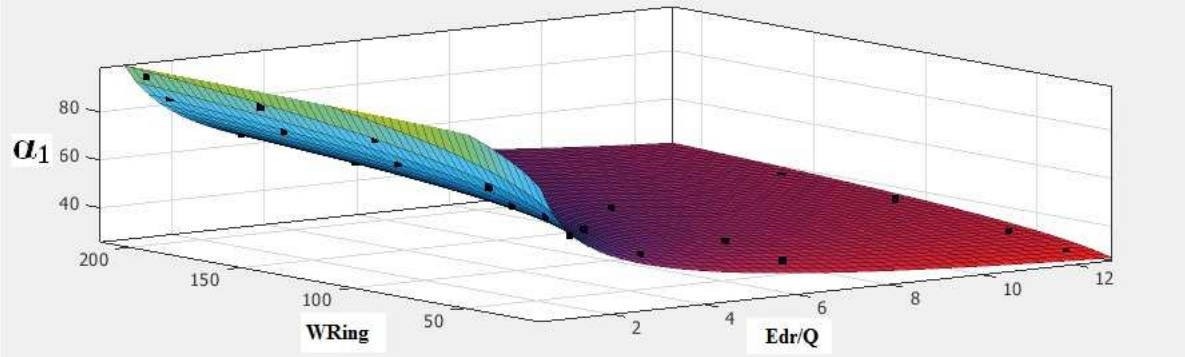

FIGURE 5.11 Presentation of the function obtained from step 1

method results. As it is clear from the figure, Persson method values do not provide accurate results for disk and ring case.

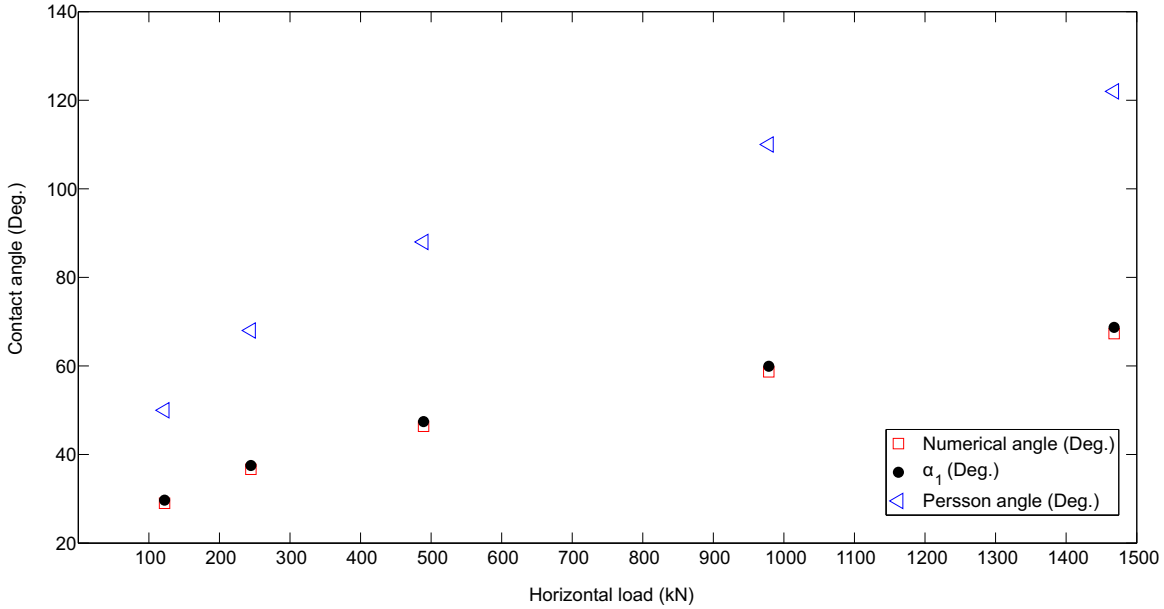

FIGURE 5.12 Comparing α_1 with numerical and persson results for $0.5w_{\text{Ring}}$

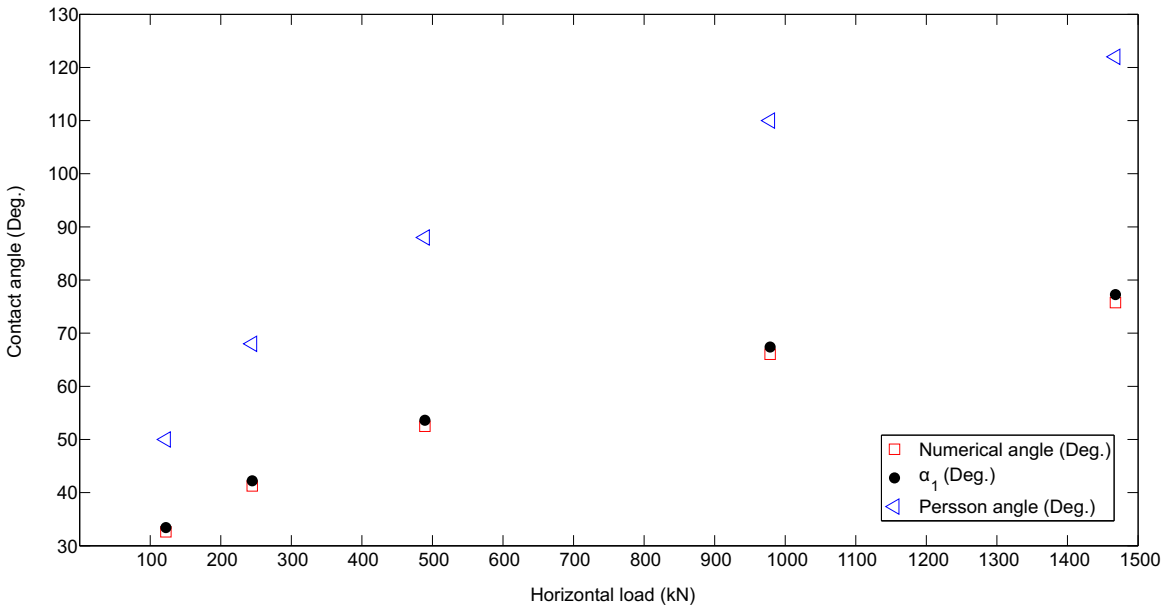

FIGURE 5.13 Comparing α_1 with numerical and persson results for $1w_{\text{Ring}}$

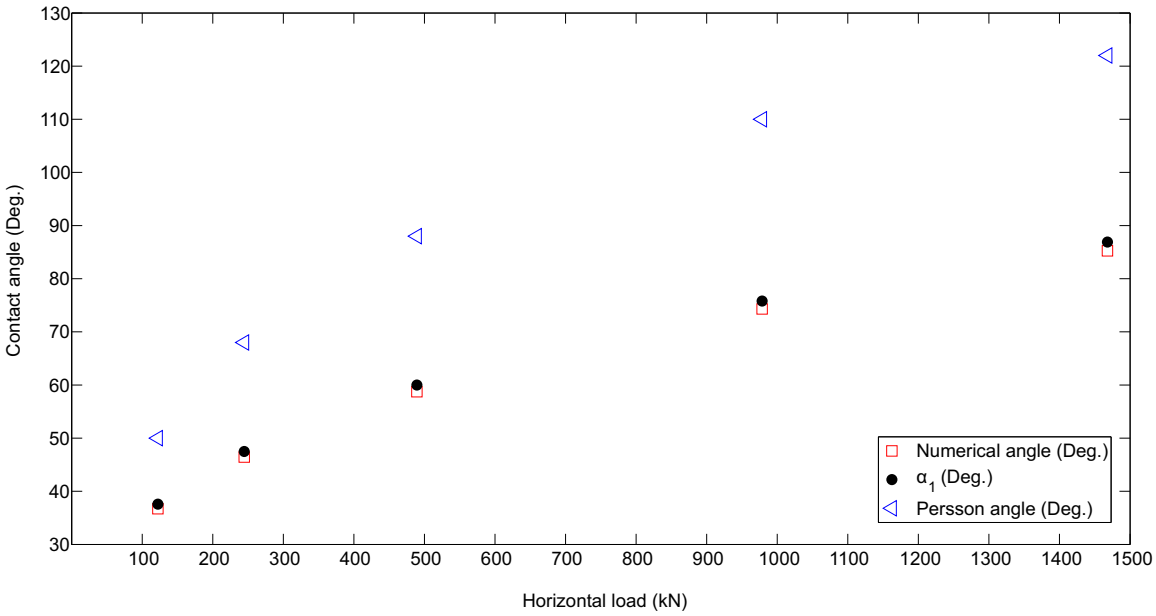

FIGURE 5.14 Comparing α_1 with numerical and persson results for $2w_{\text{Ring}}$

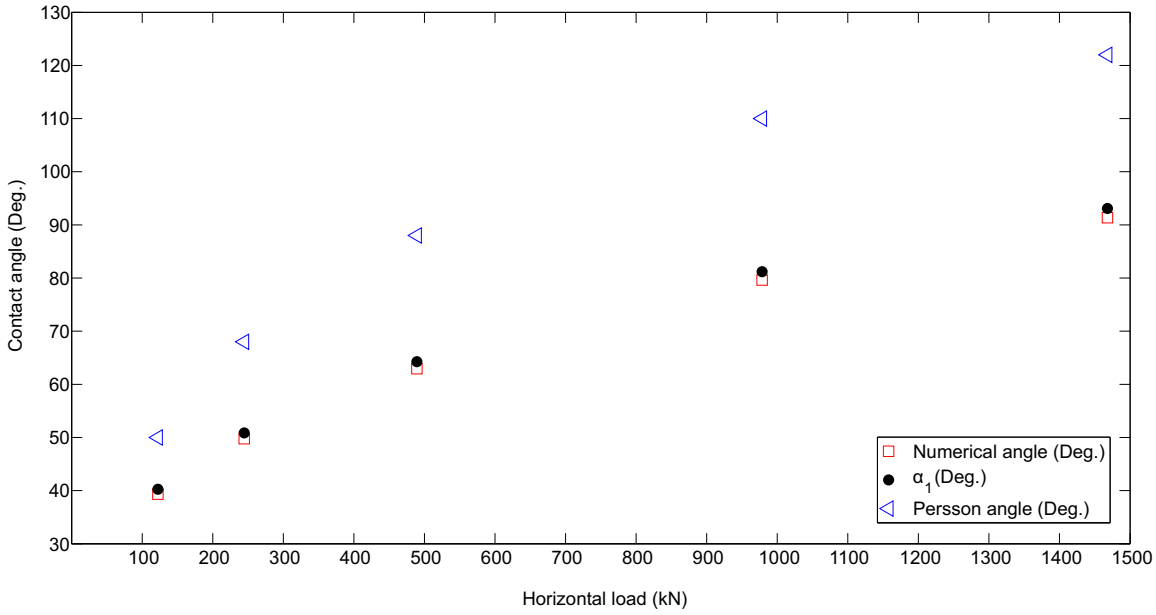

FIGURE 5.15 Comparing α_1 with numerical and persson results for $3w_{\text{Ring}}$

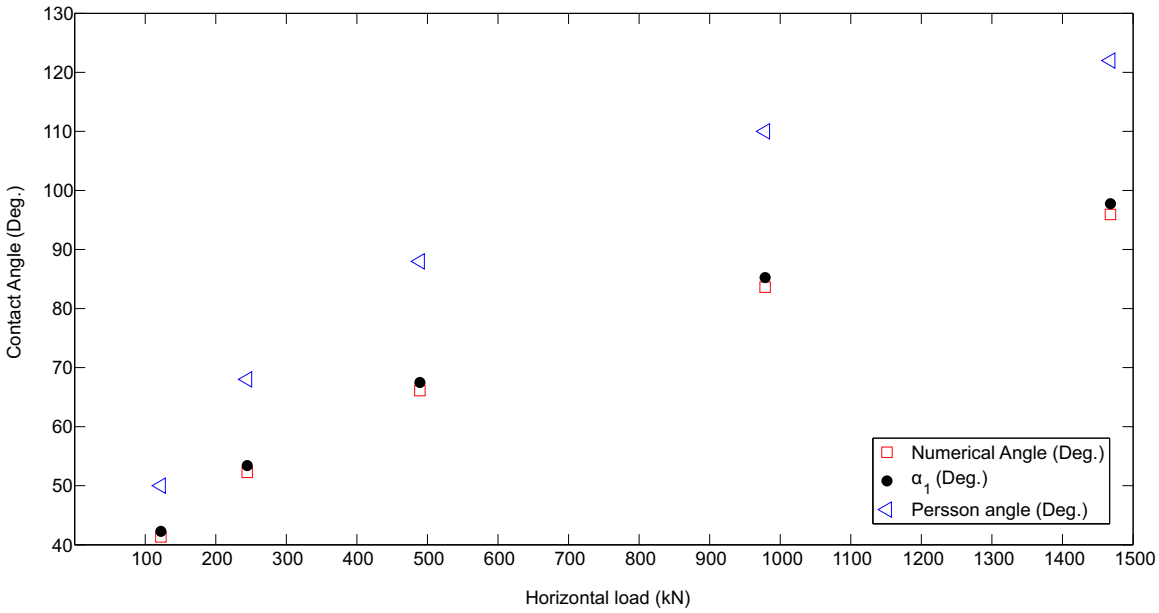

FIGURE 5.16 Comparing α_1 with numerical and persson results for $4w_{\text{Ring}}$

The second part of parametric analysis was performed by taking into account all the models generated for disk and ring models (models 1 to 50 from annex A.1 and A.2). In this step α_1 and r_{Ring} were assigned to fitting feature of MATLAB as x and y values and the numerical outputs obtained from finite element modeling az z values. The equation obtained from this step of regression analysis is considered as the final equation which takes account of all the variables presented before.

$$\alpha_{\text{f}} = 73.05 \times \left[\frac{E\Delta R}{Q}\right]^{-0.337} (w_{\text{Ring}})^{0.169} (r_{\text{Ring}})^{-0.1095} \tag{5.2}$$

Fig. 5.17 illustrates the numerical data and surface of α_f in terms of the α_1 and r_{Ring}. As mentioned before this equation is generated from disk-ring models of bearings with small ratios of pad thickness to piston contact width. Thus this method can be used for such bearings. Also in figures 5.18 to 5.21 variation of contact angle obtained from Eq. (5.2) is compared with numerical and Persson method results in terms of different variables for models 26 to 50.

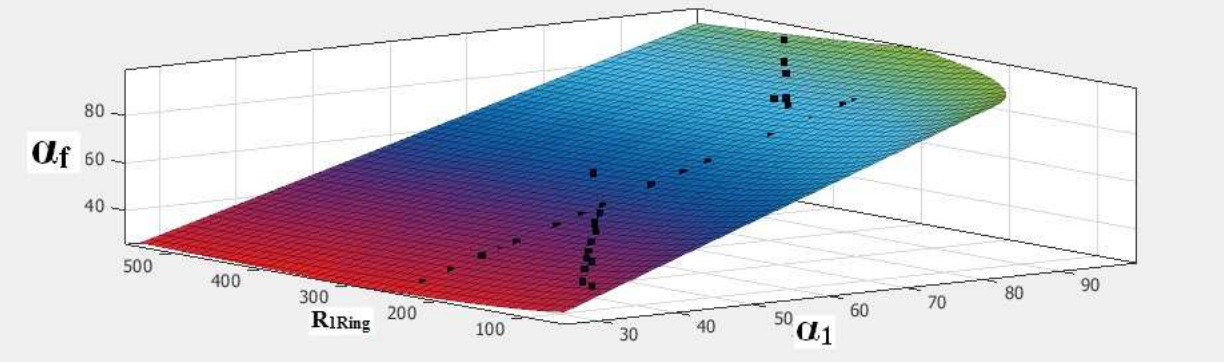

FIGURE 5.17 Presentation of the final function to obtain angle of contact

5.6 Verification of the developed equation

In the previous section Eq. (5.2) was developed as a method to estimate contact angle in disk and ring model. In this section the accuracy of this method is assessed by performing finite element analysis on some models not included in the regression analysis. The properties of these models are presented in Annex A (models 51 to 73 from annex A.3) and the contact angles obtained from Eq. (5.2) are compared to the numerical outputs as presented in figures 5.22 to figures 5.25 in terms of different variables. As it is clear from these figures, the equation developed can estimate the numerical angle of contact with acceptable

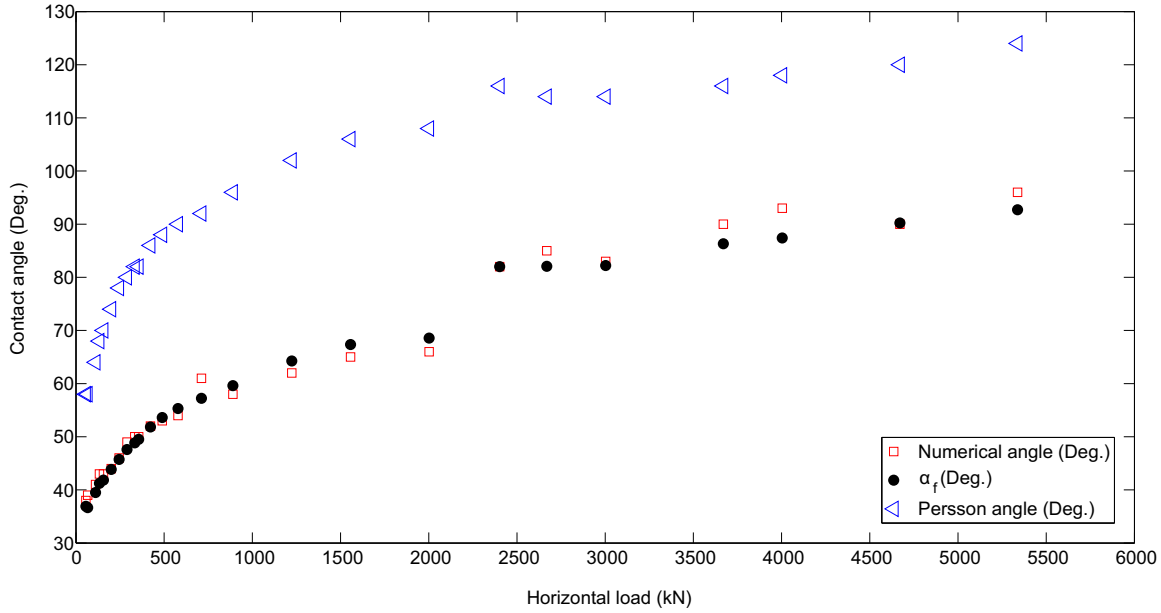

FIGURE 5.18 Variation of contact angle in terms of horizontal loads

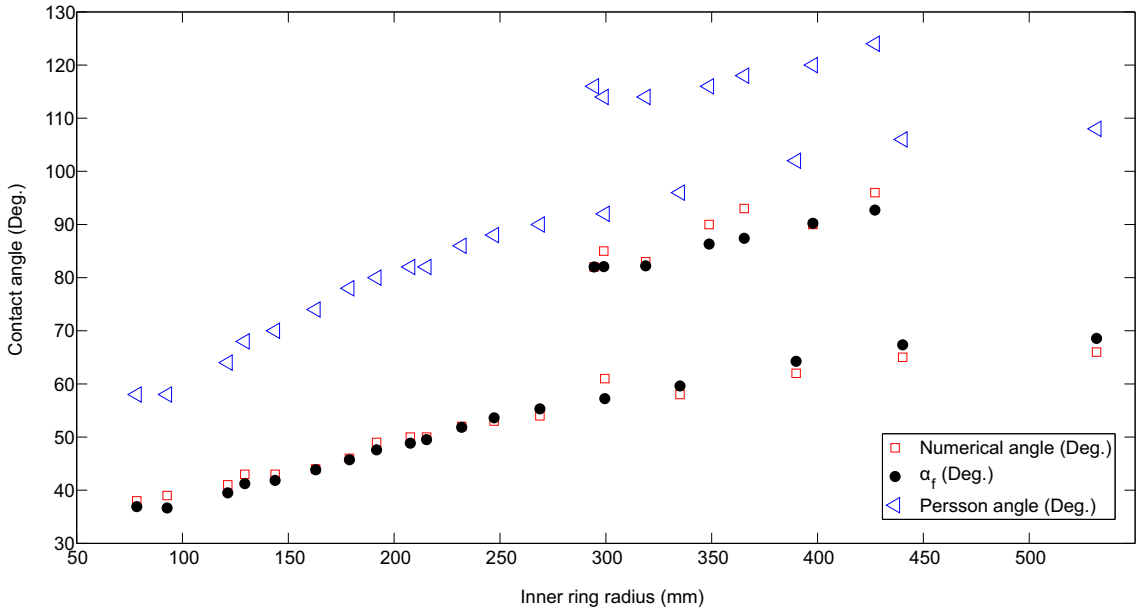

FIGURE 5.19 Variation of contact angle in terms of inner radius of ring

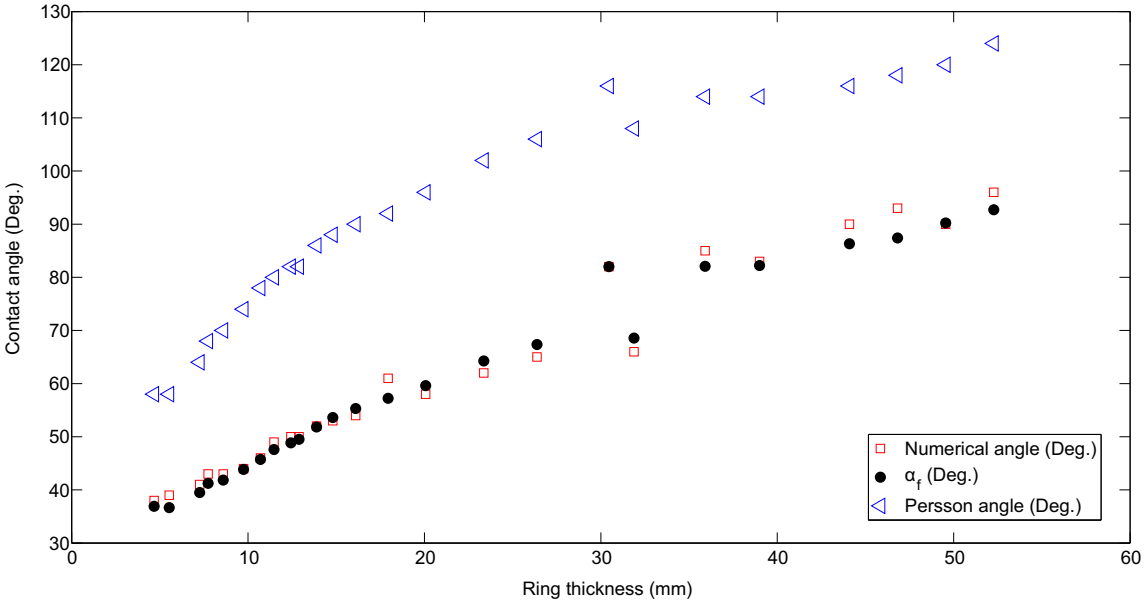

FIGURE 5.20 Variation of contact angle in terms of ring thickness

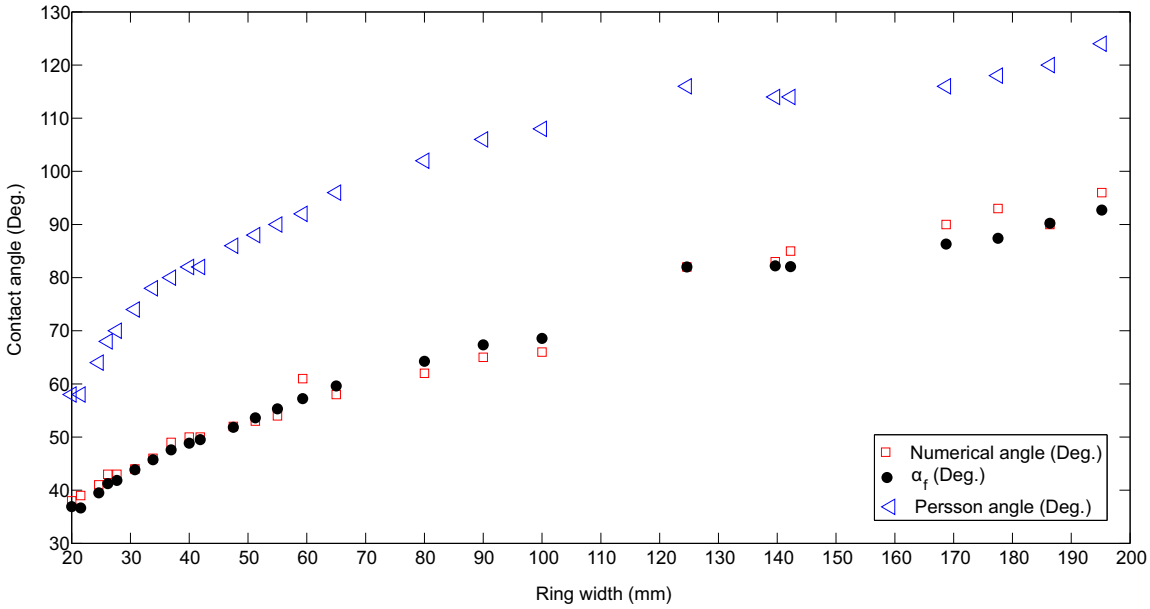

FIGURE 5.21 Variation of contact angle in terms of ring width

approximation.

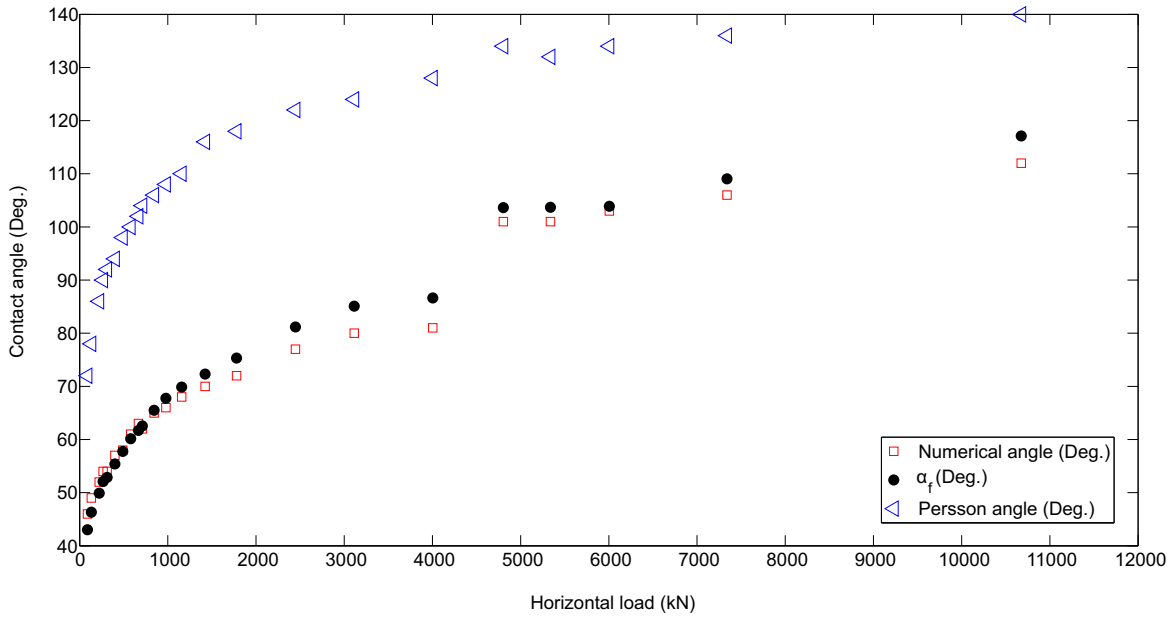

FIGURE 5.22 Variation of contact angle in terms of loading for additional models

5.7 Effects of angle of contact on design method

Method of pot bearing design specified in codes of practice can be optimized by applying Eq. (5.2) obtained from nonlinear regression analysis. This step can be taken by calculating maximum contact pressure from angle of contact obtained. As discussed in chapter 2 maximum contact pressure between piston and the pot plays an effective role in determining design parameter according to the following specifications as,

- EN 1337 :

  According to this specification maximum contact pressure is effective in determining external diameter of the pot (D_{Pot},Eq. (4.10)) due to taking into account shear forces in the pot walls. Also regarding to design of piston this parameter plays role in determining width of piston face for flat piston (w, Eq. (4.5)), radius of piston wall (R, Eq. (4.6)) and contact width between piston and pot (b, Eq. (4.7)) for curved piston walls to resist transverse forces transferred to the piston.
- AASHTO and CHBDC :

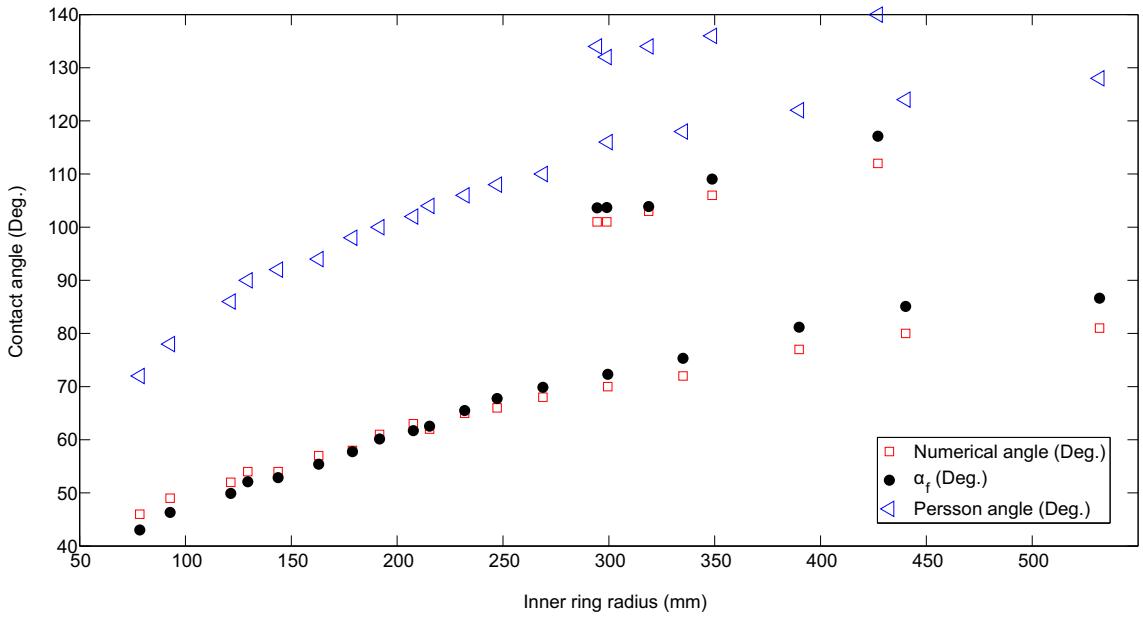

FIGURE 5.23 Variation of contact angle in terms of inner radius additional models

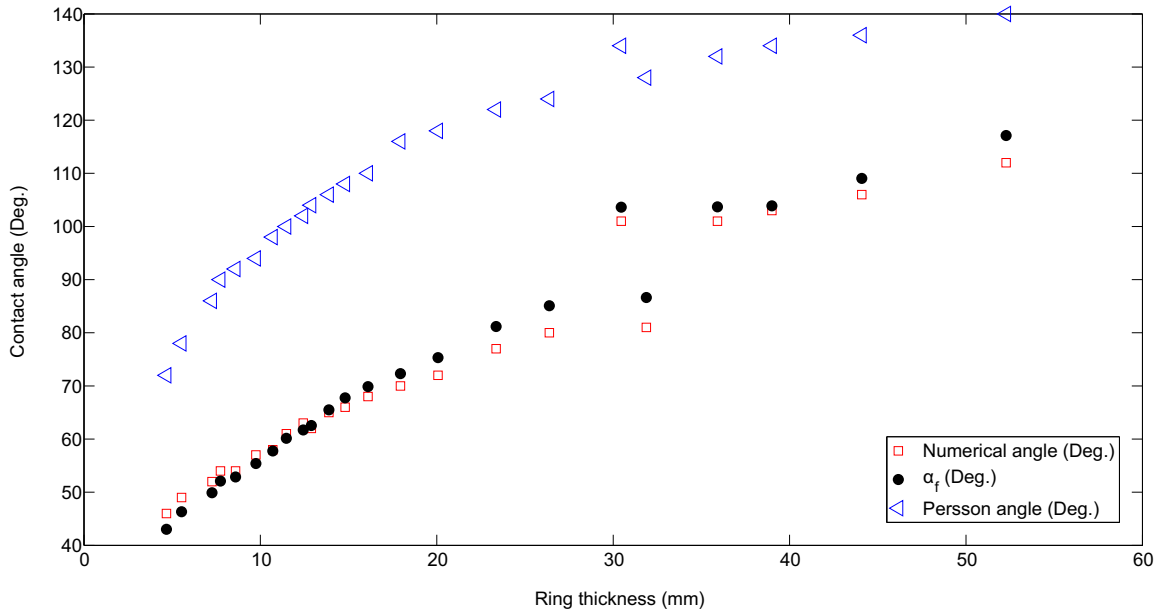

FIGURE 5.24 Variation of contact angle in terms of thickness for additional models

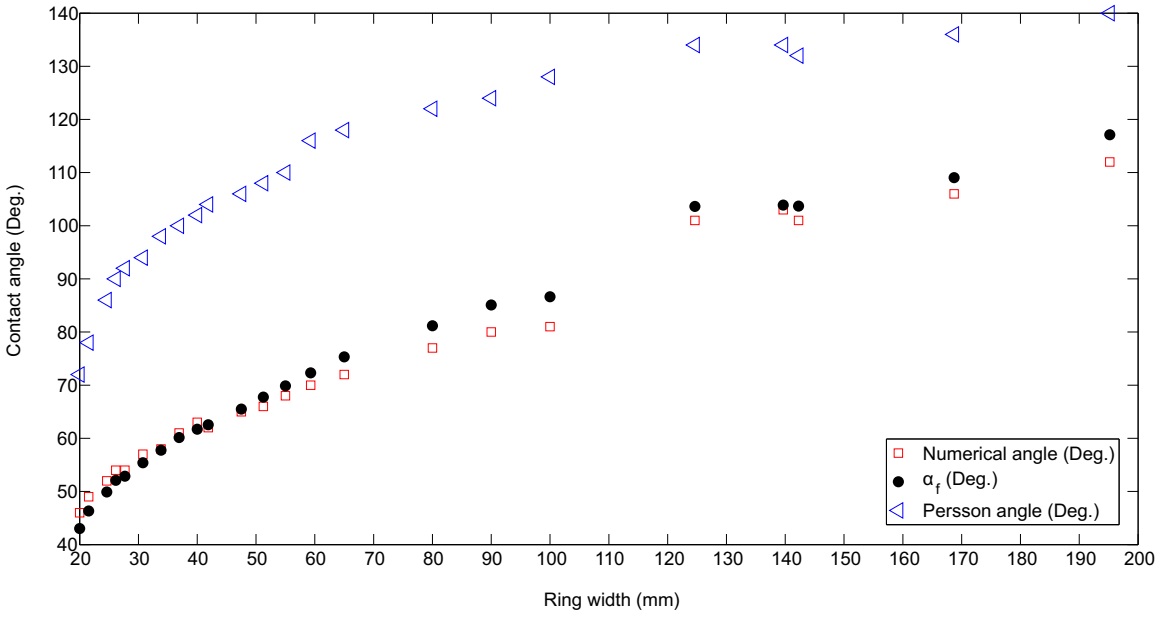

FIGURE 5.25 Variation of contact angle in terms of ring width for additional models

Compering to EN 1337, for these specifications contact pressure is effective only in determining width of piston face (w) for flat piston. In these specifications there is no indication to possibility of designing the piston as curved.

Thus the maximum contact pressure of P_0 can be obtained from the equation below by assigning α_f

$$V_{\mathrm{Fx,\,Sd}} = \int_{-r_{\mathrm{Pad}}\sin(\alpha_f/2)}^{r_{\mathrm{Pad}}\sin(\alpha_f/2)} P(x)\,\mathrm{d}x \tag{5.3}$$

or

$$V_{\mathrm{Fx,\,Sd}} = 2\int_{0}^{(\alpha_f/2)} P(\phi)\,\mathrm{d}\phi \tag{5.4}$$

Also assuming a parabolic distribution of contact forces the boundary conditions for contact pressures for Fig. 5.26 change to,

$$P(x) = 0 \text{ at } x = -r_{\mathrm{Pad}}\sin(\frac{\alpha}{2})\,; \qquad P(x) = 0 \text{ at } x = r_{\mathrm{Pad}}\sin(\frac{\alpha}{2})\,; \qquad P(x) = P_0 \text{ at } x = 0 \tag{5.5}$$

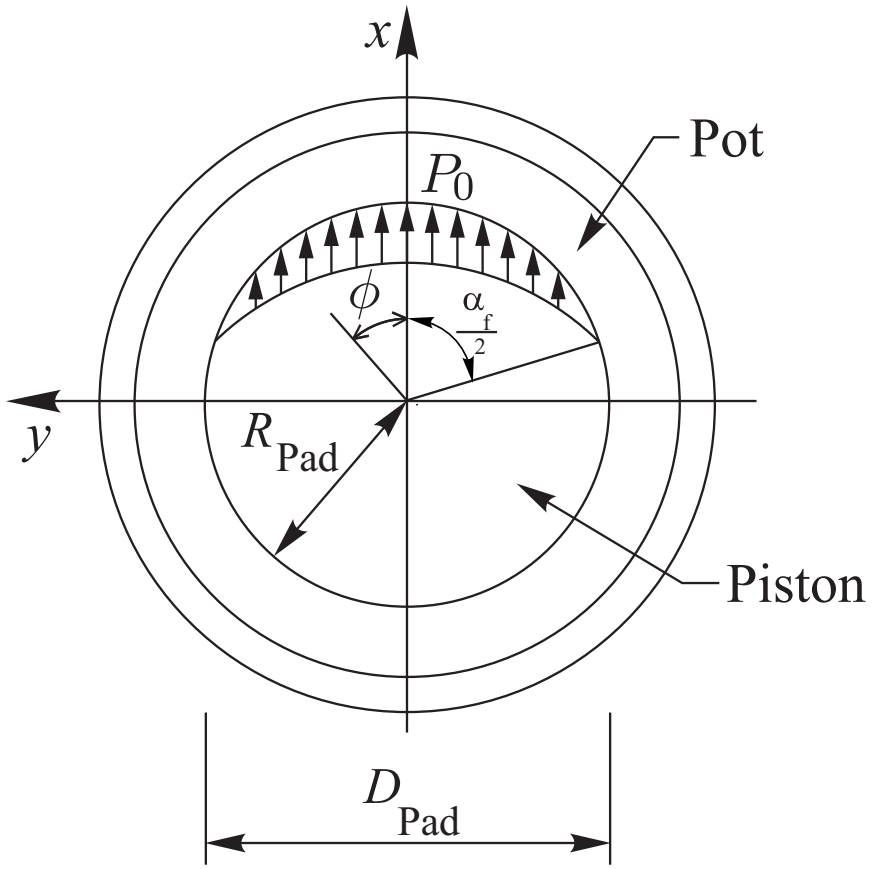

FIGURE 5.26 Horizontal distribution of contact forces in a pot bearing

leading to,

$$P_0 = \frac{\gamma V_{\mathrm{Fx,\,Sd}}}{d_{\mathrm{Pad}}} \tag{5.6}$$

Annex A.4, presents value of γ for models 1 to 73. As it is clear from the results γ exceeds 1.5 when angle of contact is less than 180 °.

5.8 Conclusion

Numerical values of contact angle from finite element modeling of pot bearings show that angle of contact depends on different geometrical and loading parameters that should be considered. These results also show that the simplifying assumption in design specifications considering only horizontal transmission of contact forces along half of bearing perimeter is not accurate. Also the maximum pressures obtained from Eq. (5.6) prove that contact pressure will be more than what is assigned in the specifications. when angle of contact is less than 180 °.

CHAPTER 6

CONCLUSIONS AND RECOMMENDATIONS

6.1 Reminder of research objectives

The main objective of this research is to investigate structural performance of fixed pot bearings through finite element modeling and simplified analytical formulations. For this purpose, the following phases were followed : (i) preparation of an exhaustive literature review, (ii) verification of finite element modeling by referring to analytical formulations of contact problem, (iii) finite element modeling of elastomeric pot bearing and disk and ring model, (iv) performing parametric regression analysis on contact angles obtained from numerical modeling. In the first phase of this research, a detailed literature review was conducted on pot bearings. Finite element results were assessed through comparison with available analytical formulations for typical bodies. In the next phase of the research, finite element modeling of a series of pot bearings from various manufacturers was conducted. The results of these analyses confirmed that the angle of contact between piston and the pot is generally different from 180 ° as assumed in design specifications. A simplified FE model including only a disk and truncated pot was proposed and validated to simulate contact conditions in actual pot bearings. The results were exploited to develop an equation for angle of contact, an important factor in design of pot bearings. For this purpose, a nonlinear regression analysis including the most important design parameters was conducted. The equation developed is the first numerical equation that estimates angle of contact between bearing parts in lieu of assuming distribution of contact forces along half of bearing perimeter as stated in the specifications.

6.2 Conclusions

The detailed literature review showed that the among the important specifications in design of pot bearings, code EN 1337 takes into account contact conditions between pot and the piston more effectively by stating that piston walls can be designed as either flat or curved for vertical transmission of forces. However for transmission of horizontal loads, all the specifications assume that contact stresses are transmitted from the piston to the wall along half of pot perimeter. Also it is concluded that another main difference between EN 1337 and the two specifications (AASHTO and CHBDC) is in design method of pot. In EN 1337 pot parts are assumed as separate components which transfer tensile and shear forces. However according to AASHTO and CHBDC pot is designed as a single structural unit which resists

bending moments due to the applied loads.

The results from finite element models of typical contact problems were validated against analytical formulations when available. It is concluded that (i) for two cylinders with positive curvature signs contact Hertz can be used as an accurate method to obtain contact parameters (ii) For two cylinders with different curvature signs, Hertz provides accurate results only when the contact area is small. However persson method proved to be accurate to obtain contact parameters for both small and large areas of contact.

The results obtained from 3D finite element models proved that angle of contact between piston and pot can be obtained by simplifying the bearing to a piston and truncated pot to avoid computation burden. However this angle cannot be obtained from Persson analytical method. The results of finite element analysis of the disk-ring models showed that angle of contact in a bearing is usually less than 180 ° (assumed in the specifications) which depends on on various geometrical and loading parameters. Angle of contact obtained from the developed equation by nonlinear regression method proved that this method can be used as a satisfactory means to estimate this parameter. Also the values of contact pressure obtained from the equation showed that for bearings with angle of contact less than 180 °, contact pressure will be more than what is stated in specifications. Thus the design method of pot bearings can be optimized by applying the modified value of contact pressure.

6.3 Recommendations

Due to the complex mechanisms present in a pot bearing such as nonlinear contact interactions and sophisticated boundary conditions it is recommended that the designer perform finite element analysis on pot bearings as well. This will help the designer to have a better understanding of the behaviour of the bearing. Also the design method of pot bearings should be optimized by the designer due to approximate design methods prescribed in the specifications. Also as further research in this area it is suggested to perform experimental tests on elastomeric pot bearings and compare the results with the ones corresponding to numerical methods.

REFERENCES

AASHTO-NSBA Steel bridge collaboration. 2004. Steel bridge bearings and detailing guidelines.

American Association of State Highway and Transportation Officials. 2012. AASHTO LRFD bridge design specifications.

ADINA Theory and modeling guide. 2010. Report ARD 10-7. ADINA R & D, Inc.

Agrawal, A.K., Subramaniam, K. and Pan, Y. 2005. Development of smart bridge bearings system a feasibility study, New York, University transportation research center.

Alampalli, S., O'Connor, J., Yannotti, A. P. 2002. Fiber reinforced polymer composites for the superstructure of a short-span rural bridge. Composite Structures. 58 (1) : 21-27

Andrá, W. and Leonhardt, F. 1962. New developments in structural bearings, rubber bearings and rubber pot bearings, Die Bautechnik, no. 2, pp. 37-50.

American Society for Testing and Materials (ASTM). 2012. Accessed online.

Atkinson, B. 1991. Pot bearing design and specification trends : 1960-1991, Third world congress on joint sealing and bearing systems for concrete structures, Toronto, Canada, pp. 817-828.

Baker, M. 2006. Development of pot bearing standards.

Bhandari, V. B. 2010. Design of machine elements.

Boresi, A. P., Sidebottom, O. M., Seely, B. and Smith, J. O. 1978. Advanced mechanics of materials, New York : Wiley., pp. 581-627.

Budinski, K.G. and Budinski, M.K. 2002. Engineering materials properties and selection.

Canadian Highway Bridge Design Code. 2006. Canadian standards association, Section 11, Joints and bearings.

Chen, W. and Lian D. 2000. Bridge engineering handbook.

Ciavarella, M., and P. Decuzzi. 2001. The state of stress induced by the plane frictionless cylindrical contact. I. The case of elastic similarity. International journal of solids and structures.

www.dsbrown.com. 2013. accessed online.

Eggert, H. and Kauschke, W. 2002. Structural bearings, Ernest and Sohn a Wiley Company.

European Standard. 2005. EN 1337-5 Structural bearings, Part 5 : Pot bearings.

Flynn, P. D., and A. A. Roll. 1967. A comparison of stress-concentration factors in hyperbolic and U-shaped grooves. Experimental Mechanics.

Gagnon, M. Gaudreault V., Overton D. 2011. Age of public infrastructure : a provincial perspective. Ontario : Investment and Capital Stock Division, Statistics Canada. Web site : www.statcan.gc.ca, accessed online.

Gase, P. 2011. Long term deterioration testing of HLMR bearings, Seventh world congress on joints and bearing, and seismic syetems for concrete Structures.

Get Toronto moving transportation commitee, 2011. Accessed online www.gettorontomoving.ca.

Hourigan, E. and Malik, A. 1986. Selection criteria for bridge bearings, Second world congress on joint sealants and bearing systems for concrete structures, San Antonio, U.S.A., pp. 817-824.

Huth, o. and Khbeis, H. 2007. Pot bearings bahavior after 32 years of service : In situ and laboratory tests, Engineering Structures, Elsevier.

Indian Railways Institute of Civil Engineering. 2006. Bridge bearings, Pune.

Jacobsen, F. K. 1985. Final report for confined or pot type elastomeric bridge bearings, Final report to Illinoise DOT.

Johnson, K. L. 1985. Contact mechanics. Cambridge University Press.

koelnwiki.de. 2011. Accessed online.

Lee, D. J. 1981. Recent experience in the specification, design, installation, and maintenance of bridge bearings, Fourth world congress on joint sealants and bearing systems for concrete structures.

Lee, J. 1994. Bridge bearing and expansion joints.

Lindley, Peter B. 1992. Engineering design with natural rubber, Malaysian Rubber Producers Research Association.

Lipson, C., Juvinall, R.C. 1963. Handbook of Stress and Strength.

Liu, C.S., K. Zhang, and R. Yang. 2007. The FEM analysis and approximate model for cylindrical joints with clearances, Mechanism and Machine Theory.

Long, J. E. 1974. Bearings in structural engineering, Newnes-Butterworths Publishing.

Marioni, A. 2006. The European standard EN 1337 on structural bearings, Sixth world congress on joints, bearings and seismic systems for concrete structures.

magebausa.com, 2011. Accessed online.

Muscarella, J. 1995. An experimental study of elastomeric bridge bearings with design recommendations, Center for transportation research, Bureau of engineering research, The University of Texas at Austin.

NCHRP Report432, 1999. Highload-multi rotational bridge bearing, Transportation research board, National research council.

Nystrom, H. E., Steve, E. W., Nanni, A.,ASCE, P.E. and Murray, S. 2003. Financial viability of fiber-reinforced polymer (FRP) bridges. Journal of Management in Engineering.

Persson, Allan. 1964. On the stress distribution of cylindrical elastic bodies in contact. Goteborg, Sweden : Chalmers Tekniska Hogskola.

Popov, V. L. 2010. Contact mechanics and friction Physical Principles and Applications, Springer.

Redfield, C. and Seim, C. 1986. Pot beaing replacements- two case studies : Cline Avenue Interchange and I-285/I-85 Interchange, Second world congress on joint sealants and bearing systems for concrete structures.

Roeder, C.W., Stanton, J.F. and Campbell, T. I. 1991. Behavior of high load multi-rotational bridge bearings, Third world congress on joint sealants and bearing systems for concrete structures.

Roeder, C. and Stanton J. 1998. Pot bearings and PTFE sliding surfaces : a state of the art report, Interim report to NCHRP project 10-20.

Roark, Raymond J., and Warren C. Young. 1989. Roark's formulas for stress and strain. New York : McGraw-Hill.

SETRA, 2009. Technical Guide for Pot Bearings Use on Bridges, Viaducts and similar structures.

Sorensen, J. D. 2011. Structural reliability, Institute of building technology and structural engineering Aalborg University, Accessed Online.

Srinath, L. S. 2009. Advanced mechanics of solids, New Delhi : Tata McGraw-Hill, pp. 446-455.

Steel bridge bearing selection and design Guide. 2011. American Iron and Steel Institute, Highway Structures Design Handbook.

Trahair, N. S., Bradford M. A., Nethercot, D. A. and Gardner, L. 2008. The bahaviour and design of steel structures to EC3.

Tonias, D.E. 1994. Bridge engineering, design, rehabilitation and maintenace of modern highway bridges.

Valvezan, J., Gilstad, D. and Farhangi, F. 1996. New bearings for Washington metro, Fourth world congress on joints, sealants and bearing systems for concrete structures.

Watson, s. 1996. A half-century of involvement with joints and bearings and some lessons learned, Fourth world congress on joints, sealants and bearing systems for concrete structures.

Wetzk, Volker. 2011. Bridge bearings a historical survey (From the German by Barthold Pelzer, Berlin), Accessed online.

ANNEXE A

SPECIFICATIONS OF DEVELOPED DISK-RING MODELS

TABLE A.1 Horizontal and geometrical properties of disk-ring models (continue)

model #	H (kN)	b_{Ring} (mm)	w_{Ring} (mm)	r_{1Ring} (mm)
1	489	15	51	247
2	122	15	102	247
3	245	15	102	247
4	489	15	102	247
5	979	15	102	247
6	1468	15	102	247
7	122	15	153	247
8	245	15	153	247
9	489	15	153	247
10	979	15	153	247
11	1468	15	153	247
12	122	15	204	247
13	245	15	204	247
14	489	15	204	247
15	979	15	204	247
16	1468	15	204	247
17	122	15	26	247
18	245	15	26	247
19	489	15	26	247
20	979	15	26	247
21	1468	15	26	247
22	122	15	51	247
23	245	15	51	247
24	979	15	51	247
25	1468	15	51	247

TABLE A.2 Horizontal and geometrical properties of disk-ring models

model #	H (kN)	b_{Ring} (mm)	w_{Ring} (mm)	r_{1Ring} (mm)
26	56	5	20	78
27	67	6	22	93
28	111	7	25	121
29	133	8	26	129
30	156	9	28	144
31	200	10	31	163
32	245	11	34	179
33	289	11	37	192
34	334	12	40	208
35	356	13	42	215
36	423	14	47	232
37	489	15	51	247
38	578	16	55	269
39	712	18	59	299
40	890	20	65	335
41	1223	23	80	390
42	1557	26	90	440
43	2002	32	100	532
44	2402	30	125	294
45	2669	36	142	299
46	3003	39	140	319
47	3670	44	169	349
48	4003	47	178	365
49	4671	50	186	398
50	5338	52	195	427

TABLE A.3 Specifications disk-ring models generated to verify developed equation

model #	H (kN)	b_{Ring} (mm)	w_{Ring} (mm)	r_{1Ring} (mm)
51	89	5	20	78
52	133	6	22	93
53	222	7	25	121
54	267	8	26	129
55	311	9	28	144
56	400	10	31	163
57	489	11	34	179
58	578	11	37	192
59	667	12	40	208
60	712	13	42	215
61	845	14	47	232
62	979	15	51	247
63	1157	16	55	269
64	1423	18	59	299
65	1779	20	65	335
66	2447	23	80	390
67	3114	26	90	440
68	4003	32	100	532
69	4804	30	125	294
70	5338	36	142	299
71	6005	39	140	319
72	7340	44	169	349
73	10676	52	195	427

TABLE A.4 Value of γ for the models developed

model #	γ	model #	γ	model #	γ
1	3.3	26	4.7	51	4.1
2	4.7	27	4.8	52	3.8
3	3.7	28	4.4	53	3.6
4	3.0	29	4.3	54	3.4
5	2.4	30	4.2	55	3.4
6	2.2	31	4.0	56	3.2
7	4.4	32	3.9	57	3.1
8	3.5	33	3.7	58	3.0
9	2.8	34	3.6	59	2.9
10	2.3	35	3.6	60	2.9
11	2.1	36	3.4	61	2.8
12	4.2	37	3.3	62	2.7
13	3.3	38	3.2	63	2.6
14	2.7	39	3.1	64	2.5
15	2.2	40	3.0	65	2.5
16	2.0	41	2.8	66	2.3
17	5.9	42	2.7	67	2.2
18	4.7	43	2.7	68	2.2
19	3.7	44	2.3	69	1.9
20	3.0	45	2.3	70	1.9
21	2.7	46	2.3	71	1.9
22	5.2	47	2.2	72	1.8
23	4.2	48	2.2	73	1.8
24	2.7	49	2.1		
25	2.4	50	2.1		